1-1-2011

Mechanisms of Observed Neuroprotection of Dopaminergic Neurons in Wallerian Degeneration Slow (WldS) Mice

Jo Ann Antenor-Dorsey
Washington University in St. Louis

WASHINGTON UNIVERSITY IN ST. LOUIS

Division of Biology and Biomedical Science

Neurosciences

Dissertation Examination Committee:
Karen O'Malley, Chairperson
Valeria Cavalli
Marc Diamond
Aaron DiAntonio
Paul Kotzbauer
Joel Perlmutter

Mechanisms of Observed Neuroprotection of Dopaminergic Neurons in Wallerian Degeneration Slow (*Wld*^{S}) Mice

By

Jo Ann V. Antenor-Dorsey

A dissertation presented to the
Graduate School of Arts and Sciences
of Washington University in
partial fulfillment of the
requirements for the degree
of Doctor of Philosophy

December 2011

Saint Louis, Missouri

Abstract

An emerging hypothesis in Parkinson's disease (PD) is that dopaminergic (DA) neurons degenerate through a "dying back" axonopathy wherein degeneration begins in the distal axon and progresses over time towards the cell body. Impaired axonal transport also appears to play an early, pivotal role in PD. Thus processes that delay axonal transport dysfunction and/or axonal degeneration might slow PD progression. Previously, we and others have found that the *Wld*^{S} mouse mutant ("Wallerian degeneration-slow"), which exhibits delayed axonal degeneration after peripheral axonopathy, also protects DA terminal fields from the PD-mimetics 1-methyl-4-phenyl-1,2,3,6-tetrahydropyridine (MPTP) and 6-hydroxydopamine (6-OHDA) *in vivo*. To understand the mechanisms underlying *Wld*^{S}-mediated axonal protection, we tested whether *Wld*^{S} rescued DA neurons *in vitro* after treatment with either MPP^+, the active component of MPTP, or 6-OHDA. *Wld*^{S}*,* but not its component parts, UbE4b and Nmnat1, robustly rescued neurites in dissociated DA cultures following either MPP^+ or 6-OHDA treatment. To extend these results, compartmented chambers were developed such that axons could be segregated from cell bodies and dendrites. Using these devices, we found that MPP^+ impaired mitochondrial, but not synaptic vesicle transport, in DA axons and that *Wld*^{S} rescued MPP^+-mediated impairment of mitochondrial transport in DA axons. Mechanistically, this appears to be due to *Wld*^{S}-mediated protection from toxin-induced loss of mitochondrial membrane potential. These results extend *Wld*^{S} protection to CNS DA neurons and suggest that *Wld*^{S} confers a gain-of-function phenotype that attenuates mitochondrial dysfunction. This study, together with the large amount of evidence suggesting PD is associated with axonal "dying-back", also underscores the necessity of developing therapeutics aimed at axons as well as cell bodies so as to preserve circuitry and function.

Acknowledgements

This dissertation is dedicated to my children, Mackenzie Josephine Antenor-Dorsey and Jameson Connor Antenor-Dorsey. Always remember that both of you are my ultimate pride and joy, now and forever. Mommy loves both of you … A LOT.

I want to thank my husband, Michael Dorsey. From being my "sugar daddy", to my first "victim" for a talk, to the ultimate back massager, I know I could not have survived this journey without you. Thank you for being a loving father, a sweet husband, and being my best friend. We make cute kids, don't we? I love you so much.

To my Nanay and Tatay, who have sacrificed so much of their lives in order to help me succeed in pursuing a career as a scientist, maraming salamat po. I owe you (and continue to owe you) so much. Both of you are such great role models for my brother and I to exemplify. Mahal na mahal ko po kayo.

I'd like to thank my Ate Linda, my second mother. She may be half my height, but her love for my brother and I know no bounds. She is the epitome of "small, but fierce", and I miss her so much. I promise, I'll come home soon!

I'd also like to thank my Kuya (brother), who helped me get started on my science career by making my PowerPoint presentations for my National Science Fair competitions back in the Philippines.

I like to extend my gratitude to the rest of my family and my friends, especially: Amanda, the godmother of my children and my sister from another mother, Alison, a true friend who always puts up with my venting, Cass, who is always supportive and initiates the best "themed" lunches for the 9th floor, Indra, a selfless friend and my fashionably fabulous cheerleader, Jen, who gave great and helpful suggestions on my dissertation, and Tunde, who always supplied me with compliments and comic books, the two things a geeky girl can never be without. You guys made my life, inside and outside the lab, full of laughter and joy, and I thank you.

I'd like to thank all the past and present members of the O'Malley Lab. A shout-out is in order to the undergrad students who were instrumental in getting my huge data sets analyzed: Manouela Valtcheva, Diane Ma, and Anna Dardick. I'd also like to thank

Steve Harmon for assisting me in the lab, especially in regards to maintaining my mice colony and for teaching me about my bread and butter in the lab, primary midbrain cultures. I'd also like to thank Dr. Ivy Jong, who was helpful in giving me the tools to transform myself from a systems neuroscientist into a cell neuroscientist. Finally, I'd like to express my utmost gratitude to Dr. Jeong Sook Kim-Han, whose generosity knows no bounds. I thank you for teaching me so much about science, but I am most grateful for your insight on family and God. You have made me into a stronger Catholic scientist, and I cannot repay you enough for that.

I'd also like to extend my gratitude to past and present members of my committee, Dr. Guojun Bu and Dr. Valeria Cavalli, who gave me helpful discussions about my science, Dr. Paul Kotzbauer, who let me rotate in his lab, Dr. Aaron DiAntonio and Dr. Marc Diamond, who may have "joined" the party later but gave such insightful suggestions, and Dr. Joel Perlmutter, who always believed in me.

I want to express my sincere thanks to my thesis mentor, Dr. Karen O'Malley, for giving me the opportunity to be part of her lab. I am very grateful for the mentorship and guidance she has provided me over the past 5 years. She gave me the freedom to learn and grow as a scientist, but was always there with a helping and guiding hand when I needed it.

Finally, I'd like to thank my Lord and Savior, Jesus Christ. All things are possible through You. To God be the Glory.

Table of Contents

List of Tables

List of Figures

Chapter 1

Introduction

1.1 Parkinson's disease: Overview

Parkinson's disease (PD) is the second most common neurodegenerative disease in the United States. Presenting late in life, it affects 1% of the population over the age of 55. This progressive neurodegenerative disease is characterized by the loss of dopaminergic neurons in the substantia nigra (SN) which project to the striatum [1-2]. PD is also associated with the formation of cytoplasmic inclusions in the nervous system called Lewy bodies. Lewy bodies are spherical eosinophilic aggregates composed of proteins such as α-synuclein, parkin, and ubiquitin [4]. Striatal dopamine (DA) deficiency results in diminished motor control in PD, characterized by resting tremor, rigidity, bradykinesia and postural instability [5-6]. These motor symptoms do not appear until there is approximately a 30% loss of DA neurons and about 50-60% loss of DA [7]. Although positron emission tomography (PET) imaging shows decreased fluorodopa uptake in the striatum indicating a loss of DA innervation, the clinical diagnosis of PD can only be confirmed by post-mortem pathology.

PD-related neurodegeneration extends beyond the DA neurons of the SN. It is evident in noradrenergic [8], serotonergic [9], and cholinergic systems [10] as well as the cerebral cortex, olfactory bulb and autonomic nervous system [5]. In fact, the earliest pathology of PD is the presence of thread-like inclusion bodies, or Lewy neurites, in the axons of peripheral neurons [5]. Moreover, degeneration of hippocampal structures and cholinergic inputs to the cortex have been known to contribute to the comorbidity of dementia in PD [11].

At present, there is no known cure for PD. Current treatments target replenishment of striatal DA via administration of the DA precursor, levodopa, which initially alleviates most of the symptoms of PD. However, this treatment does not prevent or slow the progression of the disease. It often produces severe dyskinetic side effects and may decrease in efficacy throughout disease progression [12]. The etiology of PD is still unknown, but much about PD has been learned from epidemiological studies, post-mortem studies, and animal model systems.

1.2 Genetic factors

Genetic studies of individuals with familial PD have led to the identification of fifteen loci (PARK1-15) that are linked to PD [13]. Genes associated with the disease at eleven of these loci have been identified: α-synuclein, Parkin, α-synuclein duplications and triplications, ubiquitin C-terminal hydrolase L1 (UCH-L1), PTEN-induced putative kinase 1 (PINK1), DJ-1, leucine-rich repeat kinase 2 (LRRK2), ATP13A2, Omi/HtrA2, PLA2G6, and FBXO7. Although the majority of PD cases are idiopathic, studies on mutations in the α-synuclein, Parkin, PINK1, and LRRK2 genes that lead to familial PD have given clues to the molecular mechanisms that result in DA cell loss in PD.

1.2.1 α-synuclein

Missense mutations in the gene encoding α-synuclein (A53T, A30P and E46K) and triplications of a portion of α-synuclein have been linked to autosomal dominant PD [14-18]. α-synuclein is a presynaptic protein of unknown function, but is abundant in the brain and associated with vesicles and membranes. Thus, it is thought to be involved in synaptic vesicle trafficking, storage and compartmentalization of neurotransmitters [19-22], perhaps as a co-chaperone [18]. Because α-synuclein tends to aggregate, it has been implicated in PD pathogenesis. This is consistent with studies showing that α-synuclein is the major fibrillar component of Lewy bodies in both familial and sporadic PD [4].

1.2.2 LRRK2

Mutations in LRRK2 are the most common known cause of late-onset autosomal dominant PD and are seen in idiopathic cases of PD [23-25]. LRRK2 is a multi-domain protein that contains a Rho/Ras-like GTPase domain, a MAPKKK kinase domain, a WD40-repeat domain, a leucine-rich repeat domain, and a C-terminal of RAS domain. LRRK2 is expressed in forebrain structures including nigrostriatal DA neurons and localizes to the Golgi, synaptic vesicles, plasma membrane, lysosomes and outer mitochondrial membranes [26-31]. Although the function of LRRK2 is unknown, deletion of the LRRK2 homolog, LRK-1, in C. elegans leads to depletion of synaptic vesicle proteins [32]. LRRK2 has also been shown to associate with lipid rafts, localize to Lewy bodies and

regulate neurite length and branching [33-35]. The G2019S and I2020T mutations are located in the kinase domain and are associated with increased kinase activity [36-39]. Many studies have shown that alterations in the kinase activity of LRRK2 due to disease-linked mutations affect apoptosis and neurodegeneration; however it is unclear how these changes in kinase activity lead to PD [38-40].

1.2.3 Parkin

A loss-of-function mutation in the parkin gene was identified at the PARK2 locus and linked to autosomal recessive juvenile parkinsonism (AR-JP) [41]. Mutations in Parkin are one of the most common known genetic causes of early-onset PD. Parkin is an E3 ubiquitin-protein ligase that acts in conjunction with E2 ubiquitin-conjugating enzymes to target proteins for degradation via the proteasome by adding ubiquitin chains to specific substrates [42-44]. Mutations associated with AR-JP disrupt the E3 ligase activity of parkin, preventing the targeting of specific proteins to the proteasome. Parkin is neuroprotective against a variety of toxic insults in DA neurons [45]. Post-translation modifications of parkin by oxidative stress can inhibit its protective function by impairing its E3 ligase activity [46-47]. Recent data suggests that Parkin is neuroprotective through its action on mitochondria. Data from *Drosophila* and mammalian neuronal cell lines indicates that Parkin is recruited to the mitochondria following the loss of its membrane potential ($\Delta\Psi_m$) in response to various toxic insults. Relocated Parkin serves as a signal for the induction of mitophagy, suggesting

that loss of Parkin activity allows the accumulation of dysfunctional mitochondria that leads to neuron loss in PD [48]. Therefore, another role of Parkin may be to monitor activity and maintain mitochondrial fidelity by triggering mitophagy if necessary.

1.2.4 PINK1

Loss-of-function mutations in PINK1 cause autosomal recessive early onset PD and are found in rare sporadic early onset cases [49-50]. PINK1 is a serine/threonine kinase that localizes to the mitochondrial intermembrane space and membranes of the mitochondria [49]. PINK1 is thought to play a role in cell death pathways as wild-type PINK1 can protect against staurosporine-induced cytochrome-c release but PD-linked mutations do not. [51]. Data suggest that PINK1's kinase activity may play a role in mitochondrial biogenesis and function [52-53]. In flies, loss of PINK1 by siRNA causes mitochondrial dysfunction and DA cell loss which is rescued by overexpression of Parkin [54-56], suggesting that PINK1 is upstream of Parkin. Due to its high turnover rate, PINK1 is normally present at only low levels on bioenergetically active mitochondria. Mitochondrial depolarization leads to PINK1's stabilization and accumulation on mitochondria. In turn, PINK1 accumulation appears to recruit Parkin to mitochondria in various cell lines inducing mitophagy. So PINK1 may also protect DA neurons by activating the removal of damaged mitochondria [57].

1.3 Toxin Models

Epidemiological data on PD suggests that various environmental toxins may also play a role in the etiology of the disease. A number of Parkinsonian mimetics have been identified, of which, 1-methyl-4-phenyl-1,2,3,6-tetrahydropyridine (MPTP) or its active metabolite spell out (MPP^+) and 6-hydroxydopamine (6-OHDA) are the two most commonly used. Each of these toxins has been shown to recapitulate, many, but not all, of the behavioral, pharmacological, and pathological hallmarks that characterize PD.

1.3.1 MPTP and MPP^+

MPTP, a meperidine analog, mimics both the motor deficits and pathology characteristic of PD in humans [58-59]. Accidental ingestion of MPTP by humans led to motor deficits characteristic of PD. Similar to PD patients, these patients responded to L-DOPA treatment and DA agonist therapy [59]. Autopsy on one patient confirmed severe loss of DA neurons in the SN, but a noticeable lack of Lewy bodies, in comparison to what is seen in *bona fide* PD [58].

Administration of MPTP to non-human primates and rodents also produces PD-like symptoms which respond positively to L-DOPA and selective DA loss [60]. There is specific loss of DA neurons in the SN with a more dramatic reduction of striatal axons and DA levels that persist following MPTP exposure in mice [61-62]. Cytoplasmic inclusions have been shown to develop in MPTP-treated primates [63], although traditional Lewy bodies have not been described

[64]. A robust inflammatory response has been shown, including chronic microgliosis and astrocytosis, which contributes to DA cell loss, as microglial inhibition protects DA neurons following MPTP administration in rodents [65].

MPTP is able to cross the blood-brain barrier and is rapidly converted to MPP^+ by monoamine oxidase B (MAOB) in glial cells [66]. Despite expression of MAOB and production of MPP^+ in non-DA neurons, MPP^+ toxicity is specific to catecholaminergic neurons because of its high affinity for the DA plasma membrane transporter (DAT) and other catecholamine uptake systems. In *in vitro* systems, direct application of MPP^+ induces cell death specifically in DA neurons. Inside the cell, MPP^+ is sequestered into vesicles by the vesicular monoamine transporter (VMAT2), displacing DA [67]. MPP^+ that is not sequestered into vesicles can enter mitochondria where it inhibits complex I of the electron transport chain. This leads to ATP depletion, generation of reactive oxygen species (ROS) and cell death [1, 68].

1.3.2 6-OHDA

6-OHDA is a neurotoxin formed from the auto-oxidation of DA and is found endogenously in the nigrostriatal pathway [69]. 6-OHDA was the first toxin used in an animal model to study neurodegeneration in PD [70]. Since 6-OHDA cannot cross the blood-brain barrier, experimental models of PD require that it is stereotactically injected into the striatum, the SN or the medial forebrain bundle (MFB). Similar to MPTP, rodent models utilizing 6-OHDA also lead to depletion of

striatal DA and degeneration of striatal nerve terminals followed by retrograde degeneration of neurons in the SN [71]

The specificity of 6-OHDA *in vivo* towards catecholaminergic cells is due to its structural similarity to DA and norepinephrine. 6-OHDA is taken up by catecholaminergic neurons specifically by the DAT and noradrenergic transporter [72]. Once uptake into DA nerve terminals occurs, 6-OHDA accumulates in the cytosol and generates ROS by conversion into hydroxyl radicals and 6-OHDA quinone [73]. Inhibition of 6-OHDA uptake by catecholamine uptake inhibitors blocks 6-OHDA-induced toxicity *in vivo* [74]. 6-OHDA also induces cell death in primary mesencephalic cultures; however, because it is readily oxidized to hydrogen peroxide in tissue culture buffers, 6-OHDA is not selective for DA neurons *in vitro* [75].

6-OHDA inhibits mitochondrial complex I in cell-free assays [76]. However, in whole cells, 6-OHDA does not cause ATP depletion [77], suggesting that this is not its main mechanism of action. 6-OHDA induces a collapse in $\Delta\Psi_m$ in primary DA cultures that is dependent on ROS [78] and p53 [79]. 6-OHDA treatment also causes release of cytochrome C, activation of caspase 3, DNA fragmentation [80] and damage [79], and annexin V staining [78], consistent with an apoptotic type of cell death.

1.4 Axonal dysfunction in PD

Although the molecular mechanisms underlying the etiology of PD remain unclear, the genetic factors and toxin models previously discussed support the contention that four possibly interchangeable mechanisms underlie PD. These include: (1) death via impairment of the ubiquitin proteasome system (UPS), wherein increased levels of misfolded proteins overwhelm the UPS and accumulate as aggregates in the neuron; (2) death via impairment of mitochondrial function, specifically, inhibition of mitochondrial complex I leading to decreased ATP levels and increased levels of ROS; (3) death via oxidative stress due to internal DA autooxidation, mitochondrial dysfunction, or external oxidative stresses, and (4) neuroinflammation. Although all of these models may be true for the death of DA cell bodies, a new emerging hypothesis regarding DA dysfunction is based on the “dying-back” pattern of neuronal degeneration seen in PD models. In this model, axonal degeneration begins distally and progresses proximally over a period of time. This model hypothesizes that the initial insult in PD occurs at the level of the axon, rather than at the cell body.

1.4.1 Post-mortem PD patient data

Initial support for this hypothesis comes from studies on post-mortem PD patient brains. As described, Braak *et al.* have reported that the earliest pathology of PD is the presence of Lewy neurites in the dorsal motor nucleus and preganglionic axons of the vagal nerve [5]. These data suggest that the axonal

compartment is affected very early in the disease process. By observing patterns of α-synuclein pathology and tyrosine hydroxylase (TH) immunostaining in the cardiac sympathetic axons and ganglia of PD patients, Orimo *et al.* proposed that the PD disease process begins in the distal axon and proceeds retrogradely [81]. In the DA system, dystrophic neurites have been described in the caudate nucleus of post-mortem brains from PD patients [82]. In addition, multiple studies done on postmortem brains of PD patients have observed an 80% loss of putamenal DA [6] and a 68-82% decrease in DA levels in the caudate of PD patients [83] with only a corresponding 30% cell death in SN neurons [84-86] at the time of onset of PD motor symptoms. Although postmortem studies may be subject to misinterpretation due to the effects of postmortem delay, measurement of another DA marker, VMAT binding, in postmortem caudate of PD patients and controls led Scherman *et al*. to conclude that PD motor signs become apparent when there is about a 50% decrease in VMAT binding relative to age-matched controls [85]. Consequently, either study revealed significantly more loss of nigrostriatal terminal field markers compared to the loss of SN DA neurons in PD. Taken together, the patient data suggest that the initial insult in PD occurs at the axon versus the cell body.

1.4.2 Functional imaging data

Numerous studies have also examined the relationship between DA terminal loss and the onset of PD symptoms using radioligand imaging. Three

types of PET radioligands have been used to assess striatal degeneration: (1) 18F-dopa to assess L-dopa metabolism, (2) ligands to assess DAT binding, and (3) ligands to assess VMAT2 binding [87]. A 20-50% decrease in putamenal DA has been reported with 18F-dopa [88-91], while a 50-70% decrease in putamenal DA was seen using ligands for either DAT or VMAT2 [90, 92-93]. The discrepancy between neurotransmitter levels versus transporter levels may be due to a compensatory upregulation of aromatic acid decarboxylase resulting in the underestimation of terminal losses by 18F-dopa PET [87, 90]. But the 50-70% striatal DA loss measured by DAT or VMAT radioligands is consistent with the 50% striatal DA loss seen in postmortem studies. In addition, both sets of data show a greater decrease of striatal DA versus the 30% loss of DA neurons seen in the SN at disease symptom onset. Hence, functional imaging data provide further support for the idea that degeneration of the axon plays an important role in the pathogenesis of the disease.

1.4.3 Genetic studies

Early evidence for axonal degeneration is also apparent in several PD-linked gene models. For example, post mortem studies of patients with an α-synuclein gene triplication reveal widespread and severe neuritic pathology [94]. Dystrophic neurites are also evident in transgenic mice and primate models that overexpress α-synuclein [95-96]. Transgenic mice exhibiting the mutant α-synuclein gene associated with familial PD (A53T) exhibit intra-axonal

accumulation of a-synuclein aggregates, vesicles, mitochondria, vacuoles and neurofilaments, suggesting an interruption of axonal transport and, subsequently, axonal degeneration [97-98]. Moreover, overexpression of α-synuclein causes neurite degeneration in primary neuronal cultures [99] as well as defective axonal transport [100]. The latter may be due to the reported association of α-synuclein with complexes containing the molecular motors kinesin and dynein that are responsible for microtubule-based axonal transport [101]. This suggests that axonal transport dysfunction can lead to axonal degeneration and that defective axonal transport may play a role in the etiology of PD.

Mice expressing the PD-associated LRRK2 mutation (R1441G) exhibit PD-like motor symptoms that respond to L-dopa. These mice do not have SN DA neuron loss but exhibit fragmented DA axons that have axonal spheroids and form dystrophic neurites [102]. Meanwhile, the G2019S and I2020T LRRK2 mutations exhibit dramatic reductions in neurite length and branching yet only slight changes in cell soma diameter in primary neuronal cultures [35]. Similar findings were made for the G2019S mutant in differentiated neuroblastoma cells [103] and in primary neurons derived from transgenic mice [104]. In addition, Parkin protects DA neurons against colchicine, a known microtubule-depolymerizing agent [105]. Lastly, PINK1 may also play a role in axonal trafficking and hence the health of the axonal compartment via its association with Miro and Milton, two proteins that are involved in axonal mitochondrial transport [106]. Taken together, these data support the notion that there are

persistent early changes in axonal health and trafficking in PD, changes that may contribute to PD pathogenesis.

1.4.4 Toxin studies

A similar pattern of neurodegeneration is also evident in toxin models of PD. For example, severe terminal field loss yet relatively mild nigral changes are also observed in response to MPTP treatment in primates [107-108]. This specific terminal field effect is consistent with data showing that this toxin can destabilize microtubules in cell-free assays, affect tubulin levels in differentiated PC12 cells [109-110], and impede the clearance of α-synuclein by impairing dynein activity [111]. More directly, MPP^+ affects axonal transport in the squid giant axon by increasing retrograde transport and decreasing anterograde transport independent of the cell's ATP production [112]. In the mammalian PC12 cell line MPP^+ also affects axonal mitochondrial trafficking by destabilizing microtubules [113]. Thus, toxin models of PD also support the idea that axonal transport dysfunction, and subsequent axonal degeneration, is important in the progression of PD.

Rodent models lesioned with 6-OHDA also lead to depletion of striatal nerve terminals followed by retrograde degeneration of neurons in the SN [71]. Like MPP+, 6-OHDA also destabilizes microtubules in *in vitro* cell-free assays suggesting that microtubule destabilization is a common pathway to axon degeneration [114]. Consistent with this notion, rotenone, another well known PD mimetic, was reported to induce DA neuron death through microtubule depolymerization [115]. In addition, rotenone impairs mitochondrial transport in

differentiated SH-SY5Y cells, a neuroblastoma cell line that exhibits a DA phenotype [116]. Finally, intrastriatal injection of colchicines blocks retrograde axonal transport and subsequently causes degeneration of the striatonigral pathway [117]. Therefore, changes in axonal structure or transport can potentially mediate the “dying back” mechanism observed in PD.

Taken together, there is a growing body of data from post mortem studies, genetic and toxin models indicating that axon dysfunction plays a key role in PD.

1.4.5 Programmed cell death versus axonal degeneration

It was initially thought that axons were highly dependent on cell bodies for long-term survival. However, recent studies reveal the existence of axon-autonomous mechanism(s) that regulate rapid axon degeneration after injury [118]. For example, axons of sympathetic neurons die back after localized NGF withdrawal, while the cell body survives [119]. In contrast, local application of NGF to the axonal terminal promotes survival of both the axon and cell body [120]. More directly, caspase-3, which is involved in programmed cell death, is not activated in a variety of axonal degeneration models [121]. In the context of PD, Ries *et al.* examined how c-jun N-terminal kinases (JNKs), which play a central role in mitogen-activated protein kinase (MAPK)-mediated apoptosis of SN DA neurons, affect 6-OHDA-mediated degeneration of DA axons. They found that homologous JNK2/JNK3 null mice show almost complete protection of their SN cell bodies but no protection of axons against 6-OHDA [122]. Further

evidence that axons can survive even in the presence of cell body death is seen from Wallerian degeneration-slow (*Wld*^{S}) mice. This mutation arose spontaneously from C57/Bl/6 mice and has been demonstrated to cause delayed Wallerian degeneration in the peripheral nerve after axotomy [123]. Studies show that the cell bodies of sympathetic neurons from *Wld*^{S} mice degenerate with a normal timecourse and morphology but that *Wld*^{S} neurites remain metabolically active in response to injury [124]. These studies suggest that the degeneration of neurites and cell bodies occur through mutually exclusive processes, and that the protection of one compartment does not necessarily lead to protection of the other.

1.5 Wallerian degeneration-slow (*Wld*^{S}) mice

Wallerian degeneration is similar to the “dying back” phenomenon in that the distal stump of an injured axon degenerates first. This occurs in four phases: 1) the distal stump loses the ability to transmit action potentials; 2) the axon and synaptic terminals fragment; 3) the cytoskeleton degenerates; and 4) Schwann cells and invading macrophages remove axonal and nerve terminal debris [125]. As their names suggests, *Wld*^{S} mice exhibit delayed degeneration of neurites following axotomy or vincristine treatment but does not delay neuronal cell death following such insults [123]. This phenomenon is also observed in other axon disease models. For example, in the mouse model for progressive motor neuron (*pmn*) disease, crossing *Wld*^{S} mice with *pmn* mice protects neurites but not cell bodies against degeneration [126]. In contrast,, crossing *pmn* mice with

mice overexpressing Bcl-2, an anti-apoptotic protein, protects motorneuron cell bodies but not axonal degeneration [127]. These results suggest that Wallerian degeneration appears to occur through a different mechanism than apoptosis.

Wld^S mice also protect axons in other disease models such as myelin-related axonopathy [128], gracile axonal dystrophy [129], autoimmune encephalomyelitis [130], ischemia [131], Alzheimer's disease [132], and the toxin models of PD [62, 133]. In terms of the latter, Sajadi *et al.* have shown that unlike wild type mice, *Wld*^{S} preserves nigrostriatal projections but not SN cell bodies following 6-OHDA administration [133]. Similarly, Hasbani and O'Malley observed an even more pronounced preservation of terminal fields after MPTP treatment in *Wld*^{S} versus wild type animals [62]. Taken together, these data suggest that understanding the mechanisms underlying *Wld*^{S} axon protection may aid in the development of potential therapies for many neurodegenerative diseases, including PD.

The *Wld*^{S} gene encodes an in-frame fusion protein of the amino (N)-terminal 70 (N70) amino acids of ubiquination factor E4B (Ube4b), which is linked by a unique 18-amino acid region to the complete coding region of the nicotinamide adenine dinucleotide (NAD^+) synthesizing enzyme, nicotinamide adenylytransferase 1 (Nmnat1) [134] (Figure 1). The fusion protein is localized to the nucleus due to the nuclear localization signal present on the Nmnat1 portion of the protein [135]. Coleman and colleagues have shown that transgenic animals expressing this fusion protein recapitulate the *Wld*^{S} phenotype [136]. At present, the components of the *Wld*^{S} sequence that are required for axon

protection and which downstream factors are involved in this process remains controversial. Several mechanistic hypotheses have been proposed.

1.5.1 Ube4b

Because inhibiting UPS delays axonal degeneration [136], the Ube4b part of the *Wld*^{S} fusion protein may be responsible for its neuroprotective effect. However, the *Wld*^{S} fusion gene contains only the first 70 amino acids of Ube4b, not the 123 amino acid sequence essential for its ubiquination activity. Hence, gain of multi-ubiquitination function is unlikely as the *Wld*^{S} protein lacks the U-box motif. Dominant-negative inhibition of Ube4b is another possibility since expression of the yeast deubiquitinating enzyme UBP2 delays axonal degeneration in olfactory receptor neurons [137]. However, Ufd2, the yeast homologue of Ube4b, is a positive survival factor [138] and inhibition of UPS is linked to neurodegeneration rather than neuroprotection [139]. UPS has also been shown to be required for both developmental neuronal pruning and injury-induced axon degeneration, while *Wld*^{S} has no effect on neuronal pruning [137]. Moreover, overexpression of Ube4b does not protect differentiated Neuro2A cells against vincristine [140] or dorsal root ganglion cells (DRGs) against axotomy [141].

Although Ube4b activity may not be critical to *Wld*^{S} actions, the deletion of 16 amino acids (N16) of the Ube4b portion of *Wld*^{S} completely suppresses the axon protection afforded by *Wld*^{S} in mice [142] and greatly weakens the protection of axons in *Drosophila* [143]. Mechanistically, the N16 portion of the

fusion protein co-immunoprecipitates with valosin containing protein (VCP/p97) [144]. VCP is a AAA-ATPase with key roles in UPS and membrane fusion [145]. Consequently, although *Wld*^{S} lacks Ube4b's ligase activity, it maintains its ability to bind VCP which may target the fusion protein to areas critical for its activity.

1.5.2 Nmnat1

In contrast to Ube4b, in certain experimental paradigms the Nmnat1 portion of *Wld*^{S} is sufficient for axon protection *in vitro*, acting either through the silent information regulator (SIRT1) [146] or through local NAD^+ synthesis in neurites [147]. Consistent with Nmnat1's NAD^+ synthesizing capabilities, exogenous application of NAD^+ can protect DRGs against degeneration [141]. Not all studies have shown the same results, however, even in the same model system [148]. In support of a model requiring the complete *Wld*^{S} fusion protein, transgenic mice that only overexpress Nmnat1 show normal rates of Wallerian degeneration [148]. However, cytoplasmically [149] or axonally targeted Nmnat1 transgenic animals [150] are equally if not more effective at protecting at least peripheral model systems than *Wld*^{S}. Thus, cell type specific effects must exist with needing the complete *Wld*^{S} fusion gene to protect some axons but have Nmnat1 to be sufficient in other cases.

Disparity in results hold true in *Drosophila*, as well since Avery *et al.* [151], showed that Nmnat's enzymatic activity is required to protect axons following axotomy whereas Zhai *et al*., [152] found that Nmnat does not need its catalytic domain to protect axons. The latter study [152], as well as a new study

demonstrating that Nmnat also protects dendrites [153], both indicate that Nmnat exhibits a separate chaperone-like activity which protects axons and dendrites [152, 154]. These studies support the role of Nmnat in protecting against degeneration, but not though its traditional role in NAD^+ synthesis.

Two other isoforms of Nmnat exist, Nmnat2 and Nmnat3. Nmnat2 is highly expressed in the brain compared to Nmnat1 and 3 and is primarily localized in the Golgi complex [155]. Overexpression of Nmnat2 protects DRG and superior cervical ganglia (SCG) axons following axotomy [156] [157]. In either case, protection is dependent upon Nmnat2's NAD^+ synthesizing activity [156,157]. Similar results are true for Nmnat3, a mitochondrially localized isoform of Nmnat [158]. Nmnat3 is thought to promote axonal protection by mitigating the effects of ROS [159]. Based on these studies, it appears that the site of action plays a role in Nmnat's effectiveness in protecting against axonal degeneration [160].

Despite the data in Drosophila, in peripheral vertebrate model systems it appears that the NAD^+ enzymatic activity of *Wld*^{S} is required since mutating key amino acids abolishes the neuroprotection [135-136]. Collectively, these studies suggest that the fusion protein has acquired a gain of function not normally present in the neuron and that the entire fusion gene is necessary for protection.

1.5.3 Axonal structure and function

Other studies have attempted to determine how the *Wld*^{S} protein protects through a more localized analysis of its effects on the axon. Suzuki *et al.* found that microtubule acetylation, a post-translational modification associated with

microtubule stability, is enhanced in cultured cerebellar granule cells in *Wld*^{S} mice [161]. In other studies, activation of SIRT2, a NAD^+-dependent tubulin deacetylase, abolishes *Wld*^{S} resistance to axonal degeneration by colchicine [162]. Specific to PD, inhibition of SIRT2 using small interfering RNA rescued cells from α-synuclein mediated toxicity [163]. These data suggest that the neuroprotective effect of *Wld*^{S} may be mediated by its effect on microtubule stabilization.

Consistent with a role in stabilizing microtubule tracks, a microarray study using *Wld*^{S} mice crossed with *pmn* mice reported that 56 genes were differentially expressed between *pmn* and *pmn* x *Wld*^{S} mice [164]. None of the canonical "apoptosis" genes were altered, rather a large proportion of the genes that were upregulated were related to retrograde and anterograde transport (e.g. dynactin and kinesin) [164]. These studies suggest that *Wld*^{S} protects axons by maintaining proper axonal transport after injury.

1.5.4 Mitochondrial function

Mitochondrial dysfunction appears to be an early event in the degeneration of neurites [165]. For example, treatment of SCG neurons with the microtubule-disrupting agent, vinblastine, decreases $\Delta\Psi_m$ and induces neurite degeneration. In contrast, *Wld*^{S} mice maintain their $\Delta\Psi_m$ and have intact neurites leading to the proposal that preservation of $\Delta\Psi_m$ may mediate the axonal protection seen with *Wld*^{S} [166]. Recently, Barrientos *et al.* reported that *Wld*^{S} is able to regulate the mitochondrial permeability transition pore and prevent

calcium release, ATP loss, oxidative stress and release of proteins involved in axonal degeneration [167]. Although *Wld*^{S} is primarily in the nucleus, it appears to associate with mitochondria, albeit in lower levels than seen in the nucleus [162]. In addition, differential proteomics analysis comparing WT and *Wld*^{S} striatal synaptosomes identified 16 protein that were differentially expressed, 8 of which are mitochondrially-associated proteins [132]. Finally, Shen *et al.* has shown that *Wld*^{S} preserves mitochondrial trafficking in isolated cortical axons during chemical ischemia [168]. Taken together, *Wld*^{S} may protect axons by preserving or enhancing mitochondrial function.

Collectively, the current body of literature suggest that *Wld*^{S} may protect axons by (1) preventing a decline in energy, (2) preventing degradation of axonal structure, (3) preventing the impairment of key motor proteins involved in axonal transport, and/or (4) by priming mitochondria to have a more robust response to degeneration-inducing stimuli.

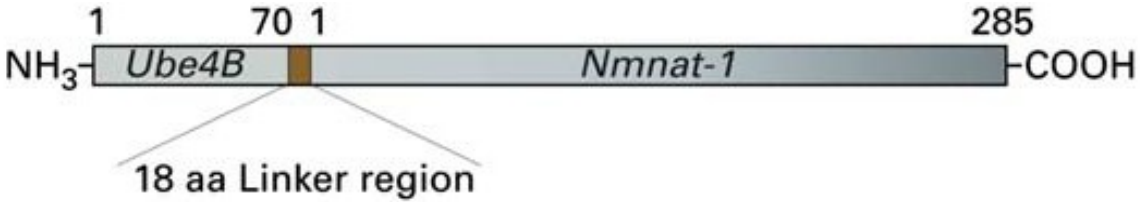

Fig 1.1 - Mouse *Wld*^{S} fusion protein structure (GenBank accession number AAG17285). Amino acid residue numbers relative to Ube4b and Nmnat1 are shown. From Fainzilber (2006) [3].

1.6 Goals of the current study

Observations from work done by our lab [62] and others [5, 169] have suggested that, in PD, DA neurons degenerate through a "dying back" axonopathy wherein degeneration begins in the distal axon and progresses over time towards the cell body. Therefore, processes that delay axonal degeneration might slow PD progression. Previous work in our lab has demonstrated that *Wld*^{S} mice protect DA terminal fields in the striatum from MPTP injury [62]. At present, the mechanisms underlying *Wld*^{S}-mediated axonal protection are unclear. Some studies have attributed *Wld*^{S} neuroprotection to the Nmnat1 portion of the protein while others have observed upregulation in genes involved in axonal structure and transport in *Wld*^{S} mice compared to controls. More recently, *Wld*^{S}, action on the mitochondria has been suggested to be important component of its neuroprotective effect. It is unknown at this time which, if any, of these mechanisms underlies *Wld*^{S} protection of DA axons. Consequently, the overall goals of this work are to 1) test the hypothesis that the entire *Wld*^{S} fusion protein is required for axonal protection from parkinsonian mimetics in DA neurons, and 2) to test the hypothesis that *Wld*^{S} protects DA axons by directly affecting axonal mitochondria such that they are not impaired following toxin treatment.

With these goals in mind, we discuss which portion of the *Wld*^{S} gene protects DA neurites from MPP^+ and 6-OHDA toxicity in Chapters 2 and 3, respectively. In addition, we test the neuroprotective effects of other isoforms of Nmnat in DA neurons as well as whether exogenous addition of NAD^+ and NAD^+

precursors are sufficient to protect DA neurons against MPP^+ and 6-OHDA in a similar manner to *Wld*^{S} neurons.

To study the effects of *Wld*^{S} specifically on DA axonal structure and function, we describe a novel system to segregate DA axons from the cell bodies in Chapter 4. Using this unique compartmented chamber, we test the hypothesis that impaired axonal transport plays a role in MPP^+-induced axonal degeneration. Finally, we evaluate whether *Wld*^{S} is able to prevent the changes in mitochondrial motility and velocity observed in wild type DA axons after MPP^+ treatment in Chapter 5.

References:

1. Dauer, W. and S. Przedborski, *Parkinson's disease: mechanisms and models.* Neuron, 2003. **39**(6): p. 889-909.
2. Blum, D., et al., *Molecular pathways involved in the neurotoxicity of 6-OHDA, dopamine and MPTP: contribution to the apoptotic theory in Parkinson's disease.* Prog Neurobiol, 2001. **65**(2): p. 135-72.
3. Fainzilber, M. and J.L. Twiss, *Tracking in the Wlds--the hunting of the SIRT and the luring of the Draper.* Neuron, 2006. **50**(6): p. 819-21.
4. Spillantini, M.G., et al., *Alpha-synuclein in Lewy bodies.* Nature, 1997. **388**(6645): p. 839-40.
5. Braak, H., et al., *Stages in the development of Parkinson's disease-related pathology.* Cell Tissue Res, 2004. **318**(1): p. 121-34.
6. Bernheimer, H., et al., *Brain dopamine and the syndromes of Parkinson and Huntington. Clinical, morphological and neurochemical correlations.* J Neurol Sci, 1973. **20**(4): p. 415-55.
7. Burke, R.E., *Intracellular signalling pathways in dopamine cell death and axonal degeneration.* Prog Brain Res, 2010. **183**: p. 79-97.
8. Greenfield, J.G. and F.D. Bosanquet, *The brain-stem lesions in Parkinsonism.* J Neurol Neurosurg Psychiatry, 1953. **16**(4): p. 213-26.
9. Scatton, B., et al., *Degeneration of noradrenergic and serotonergic but not dopaminergic neurones in the lumbar spinal cord of parkinsonian patients.* Brain Res, 1986. **380**(1): p. 181-5.
10. Candy, J.M., et al., *Pathological changes in the nucleus of Meynert in Alzheimer's and Parkinson's diseases.* J Neurol Sci, 1983. **59**(2): p. 277-89.
11. Aarsland, D., et al., *Frequency of dementia in Parkinson disease.* Arch Neurol, 1996. **53**(6): p. 538-42.
12. Olanow, C.W., et al., *Levodopa in the treatment of Parkinson's disease: current controversies.* Mov Disord, 2004. **19**(9): p. 997-1005.
13. Bekris, L.M., I.F. Mata, and C.P. Zabetian, *The genetics of Parkinson disease.* J Geriatr Psychiatry Neurol, 2010. **23**(4): p. 228-42.
14. Polymeropoulos, M.H., et al., *Mapping of a gene for Parkinson's disease to chromosome 4q21-q23.* Science, 1996. **274**(5290): p. 1197-9.
15. Polymeropoulos, M.H., et al., *Mutation in the alpha-synuclein gene identified in families with Parkinson's disease.* Science, 1997. **276**(5321): p. 2045-7.
16. Kruger, R., et al., *Ala30Pro mutation in the gene encoding alpha-synuclein in Parkinson's disease.* Nat Genet, 1998. **18**(2): p. 106-8.
17. Zarranz, J.J., et al., *The new mutation, E46K, of alpha-synuclein causes Parkinson and Lewy body dementia.* Ann Neurol, 2004. **55**(2): p. 164-73.
18. Singleton, A.B., et al., *alpha-Synuclein locus triplication causes Parkinson's disease.* Science, 2003. **302**(5646): p. 841.
19. Abeliovich, A., et al., *Mice lacking alpha-synuclein display functional deficits in the nigrostriatal dopamine system.* Neuron, 2000. **25**(1): p. 239-52.

20. Yavich, L., et al., *Role of alpha-synuclein in presynaptic dopamine recruitment.* J Neurosci, 2004. **24**(49): p. 11165-70.
21. Yavich, L., P. Jakala, and H. Tanila, *Abnormal compartmentalization of norepinephrine in mouse dentate gyrus in alpha-synuclein knockout and A30P transgenic mice.* J Neurochem, 2006. **99**(3): p. 724-32.
22. Lee, H.J., et al., *Human alpha-synuclein modulates vesicle trafficking through its interaction with prenylated Rab acceptor protein 1.* Biochem Biophys Res Commun, 2011.
23. Zimprich, A., et al., *Mutations in LRRK2 cause autosomal-dominant parkinsonism with pleomorphic pathology.* Neuron, 2004. **44**(4): p. 601-7.
24. Paisan-Ruiz, C., et al., *Cloning of the gene containing mutations that cause PARK8-linked Parkinson's disease.* Neuron, 2004. **44**(4): p. 595-600.
25. Hardy, J., et al., *Genetics of Parkinson's disease and parkinsonism.* Ann Neurol, 2006. **60**(4): p. 389-98.
26. Biskup, S., et al., *Localization of LRRK2 to membranous and vesicular structures in mammalian brain.* Ann Neurol, 2006. **60**(5): p. 557-69.
27. Higashi, S., et al., *Localization of Parkinson's disease-associated LRRK2 in normal and pathological human brain.* Brain Res, 2007. **1155**: p. 208-19.
28. Higashi, S., et al., *Expression and localization of Parkinson's disease-associated leucine-rich repeat kinase 2 in the mouse brain.* J Neurochem, 2007. **100**(2): p. 368-81.
29. Galter, D., et al., *LRRK2 expression linked to dopamine-innervated areas.* Ann Neurol, 2006. **59**(4): p. 714-9.
30. Taymans, J.M., C. Van den Haute, and V. Baekelandt, *Distribution of PINK1 and LRRK2 in rat and mouse brain.* J Neurochem, 2006. **98**(3): p. 951-61.
31. Simon-Sanchez, J., et al., *LRRK2 is expressed in areas affected by Parkinson's disease in the adult mouse brain.* Eur J Neurosci, 2006. **23**(3): p. 659-66.
32. Sakaguchi-Nakashima, A., et al., *LRK-1, a C. elegans PARK8-related kinase, regulates axonal-dendritic polarity of SV proteins.* Curr Biol, 2007. **17**(7): p. 592-8.
33. Hatano, T., et al., *Leucine-rich repeat kinase 2 associates with lipid rafts.* Hum Mol Genet, 2007. **16**(6): p. 678-90.
34. Zhu, X., et al., *LRRK2 protein is a component of Lewy bodies.* Ann Neurol, 2006. **60**(5): p. 617-8; author reply 618-9.
35. MacLeod, D., et al., *The familial Parkinsonism gene LRRK2 regulates neurite process morphology.* Neuron, 2006. **52**(4): p. 587-93.
36. West, A.B., et al., *Parkinson's disease-associated mutations in leucine-rich repeat kinase 2 augment kinase activity.* Proc Natl Acad Sci U S A, 2005. **102**(46): p. 16842-7.
37. Gloeckner, C.J., et al., *The Parkinson disease causing LRRK2 mutation I2020T is associated with increased kinase activity.* Hum Mol Genet, 2006. **15**(2): p. 223-32.

38. Greggio, E., et al., *Kinase activity is required for the toxic effects of mutant LRRK2/dardarin.* Neurobiol Dis, 2006. **23**(2): p. 329-41.
39. Smith, W.W., et al., *Kinase activity of mutant LRRK2 mediates neuronal toxicity.* Nat Neurosci, 2006. **9**(10): p. 1231-3.
40. West, A.B., et al., *Parkinson's disease-associated mutations in LRRK2 link enhanced GTP-binding and kinase activities to neuronal toxicity.* Hum Mol Genet, 2007. **16**(2): p. 223-32.
41. Kitada, T., et al., *Mutations in the parkin gene cause autosomal recessive juvenile parkinsonism.* Nature, 1998. **392**(6676): p. 605-8.
42. Imai, Y., M. Soda, and R. Takahashi, *Parkin suppresses unfolded protein stress-induced cell death through its E3 ubiquitin-protein ligase activity.* J Biol Chem, 2000. **275**(46): p. 35661-4.
43. Shimura, H., et al., *Familial Parkinson disease gene product, parkin, is a ubiquitin-protein ligase.* Nat Genet, 2000. **25**(3): p. 302-5.
44. Zhang, Y., et al., *Parkin functions as an E2-dependent ubiquitin- protein ligase and promotes the degradation of the synaptic vesicle-associated protein, CDCrel-1.* Proc Natl Acad Sci U S A, 2000. **97**(24): p. 13354-9.
45. Feany, M.B. and L.J. Pallanck, *Parkin: a multipurpose neuroprotective agent?* Neuron, 2003. **38**(1): p. 13-6.
46. LaVoie, M.J., et al., *Dopamine covalently modifies and functionally inactivates parkin.* Nat Med, 2005. **11**(11): p. 1214-21.
47. Chung, K.K., et al., *S-nitrosylation of parkin regulates ubiquitination and compromises parkin's protective function.* Science, 2004. **304**(5675): p. 1328-31.
48. Narendra, D., et al., *Parkin-induced mitophagy in the pathogenesis of Parkinson disease.* Autophagy, 2009. **5**(5): p. 706-8.
49. Valente, E.M., et al., *Hereditary early-onset Parkinson's disease caused by mutations in PINK1.* Science, 2004. **304**(5674): p. 1158-60.
50. Valente, E.M., et al., *PINK1 mutations are associated with sporadic early-onset parkinsonism.* Ann Neurol, 2004. **56**(3): p. 336-41.
51. Petit, A., et al., *Wild-type PINK1 prevents basal and induced neuronal apoptosis, a protective effect abrogated by Parkinson disease-related mutations.* J Biol Chem, 2005. **280**(40): p. 34025-32.
52. Silvestri, L., et al., *Mitochondrial import and enzymatic activity of PINK1 mutants associated to recessive parkinsonism.* Hum Mol Genet, 2005. **14**(22): p. 3477-92.
53. Scheele, C., et al., *The human PINK1 locus is regulated in vivo by a non-coding natural antisense RNA during modulation of mitochondrial function.* BMC Genomics, 2007. **8**: p. 74.
54. Yang, Y., et al., *Mitochondrial pathology and muscle and dopaminergic neuron degeneration caused by inactivation of Drosophila Pink1 is rescued by Parkin.* Proc Natl Acad Sci U S A, 2006. **103**(28): p. 10793-8.
55. Clark, I.E., et al., *Drosophila pink1 is required for mitochondrial function and interacts genetically with parkin.* Nature, 2006. **441**(7097): p. 1162-6.
56. Park, J., et al., *Mitochondrial dysfunction in Drosophila PINK1 mutants is complemented by parkin.* Nature, 2006. **441**(7097): p. 1157-61.

57. Narendra, D.P. and R.J. Youle, *Targeting mitochondrial dysfunction: role for PINK1 and Parkin in mitochondrial quality control.* Antioxid Redox Signal, 2011. **14**(10): p. 1929-38.
58. Davis, G.C., et al., *Chronic Parkinsonism secondary to intravenous injection of meperidine analogues.* Psychiatry Res, 1979. **1**(3): p. 249-54.
59. Langston, J.W., et al., *Chronic Parkinsonism in humans due to a product of meperidine-analog synthesis.* Science, 1983. **219**(4587): p. 979-80.
60. Kopin, I.J. and D.G. Schoenberg, *MPTP in animal models of Parkinson's disease.* Mt Sinai J Med, 1988. **55**(1): p. 43-9.
61. Fuller, R.W. and S.K. Hemrick-Luecke, *Effects of amfonelic acid, alpha-methyltyrosine, Ro 4-1284 and haloperidol pretreatment on the depletion of striatal dopamine by 1-methyl-4-phenyl-1,2,3,6-tetrahydropyridine in mice.* Res Commun Chem Pathol Pharmacol, 1985. **48**(1): p. 17-25.
62. Hasbani, D.M. and K.L. O'Malley, *Wld(S) mice are protected against the Parkinsonian mimetic MPTP.* Exp Neurol, 2006. **202**(1): p. 93-9.
63. Forno, L.S., et al., *Locus ceruleus lesions and eosinophilic inclusions in MPTP-treated monkeys.* Ann Neurol, 1986. **20**(4): p. 449-55.
64. Forno, L.S., et al., *Similarities and differences between MPTP-induced parkinsonsim and Parkinson's disease. Neuropathologic considerations.* Adv Neurol, 1993. **60**: p. 600-8.
65. Wu, D.C., et al., *Blockade of microglial activation is neuroprotective in the 1-methyl-4-phenyl-1,2,3,6-tetrahydropyridine mouse model of Parkinson disease.* J Neurosci, 2002. **22**(5): p. 1763-71.
66. Markey, S.P., et al., *Intraneuronal generation of a pyridinium metabolite may cause drug-induced parkinsonism.* Nature, 1984. **311**(5985): p. 464-7.
67. Staal, R.G. and P.K. Sonsalla, *Inhibition of brain vesicular monoamine transporter (VMAT2) enhances 1-methyl-4-phenylpyridinium neurotoxicity in vivo in rat striata.* J Pharmacol Exp Ther, 2000. **293**(2): p. 336-42.
68. Ramsay, R.R. and T.P. Singer, *Energy-dependent uptake of N-methyl-4-phenylpyridinium, the neurotoxic metabolite of 1-methyl-4-phenyl-1,2,3,6-tetrahydropyridine, by mitochondria.* J Biol Chem, 1986. **261**(17): p. 7585-7.
69. Curtius, H.C., et al., *Mass fragmentography of dopamine and 6-hydroxydopamine. Application to the determination of dopamine in human brain biopsies from the caudate nucleus.* J Chromatogr, 1974. **99**(0): p. 529-40.
70. Ungerstedt, U., *6-Hydroxy-dopamine induced degeneration of central monoamine neurons.* Eur J Pharmacol, 1968. **5**(1): p. 107-10.
71. Kirik, D., B. Georgievska, and A. Bjorklund, *Localized striatal delivery of GDNF as a treatment for Parkinson disease.* Nat Neurosci, 2004. **7**(2): p. 105-10.
72. Luthman, J., et al., *Selective lesion of central dopamine or noradrenaline neuron systems in the neonatal rat: motor behavior and monoamine alterations at adult stage.* Behav Brain Res, 1989. **33**(3): p. 267-77.

73. Monteiro, H.P. and C.C. Winterbourn, *6-Hydroxydopamine releases iron from ferritin and promotes ferritin-dependent lipid peroxidation.* Biochem Pharmacol, 1989. **38**(23): p. 4177-82.
74. Breese, G.R. and T.D. Traylor, *Effect of 6-hydroxydopamine on brain norepinephrine and dopamine evidence for selective degeneration of catecholamine neurons.* J Pharmacol Exp Ther, 1970. **174**(3): p. 413-20.
75. Clement, M.V., et al., *The cytotoxicity of dopamine may be an artefact of cell culture.* J Neurochem, 2002. **81**(3): p. 414-21.
76. Glinka, Y.Y. and M.B. Youdim, *Inhibition of mitochondrial complexes I and IV by 6-hydroxydopamine.* Eur J Pharmacol, 1995. **292**(3-4): p. 329-32.
77. Storch, A., et al., *6-Hydroxydopamine toxicity towards human SH-SY5Y dopaminergic neuroblastoma cells: independent of mitochondrial energy metabolism.* J Neural Transm, 2000. **107**(3): p. 281-93.
78. Lotharius, J., L.L. Dugan, and K.L. O'Malley, *Distinct mechanisms underlie neurotoxin-mediated cell death in cultured dopaminergic neurons.* J Neurosci, 1999. **19**(4): p. 1284-93.
79. Bernstein, A.I., et al., *6-OHDA generated ROS induces DNA damage and p53- and PUMA-dependent cell death.* Mol Neurodegener, 2011. **6**(1): p. 2.
80. Holtz, W.A. and K.L. O'Malley, *Parkinsonian mimetics induce aspects of unfolded protein response in death of dopaminergic neurons.* J Biol Chem, 2003. **278**(21): p. 19367-77.
81. Orimo, S., et al., *Axonal alpha-synuclein aggregates herald centripetal degeneration of cardiac sympathetic nerve in Parkinson's disease.* Brain, 2008. **131**(Pt 3): p. 642-50.
82. Lach, B., et al., *Caudate nucleus pathology in Parkinson's disease: ultrastructural and biochemical findings in biopsy material.* Acta Neuropathol, 1992. **83**(4): p. 352-60.
83. Riederer, P. and S. Wuketich, *Time course of nigrostriatal degeneration in parkinson's disease. A detailed study of influential factors in human brain amine analysis.* J Neural Transm, 1976. **38**(3-4): p. 277-301.
84. Fearnley, J.M. and A.J. Lees, *Ageing and Parkinson's disease: substantia nigra regional selectivity.* Brain, 1991. **114 (Pt 5)**: p. 2283-301.
85. Ma, S.Y., et al., *Correlation between neuromorphometry in the substantia nigra and clinical features in Parkinson's disease using disector counts.* J Neurol Sci, 1997. **151**(1): p. 83-7.
86. Greffard, S., et al., *Motor score of the Unified Parkinson Disease Rating Scale as a good predictor of Lewy body-associated neuronal loss in the substantia nigra.* Arch Neurol, 2006. **63**(4): p. 584-8.
87. Nandhagopal, R., M.J. McKeown, and A.J. Stoessl, *Functional imaging in Parkinson disease.* Neurology, 2008. **70**(16 Pt 2): p. 1478-88.
88. Morrish, P.K., G.V. Sawle, and D.J. Brooks, *Clinical and [18F] dopa PET findings in early Parkinson's disease.* J Neurol Neurosurg Psychiatry, 1995. **59**(6): p. 597-600.

89. Morrish, P.K., et al., *Measuring the rate of progression and estimating the preclinical period of Parkinson's disease with [18F]dopa PET.* J Neurol Neurosurg Psychiatry, 1998. **64**(3): p. 314-9.
90. Lee, C.S., et al., *In vivo positron emission tomographic evidence for compensatory changes in presynaptic dopaminergic nerve terminals in Parkinson's disease.* Ann Neurol, 2000. **47**(4): p. 493-503.
91. Hilker, R., et al., *Nonlinear progression of Parkinson disease as determined by serial positron emission tomographic imaging of striatal fluorodopa F 18 activity.* Arch Neurol, 2005. **62**(3): p. 378-82.
92. Tissingh, G., et al., *Drug-naive patients with Parkinson's disease in Hoehn and Yahr stages I and II show a bilateral decrease in striatal dopamine transporters as revealed by [123I]beta-CIT SPECT.* J Neurol, 1998. **245**(1): p. 14-20.
93. Schwartz, M., et al., *Dopamine-transporter imaging and visuo-motor testing in essential tremor, practical possibilities for detection of early stage Parkinson's disease.* Parkinsonism Relat Disord, 2004. **10**(6): p. 385-9.
94. Gwinn-Hardy, K., et al., *Distinctive neuropathology revealed by alpha-synuclein antibodies in hereditary parkinsonism and dementia linked to chromosome 4p.* Acta Neuropathol, 2000. **99**(6): p. 663-72.
95. van der Putten, H., et al., *Neuropathology in mice expressing human alpha-synuclein.* J Neurosci, 2000. **20**(16): p. 6021-9.
96. Kirik, D., et al., *Nigrostriatal alpha-synucleinopathy induced by viral vector-mediated overexpression of human alpha-synuclein: a new primate model of Parkinson's disease.* Proc Natl Acad Sci U S A, 2003. **100**(5): p. 2884-9.
97. Duda, J.E., Giasson, B. I., Lee, V. M.-Y. and Trojanowski, J. Q. , *Is the Initial Insult in Parkinson's Disease and Dementia with Lewy Bodies a Neuritic Dystrophy?* Annals of the New York Academy of Sciences, 2003. **991**: p. 295-297.
98. Duda, J.E., et al., *Concurrence of alpha-synuclein and tau brain pathology in the Contursi kindred.* Acta Neuropathol, 2002. **104**(1): p. 7-11.
99. Lee, H.J., et al., *Impairment of microtubule-dependent trafficking by overexpression of alpha-synuclein.* Eur J Neurosci, 2006. **24**(11): p. 3153-62.
100. Saha, A.R., et al., *Parkinson's disease alpha-synuclein mutations exhibit defective axonal transport in cultured neurons.* J Cell Sci, 2004. **117**(Pt 7): p. 1017-24.
101. Utton, M.A., et al., *Molecular motors implicated in the axonal transport of tau and alpha-synuclein.* J Cell Sci, 2005. **118**(Pt 20): p. 4645-54.
102. Li, Y., et al., *Mutant LRRK2(R1441G) BAC transgenic mice recapitulate cardinal features of Parkinson's disease.* Nat Neurosci, 2009. **12**(7): p. 826-8.
103. Plowey, E.D., et al., *Role of autophagy in G2019S-LRRK2-associated neurite shortening in differentiated SH-SY5Y cells.* J Neurochem, 2008. **105**(3): p. 1048-56.

104. Parisiadou, L., et al., *Phosphorylation of ezrin/radixin/moesin proteins by LRRK2 promotes the rearrangement of actin cytoskeleton in neuronal morphogenesis.* J Neurosci, 2009. **29**(44): p. 13971-80.
105. Ren, Y., et al., *Parkin protects dopaminergic neurons against microtubule-depolymerizing toxins by attenuating microtubule-associated protein kinase activation.* J Biol Chem, 2009. **284**(6): p. 4009-17.
106. Weihofen, A., et al., *Pink1 forms a multiprotein complex with Miro and Milton, linking Pink1 function to mitochondrial trafficking.* Biochemistry, 2009. **48**(9): p. 2045-52.
107. Herkenham, M., et al., *Selective retention of MPP+ within the monoaminergic systems of the primate brain following MPTP administration: an in vivo autoradiographic study.* Neuroscience, 1991. **40**(1): p. 133-58.
108. Pifl, C., G. Schingnitz, and O. Hornykiewicz, *Effect of 1-methyl-4-phenyl-1,2,3,6-tetrahydropyridine on the regional distribution of brain monoamines in the rhesus monkey.* Neuroscience, 1991. **44**(3): p. 591-605.
109. Cappelletti, G., et al., *Microtubule assembly is directly affected by MPP(+)in vitro.* Cell Biol Int, 2001. **25**(10): p. 981-4.
110. Cappelletti, G., T. Surrey, and R. Maci, *The parkinsonism producing neurotoxin MPP+ affects microtubule dynamics by acting as a destabilising factor.* FEBS Lett, 2005. **579**(21): p. 4781-6.
111. Cai, Z.L., et al., *MPP+ impairs autophagic clearance of alpha-synuclein by impairing the activity of dynein.* Neuroreport, 2009. **20**(6): p. 569-73.
112. Morfini, G., et al., *1-Methyl-4-phenylpyridinium affects fast axonal transport by activation of caspase and protein kinase C.* Proc Natl Acad Sci U S A, 2007. **104**(7): p. 2442-7.
113. Cartelli, D., et al., *Microtubule dysfunction precedes transport impairment and mitochondria damage in MPP+ -induced neurodegeneration.* J Neurochem, 2010. **115**(1): p. 247-58.
114. Davison, A.J., N.A. Legault, and D.W. Steele, *Effect of 6-hydroxydopamine on polymerization of tubulin. Protection by superoxide dismutase, catalase, or anaerobic conditions.* Biochem Pharmacol, 1986. **35**(9): p. 1411-7.
115. Choi, W.S., R.D. Palmiter, and Z. Xia, *Loss of mitochondrial complex I activity potentiates dopamine neuron death induced by microtubule dysfunction in a Parkinson's disease model.* J Cell Biol, 2011. **192**(5): p. 873-82.
116. Borland, M.K., et al., *Chronic, low-dose rotenone reproduces Lewy neurites found in early stages of Parkinson's disease, reduces mitochondrial movement and slowly kills differentiated SH-SY5Y neural cells.* Mol Neurodegener, 2008. **3**: p. 21.
117. Liang, Y., et al., *Intrastriatal injection of colchicine induces striatonigral degeneration in mice.* J Neurochem, 2008. **106**(4): p. 1815-27.
118. Raff, M.C., A.V. Whitmore, and J.T. Finn, *Axonal self-destruction and neurodegeneration.* Science, 2002. **296**(5569): p. 868-71.

119. Campenot, R.B., *Development of sympathetic neurons in compartmentalized cultures. II. Local control of neurite survival by nerve growth factor.* Dev Biol, 1982. **93**(1): p. 13-21.
120. Campenot, R.B., *NGF and the local control of nerve terminal growth.* J Neurobiol, 1994. **25**(6): p. 599-611.
121. Finn, J.T., et al., *Evidence that Wallerian degeneration and localized axon degeneration induced by local neurotrophin deprivation do not involve caspases.* J Neurosci, 2000. **20**(4): p. 1333-41.
122. Ries, V., et al., *JNK2 and JNK3 combined are essential for apoptosis in dopamine neurons of the substantia nigra, but are not required for axon degeneration.* J Neurochem, 2008. **107**(6): p. 1578-88.
123. Coleman, M., *Axon degeneration mechanisms: commonality amid diversity.* Nat Rev Neurosci, 2005. **6**(11): p. 889-98.
124. Deckwerth, T.L. and E.M. Johnson, Jr., *Neurites can remain viable after destruction of the neuronal soma by programmed cell death (apoptosis).* Dev Biol, 1994. **165**(1): p. 63-72.
125. Saxena, S. and P. Caroni, *Mechanisms of axon degeneration: from development to disease.* Prog Neurobiol, 2007. **83**(3): p. 174-91.
126. Ferri, A., et al., *Inhibiting axon degeneration and synapse loss attenuates apoptosis and disease progression in a mouse model of motoneuron disease.* Curr Biol, 2003. **13**(8): p. 669-73.
127. Sagot, Y., et al., *Bcl-2 overexpression prevents motoneuron cell body loss but not axonal degeneration in a mouse model of a neurodegenerative disease.* J Neurosci, 1995. **15**(11): p. 7727-33.
128. Samsam, M., et al., *The Wlds mutation delays robust loss of motor and sensory axons in a genetic model for myelin-related axonopathy.* J Neurosci, 2003. **23**(7): p. 2833-9.
129. Mi, W., et al., *The slow Wallerian degeneration gene, WldS, inhibits axonal spheroid pathology in gracile axonal dystrophy mice.* Brain, 2005. **128**(Pt 2): p. 405-16.
130. Chitnis, T., et al., *Elevated neuronal expression of CD200 protects Wlds mice from inflammation-mediated neurodegeneration.* Am J Pathol, 2007. **170**(5): p. 1695-712.
131. Gillingwater, T.H., et al., *Neuroprotection after transient global cerebral ischemia in Wld(s) mutant mice.* J Cereb Blood Flow Metab, 2004. **24**(1): p. 62-6.
132. Wishart, T.M., et al., *Differential proteomics analysis of synaptic proteins identifies potential cellular targets and protein mediators of synaptic neuroprotection conferred by the slow Wallerian degeneration (Wlds) gene.* Mol Cell Proteomics, 2007. **6**(8): p. 1318-30.
133. Sajadi, A., B.L. Schneider, and P. Aebischer, *Wlds-mediated protection of dopaminergic fibers in an animal model of Parkinson disease.* Curr Biol, 2004. **14**(4): p. 326-30.
134. Coleman, M.P., et al., *An 85-kb tandem triplication in the slow Wallerian degeneration (Wlds) mouse.* Proc Natl Acad Sci U S A, 1998. **95**(17): p. 9985-90.

135. Fang, C., et al., *The cellular distribution of the Wld s chimeric protein and its constituent proteins in the CNS.* Neuroscience, 2005. **135**(4): p. 1107-18.
136. Mack, T.G., et al., *Wallerian degeneration of injured axons and synapses is delayed by a Ube4b/Nmnat chimeric gene.* Nat Neurosci, 2001. **4**(12): p. 1199-206.
137. Hoopfer, E.D., et al., *Wlds protection distinguishes axon degeneration following injury from naturally occurring developmental pruning.* Neuron, 2006. **50**(6): p. 883-95.
138. Koegl, M., et al., *A novel ubiquitination factor, E4, is involved in multiubiquitin chain assembly.* Cell, 1999. **96**(5): p. 635-44.
139. Lam, Y.A., et al., *Inhibition of the ubiquitin-proteasome system in Alzheimer's disease.* Proc Natl Acad Sci U S A, 2000. **97**(18): p. 9902-6.
140. Watanabe, M., T. Tsukiyama, and S. Hatakeyama, *Protection of vincristine-induced neuropathy by WldS expression and the independence of the activity of Nmnat1.* Neurosci Lett, 2007. **411**(3): p. 228-32.
141. Sasaki, Y., T. Araki, and J. Milbrandt, *Stimulation of nicotinamide adenine dinucleotide biosynthetic pathways delays axonal degeneration after axotomy.* J Neurosci, 2006. **26**(33): p. 8484-91.
142. Conforti, L., et al., *Wld S protein requires Nmnat activity and a short N-terminal sequence to protect axons in mice.* J Cell Biol, 2009. **184**(4): p. 491-500.
143. Hatakeyama, S., et al., *U box proteins as a new family of ubiquitin-protein ligases.* J Biol Chem, 2001. **276**(35): p. 33111-20.
144. Laser, H., et al., *The slow Wallerian degeneration protein, WldS, binds directly to VCP/p97 and partially redistributes it within the nucleus.* Mol Biol Cell, 2006. **17**(3): p. 1075-84.
145. Wang, Q., C. Song, and C.C. Li, *Molecular perspectives on p97-VCP: progress in understanding its structure and diverse biological functions.* J Struct Biol, 2004. **146**(1-2): p. 44-57.
146. Araki, T., Y. Sasaki, and J. Milbrandt, *Increased nuclear NAD biosynthesis and SIRT1 activation prevent axonal degeneration.* Science, 2004. **305**(5686): p. 1010-3.
147. Wang, J., et al., *A local mechanism mediates NAD-dependent protection of axon degeneration.* J Cell Biol, 2005. **170**(3): p. 349-55.
148. Conforti, L., et al., *NAD(+) and axon degeneration revisited: Nmnat1 cannot substitute for Wld(S) to delay Wallerian degeneration.* Cell Death Differ, 2007. **14**(1): p. 116-27.
149. Sasaki, Y., et al., *Transgenic mice expressing the Nmnat1 protein manifest robust delay in axonal degeneration in vivo.* J Neurosci, 2009. **29**(20): p. 6526-34.
150. Babetto, E., et al., *Targeting NMNAT1 to axons and synapses transforms its neuroprotective potency in vivo.* J Neurosci, 2010. **30**(40): p. 13291-304.

151. Avery, M.A., et al., *Wld S requires Nmnat1 enzymatic activity and N16-VCP interactions to suppress Wallerian degeneration.* J Cell Biol, 2009. **184**(4): p. 501-13.
152. Zhai, R.G., et al., *NAD synthase NMNAT acts as a chaperone to protect against neurodegeneration.* Nature, 2008. **452**(7189): p. 887-91.
153. Wen, Y., et al., *Nmnat exerts neuroprotective effects in dendrites and axons.* Mol Cell Neurosci, 2011.
154. Zhai, R.G., et al., *Drosophila NMNAT maintains neural integrity independent of its NAD synthesis activity.* PLoS Biol, 2006. **4**(12): p. e416.
155. Mayer, P.R., et al., *Expression, localization, and biochemical characterization of nicotinamide mononucleotide adenylyltransferase 2.* J Biol Chem, 2010. **285**(51): p. 40387-96.
156. Gilley, J. and M.P. Coleman, *Endogenous Nmnat2 is an essential survival factor for maintenance of healthy axons.* PLoS Biol, 2010. **8**(1): p. e1000300.
157. Yan, T., et al., *Nmnat2 delays axon degeneration in superior cervical ganglia dependent on its NAD synthesis activity.* Neurochem Int, 2010. **56**(1): p. 101-6.
158. Yahata, N., S. Yuasa, and T. Araki, *Nicotinamide mononucleotide adenylyltransferase expression in mitochondrial matrix delays Wallerian degeneration.* J Neurosci, 2009. **29**(19): p. 6276-84.
159. Press, C. and J. Milbrandt, *Nmnat delays axonal degeneration caused by mitochondrial and oxidative stress.* J Neurosci, 2008. **28**(19): p. 4861-71.
160. Coleman, M.P. and M.R. Freeman, *Wallerian degeneration, wld(s), and nmnat.* Annu Rev Neurosci, 2010. **33**: p. 245-67.
161. Suzuki, K. and T. Koike, *Mammalian Sir2-related protein (SIRT) 2-mediated modulation of resistance to axonal degeneration in slow Wallerian degeneration mice: a crucial role of tubulin deacetylation.* Neuroscience, 2007. **147**(3): p. 599-612.
162. Suzuki, K. and T. Koike, *Resveratrol abolishes resistance to axonal degeneration in slow Wallerian degeneration (WldS) mice: activation of SIRT2, an NAD-dependent tubulin deacetylase.* Biochem Biophys Res Commun, 2007. **359**(3): p. 665-71.
163. Outeiro, T.F., et al., *Sirtuin 2 inhibitors rescue alpha-synuclein-mediated toxicity in models of Parkinson's disease.* Science, 2007. **317**(5837): p. 516-9.
164. Simonin, Y., F.E. Perrin, and A.C. Kato, *Axonal involvement in the Wlds neuroprotective effect: analysis of pure motoneurons in a mouse model protected from motor neuron disease at a pre-symptomatic age.* J Neurochem, 2007. **101**(2): p. 530-42.
165. Sievers, C., et al., *Neurites undergoing Wallerian degeneration show an apoptotic-like process with Annexin V positive staining and loss of mitochondrial membrane potential.* Neurosci Res, 2003. **46**(2): p. 161-9.
166. Ikegami, K. and T. Koike, *Non-apoptotic neurite degeneration in apoptotic neuronal death: pivotal role of mitochondrial function in neurites.* Neuroscience, 2003. **122**(3): p. 617-26.

167. Barrientos, S.A., et al., *Axonal degeneration is mediated by the mitochondrial permeability transition pore.* J Neurosci, 2011. **31**(3): p. 966-78.
168. Shen, H., K. Hyrc, and M.P. Goldberg. *WldS mutation slows calcium accumulation and preserves mitochondrial trafficking in isolated cortical axons during chemical ischemia*. in *Society for Neuroscience Annual Meeting*. 2008. Washington, DC.
169. Cheng, H.C., C.M. Ulane, and R.E. Burke, *Clinical progression in Parkinson disease and the neurobiology of axons.* Ann Neurol, 2010. **67**(6): p. 715-25.

Chapter 2

Wld^{S} but not Nmnat1 protects dopaminergic neurites from MPP^{+} neurotoxicity

This chapter is under review for publication:

Antenor-Dorsey JA and O'Malley K. *Wld*^{S} but not Nmnat1 protects dopaminergic neurites from MPP^{+} neurotoxicity, Molecular Neurodegeneration

Abstract

The *Wld*^{S} mouse mutant ("Wallerian degeneration-slow") delays axonal degeneration in a variety of disorders including *in vivo* models of Parkinson's disease. The mechanisms underlying *Wld*^{S}-mediated axonal protection are unclear, although many studies have attributed *Wld*^{S} neuroprotection to the NAD^+-synthesizing Nmnat1 portion of the fusion protein. Here, we used dissociated dopaminergic (DA) cultures to test the hypothesis that catalytically active Nmnat1 protects DA neurons from toxin-mediated axonal injury. Using mutant mice and lentiviral transduction of DA neurons, the present findings demonstrate that *Wld*^{S} but not Nmnat1, Nmnat3, or cytoplasmically-targeted Nmnat1 protects DA axons from the parkinsonian mimetic N-methyl-4-phenylpyridinium (MPP^+). Moreover, NAD^+ synthesis is not required since enzymatically-inactive *Wld*^{S} still protects. In addition, NAD^+ by itself is axonally protective and together with *Wld*^{S} is additive in the MPP^+ model. Our data suggest that NAD^+ and *Wld*^{S} act through separate and possibly parallel mechanisms to protect DA axons. As MPP^+ is thought to impair mitochondrial function, these results suggest that *Wld*^{S} might be involved in preserving mitochondrial health or maintaining cellular metabolism.

2.1 Introduction

Parkinson's disease (PD) is the second most common neurodegenerative disorder in the U.S., affecting 1-2% of people over the age of 55. Characterized by loss of dopaminergic neurons in the substantia nigra (SN) [1-2], the cardinal motor symptoms of PD include resting tremor, bradykinesia, rigidity, and abnormal gait [3-4]. Another characteristic of PD is its late onset and progressive nature. Symptoms appear after 50-70% [5-6] of striatal dopamine (DA) has been depleted and 30-50% [7-8] of the nigral DA cells have died. Such studies suggest that the extent of striatal DA depletion is better correlated with the severity of PD symptoms than the loss of DA neurons in the SN [7].

Data from PD-linked genetic mutations also support the notion that axonal pathology and/or dysfunction occurs prior to the loss of DA cell bodies. For example, α-synuclein pathology is seen in neurites before it is observed in PD-associated cell bodies [3, 9]. α-synuclein mutants accumulate in the cell soma when overexpressed in cortical neurons, suggesting impaired axonal transport as well [10]. Moreover, transgenic models expressing the PD-linked mutant gene leucine rich repeat kinase 2 (LRRK2) also exhibit pronounced axonal loss and pathology prior to cell body loss [11]. In addition, genetic mutations in other PD-linked genes such as Parkin, an E3 ligase [12], and PINK1 (PTEN-induced putative kinase 1 protein) a mitochondrially-targeted kinase, also alter axonal transport [13-14]. Collectively, these findings have led to the idea that nigral neurons degenerate through a "dying back" axonopathy where degeneration starts in the distal axon and proceeds over time towards the cell body.

Environmental toxins known to mimic PD such as rotenone and MPP^+ also disrupt axonal function. These factors not only inhibit mitochondrial Complex I activity, but also de-polymerize microtubules leading to axon fragmentation and decreased synaptic function [15-17]. Moreover, MPP^+ can directly inhibit axon transport in the squid axoplasm [18] and DA neurons [19]. Thus, results from PD-associated environmental and genetic factors support an early, critical role for axonal impairment in PD.

Recent data suggest that the Wallerian degeneration slow fusion protein (*Wld*^{S}) can delay axonal degeneration about 10-fold from a wide variety of genetic and toxin-inducing stimuli in the peripheral nervous system [20]. *Wld*^{S} also blocks axon degeneration in several central nervous system (CNS) models of degeneration including animal models of PD [21-22]. For example, we previously found that *Wld*^{S} rescues 85% of DA axons for at least 7 days post MPTP treatment *in vivo* [23]. Because no other mutation or drug protects axons as robustly as *Wld*^{S}, understanding how the *Wld*^{S} fusion protein is able to prevent axon degeneration is the first step towards defining an intervention that would leave axons intact.

Wld^S is a chimeric protein composed of the first 70 amino acids of the ubiquitination factor E4b (Ube4b) followed by an 18-amino acid linker region and then the entire coding sequence for nicotinamide mononucleotide adenylyltransferase (Nmnat1), a nicotinamide adenine dinucleotide (NAD^+) synthesizing enzyme [20]. Most studies suggest that catalytically active Nmnat1 is necessary for axonal protection [24-25], hence, exogenous addition of NAD^+

has been reported to delay Wallerian degeneration in response to axotomy in dorsal root ganglion (DRG) cells [26]. In *Drosophila*, however, the picture is more complex in that Avery *et al.* [27] showed that Nmnat enzymatic activity is required following axotomy whereas Zhai *et al*. [28] found that Nmnat does not need its catalytic domain to protect axons. In this model [28], as well as in a new study demonstrating that Nmnat also protects dendrites [29], Nmnat exhibits a separate chaperone-like activity which protects axons and dendrites [28, 30].

Inasmuch as most studies have been done in peripheral model systems and because we have previously shown that *Wld*^{S} protects DA terminal fields from MPTP *in vivo*, we used a dissociated midbrain culture system to determine the mechanism of *Wld*^{S}-mediated neurite protection in DA neurons. Here, we show that, regardless of its enzymatic activity, the entire *Wld*^{S} sequence is needed for the *Wld*^{S}' neuroprotective phenotype in DA neurons. Our data also illustrate that NAD^+ has a neuroprotective effect that is different from *Wld*^{S}-mediated protection.

2.2 Materials and methods

2.2.1 Cell culture and toxin treatment

For primary midbrain cultures, the ventral mesencephalon was removed from embryonic day 14 (E14) murine embryos as previously described [31-32]. Wild-type (C57/Bl6) and *Wld*^{S} (C57Bl/OlaHsd-WldS) mice were ordered from Harlan (Bichester, UK). SIRT1 knockout mice were obtained from Dr. Christian

Sheline (Louisiana State University – Health Science Center, New Orleans, LA). Cytoplasmic *Wld*^{S} (*Cyto Wld*^{S}*)* mice were obtained from Dr. Michael Coleman (Babraham Institute, UK). Animals were treated in accordance with the National Institutes of Health *Guide for the Care and Use of Laboratory Animals.* All procedures were approved by the Washington University School of Medicine animal experimentation committee. Plates were pre-coated overnight with 0.2 mg/ml poly-D-lysine (Sigma-Aldrich, St. Louis, MO). Cells were plated at a density of approximately 125,000 cells/cm^2 and maintained in serum-free Neurobasal medium (Invitrogen, Carlsbad, CA) supplemented with 1X B27 supplement (Invitrogen), 0.5 mM L-glutamine (Sigma-Aldrich), and 0.01 µg/ml streptomycin plus 100 U penicillin. Half of the culture medium was replaced with fresh Neurobasal medium after 5 days *in vitro* (DIV). Cultures were pretreated with 1 mM NAD^+, 1 mM NMN, 1 mM nicotinic acid mononucleotide (NaMN), or a comparable volume of vehicle 24 hours before toxin treatment. Cultures were treated with either 1 µM 1-methyl-4-phenylpyridinium (MPP+), the active metabolite of MPTP or vehicle on DIV 7. Dorsal root ganglion (DRG) cells were obtained from E14 murine embryos as previously described [33]. Cells were plated on coverslips precoated with 0.1 mg/ml poly-L-ornithine (Invitrogen) and 32 µg/ml laminin-1 (Invitrogen) and maintained in DRG media which consisted of Eagle Minimal Essential Media (Invitrogen) supplemented with chick embryo extract (Invitrogen), 10% fetal calf serum (Invitrogen), 50 ng/ml Nerve Growth Factor (Harlan Biosciences, Madison, WI) and 50 U/ml penicillin–50 g/ml streptomycin. Half of the culture medium was replaced with fresh DRG medium

after DIV 5. After transduction with lentivirus on DIV 2, DRG cultures were treated with 0.4 μM vincristine or vehicle on DIV 7. NAD^+, NMN, NaMN, MPP^+, and vincristine were all obtained from Sigma-Aldrich.

2.2.2 Lentiviral infection of DA neurons

The lentiviral expression plasmids FUGW, FCIV-Wld^S, FCIV-Nmnat1, FCIV-Ube4b, FCIV-Nmnat3, FCIV- Nmnat1(W170A), FCIV-cytNmnat1, and FCIV-Wld^S(W258A) were obtained from Dr. Jeff Milbrandt (Washington University, Saint Louis). Lentiviruses expressing transgenes were generated by the Hope Center for Neurological Disorders Viral Core (Washington University, Saint Louis). For infection of DRG and primary midbrain neurons, 50 μl lentivirus (10^5 infectious units/μl) was added to the well of a 7-mm dish containing approximately 70,000 neurons on DIV 2. Transduced primary midbrain and DRG neurons were treated with MPP^+ and vincristine, respectively, on DIV 7. Viral infection and transgene expression was monitored using the GFP reporter via fluorescent microscopy.

2.2.3 Immunocytochemistry

Primary DA cultures and DRGs were plated in 7 mm microwell plates (MatTek Corp., Ashland, MA). Cells treated with MPP^+ were fixed with 4% paraformaldehyde (PFA) in PBS after 48 hours. Cultures were stained with sheep polyclonal anti-tyrosine hydroxylase (TH) (Novus Biologicals, Littleton, CO) and Cy3 anti-sheep antibodies (Molecular Probes, Carlsbad, CA).

Localization of cytoplasmic *Wld*^{S} was confirmed using rabbit *Wld*^{S} (gift of M.P. Coleman) and Alexa488 anti-rabbit antibodies (Molecular Probes). TH$^+$ cells and neurites were counted using unbiased stereological methods (Stereo Investigator, MicroBrightField, Williston, VT). DRG cultures treated with vincristine were subsequently stained with mouse acetylated tubulin (Sigma-Aldrich) and Cy3 α-mouse antibodies (Molecular Probes). Neurites were counted as described above. All images were acquired by confocal microscopy (Olympus Fluoview 500, Olympus, Center Valley, PA) and processed in ImageJ (NIH).

2.2.4 Western Blotting

Primary midbrain cultures were plated in 48-well plates and transduced with the transgene of interest as described above. Lysates were collected in RIPA buffer (150 mM NaCl, 1% Nonidet P-40, 0.5% NaDoc, 0.1% SDS, 50 mM Tris pH 8.0) with protease inhibitor mixture (Roche, Mannheim, Germany) and incubated on ice for 30 minutes. Insoluble cell debris was removed by centrifugation and the protein concentration of each cell lysate was determined by Bradford protein assay (BioRad, Hercules, CA). Equal amounts of protein were run on SDS-polyacrylamide gels and transferred to polyvinylidene diflouride (PVDF) membranes (BioRad). PVDF membranes were probed with either rabbit *Wld*^{S} antibody or chicken polyclonal anti-GFP antibody (Aves Labs, Tigard, OR). As a control, PVDF membranes were also probed with goat polyclonal anti-HRP60 antibody (Santa Cruz Biotechnology, Santa Cruz, CA). The secondary antibodies used were either a HRP-linked rabbit antibody or HRP-linked anti-

chicken antibody and a HRP-linked anti-goat antibody (Jackson Immunoresearch, West Grove, PA). Membranes were developed with enhanced chemiluminescence (Amersham Biosciences), imaged with a Storm PhosphorImager (Molecular Dynamics) and band intensities were determined using ImageQuant software (Amersham Biosciences).

2.2.5 Statistical analysis

GraphPad Prism software (San Diego, CA) was used for statistical analysis. All data was collected from a minimum of three independent experiments done in triplicate. The significance of effects between control and experimental conditions was determined by a Student t-test or one-way ANOVA with Bonferroni Multiple Comparisons tests.

2.3 Results

2.3.1 *Wld*^{S} protects DA cell bodies and neurites from MPP$^+$

Previously we have shown that DA terminal fields but not cell bodies of *Wld*^{S} mice are protected against MPTP injury [23]. To confirm and extend these observations in a more tractable system, we utilized dissociated cultures of midbrain neurons in which 1-5% of the total cells plated are DA [31]. Results show that cultures from *Wld*^{S} mice exhibited significant protection of neurites not seen in wild type (WT) cultures after MPP$^+$ treatment (Fig. 2.1A,C). Moreover, DA cell death from MPP$^+$ treatment was also attenuated in *Wld*^{S} cultures, unlike

those seen *in vivo* (Fig. 2.1A,B). Thus *Wld*^{S} can effectively protect neurites (dendrites and axons) as well as cell bodies from known PD mimetics *in vitro*.

2.3.2 Cytoplasmic *Wld*^{S} protects cell bodies and neurites against MPP$^+$

Recent studies have reported that the localization of *Wld*^{S} influences its neuroprotective effect. Beirowski *et al*. have reported that a cytoplasmic version of the *Wld*^{S} protein confers a higher level of protection than the native form of *Wld*^{S} [34]. In addition, Milbrandt and colleagues have reported that cytoplasmic Nmnat1 and Nmnat3, which is primarily localized in the mitochondria, also confer a higher level of protection than Nmnat1 [35-36]. To test whether cytoplasmic localization of *Wld*^{S} rescued or changed the level of protection seen with nuclear *Wld*^{S}, primary DA neurons were prepared from WT and cyto *Wld*^{S} mice, treated with MPP$^+$, and analyzed as described. Results show that cyto *Wld*^{S} mice exhibited a similar level of protection of DA cell bodies and neurites as seen in *Wld*^{S} mice (Fig 2.2). Therefore, as reported for peripheral model systems, *Wld*^{S} does not have to be localized in the nucleus; it can also protect neurites from the cytoplasm.

2.3.3 Nmnat1 does not protect against MPP$^+$ toxicity

Many studies, especially in peripheral model systems, have shown that Nmnat1 can at least partially mimic the effects of *Wld*^{S} [24, 37]. To determine whether this is true in DA neurons, we transduced primary midbrain cultures from WT animals with either GFP, *Wld*^{S}, the 70 amino acid fragment of Ube4b found

in *Wld*^{S}, or the entire coding region of Nmnat1 using lentiviral vectors expressing GFP [37] (Fig. 2.3). We also tested the effects of Nmnat3, cytoplasmic Nmnat1 (cyto Nmnat1), and enzymatically inactive Nmnat1 (Nmnat1 (W170A)) [25-26] (Fig 2.3A). Western blotting was done to confirm that transductions led to similar expression levels in dissociated cultures (Fig. 2.3B-D). Despite equivalent levels of transgene expression, only neurites transduced with the entire coding sequence of *Wld*^{S} were protected from MPP^+ injury (Fig. 2.3F).

Because many studies have suggested that Nmnat and in particular cyto Nmnat or axonally targeted Nmnat can be as effective as *Wld*^{S} in protecting axons from mechanical or toxic insults, we used DRG cultures as a positive control [38-39]. Consistent with those studies, both *Wld*^{S} and cyto Nmnat rescued DRG neurites from the neurotoxin, vincristine, whereas the GFP-only and inactive *Wld*^{S} virus did not (Fig 2.4). Taken together, these data confirm previous results showing that cyto Nmnat is necessary and sufficient to save DRG neurites. In contrast, only *Wld*^{S} but not cyto Nmnat, Nmnat1, or Nmnat3 was able to protect DA neurons from the neurotoxic effects of MPP^+.

2.3.4 Inactive *Wld*^{S} protects cell bodies and neurites against MPP^+

To corroborate the hypothesis that Nmnat1 does not protect DA neurons from MPP^+, we transduced dissociated primary midbrain cultures with enzymatically inactive *Wld*^{S} (W258A; [37]). In contrast to our own results in DRG cultures (Fig. 2.4) as well as results published by others using this same construct [37], the inactive *Wld*^{S} plasmid was as effective as NAD^+-synthesizing

Wld^S animals in protecting DA cell bodies and neurites against MPP^+ injury (Fig. 2.5). Therefore, the entire *Wld*^{S} chimeric protein, but not its NAD^+-synthesizing activity, is required for neuroprotection of DA neurons.

2.3.5 NAD^+ protects cell bodies and neurites against MPP^+

Previous studies have shown that NAD^+ itself can be neuroprotective [37]. Although Nmnat1 by itself did not recapitulate the neuroprotective effect of *Wld*^{S} on dopaminergic neurons, we tested whether NAD^+ or one of its precursors (Fig. 2.6A) rescued cell bodies or neurites from MPP^+ treatment. Therefore, dissociated DA WT cultures were pretreated with either 1 mM of NAD^+, *nicotinamide* mononucleotide (NMN), or nicotinic acid mononucleotide (NaMN) 24 hours before MPP^+ treatment. Both NAD^+ and NMN but not NaMN protected cell bodies and neurites against MPP^+ toxicity (Fig. 2.6B,C). These findings together with the results showing that catalytically-inactive *Wld*^{S} was able to protect DA neurons (Fig. 2.5) but catalytically active Nmnat did not (Fig. 2.3F) suggest that different pathways are being invoked in response to MPP^+ toxicity.

2.3.6 SIRT1 is not responsible for the NAD^+-mediated protection of cell bodies and neurites against MPP^+

Previous studies in DRG neurons have attributed the protective phenotype of *Wld*^{S} to its action on the Nmnat1-NAD^+-SIRT1 pathway [37]. To test the involvement of SIRT1, we prepared dissociated DA cultures from SIRT1 knockout mice. Following 24 hour pretreatment with 1 mM NAD^+ or vehicle

control, cultures were exposed to MPP^+. Consistent with the notion that NAD^+ is not acting through SIRT1 but rather through a different mechanism, NAD^+ protected cell bodies and neurites in SIRT1 knockout cultures from MPP^+ toxicity (Fig. 2.7).

2.3.7 NAD^+ and *Wld*^{S} effects are additive

The data described above suggest that *Wld*^{S} is acting through a separate possibly parallel pathway from that of NAD^+ in DA neurons. If so, then adding NAD^+ to *Wld*^{S} cultures will enhance the neuroprotective phenotype of *Wld*^{S}. To see whether the NAD^+ effect overlapped with *Wld*^{S} or was additive, dissociated DA cultures were prepared from WT and *Wld*^{S} mice and pretreated with and without NAD^+ as previously described. Both NAD^+ and *Wld*^{S} alone exhibited similar levels of cell body and neurite protection (Fig. 2.8). However, NAD^+ together with *Wld*^{S} generated significantly higher levels of protection suggesting this is an additive process (Fig. 2.8). To test whether these effects were maximal, additional cultures were treated with 5 mM NAD^+; no significant differences in neuroprotection were observed when compared with the lower dose of 1 mM NAD^+ (Fig. 2.8D). These findings demonstrate that NAD^+ and *Wld*^{S} are additive in the MPP^+ model suggesting that they are acting through separate and possibly parallel neuroprotective mechanisms.

2.4 Discussion

The mechanism(s) by which *Wld*^{S} protects axons is still unclear. Peripheral model studies underscore the role of Nmnat and its product, NAD^+, in protecting axons from various injuries whereas few central nervous system studies have been done. Using cellular, molecular and pharmacological tools, the present findings show that the chimeric *Wld*^{S} gene product plays a critical role in protecting DA processes, one not dependent upon Nmnat activity. Specifically, neither Nmnat, cytoplasmically-targeted Nmnat, nor Nmnat 3 were able to prevent toxicity associated with the DA toxin, MPP^+ whereas, akin to previous reports [26, 37], cyto Nmnat protected DRG axons from known axonal toxins. In contrast, *Wld*^{S}, cytoplasmically-expressed *Wld*^{S}, and *Wld*^{S} with an inactive Nmnat domain, all significantly protected DA neurites from toxin-mediated loss. Despite the inability of Nmnat to protect DA processes, NAD^+ and its precursor, Nmn, were neuroprotective. As *Wld*^{S} and NAD^+ were additive in this model system, current results suggest that these protectants act through separate, possibly parallel pathways. Thus, NAD^+ or its derivatives as well as *Wld*^{S} and its targets protect DA processes and may aid in the development of therapeutics preserving the connections and circuitry important in PD.

The role of Nmnat and NAD^+ in recapitulating the full effect of *Wld*^{S} has been controversial. *In vitro* studies have shown that overexpression of Nmnat1 by itself protects axons from many mechanical, genetic or toxin-induced injuries [20, 40]. In contrast, transgenic animals expressing nuclear Nmnat1 did not replicate the effects of *Wld*^{S} [41-42] whereas cytoplasmically [38] or axonally

targeted Nmnat1 [39] were equally if not more effective. Thus, site of action plays a role in Nmnat1's effectiveness [20]. These data together with findings showing that the first 16 N-terminal amino acids of the *Wld*^{S} gene product are required for full *Wld*^{S} protection [24], possibly by redistributing enough *Wld*^{S} to cytoplasmic or axonal compartments, are consistent with the notion that both the N-terminal portion of *Wld*^{S} and Nmnat1 are necessary for full axonal protection [20].

The importance of Nmnat catalytic activity is reflected in several mutational studies in which Nmnat's active sites have been disrupted and neuroprotection was lost [24, 27, 37, 42]. Moreover, NAD^+ itself and/or some of its biosynthetic precursors, protect against axonal degeneration in peripheral model systems as well as in experimental autoimmune encephalomyelitis (EAE; [26, 43], ischemia [44-45], Alzheimer's disease [46], and PD [47-49]. In at least one study however, addition of NAD^+ was not effective [41]. Moreover, Drosophila Nmnat (dNmnat) did not require enzymatic activity for axon protection against insults such as excitotoxicity, polyglutamine-induced dysfunction, or mechanical injury [30] leading to the suggestion that dNmnat may perform a chaperone-like function [28]. Indeed, structural studies of various Nmnats have revealed characteristic similarities to known chaperones such as UspA and Hsp100 [50]. Consistent with this notion, dNmnat was recently shown to function as a stress protein in response to heat shock, hypoxia, and the mitochondrial Complex I toxin, paraquat [51]. However, in DA neurons, Nmnat1 does not seem to function as either an axonal protectant or a chaperone.

Studies have indicated that MPP^+ can block electron transport by acting at the same site as the Complex I inhibitor, rotenone, leading to the production of free radical species and a loss of ATP production [52-54]. MPP^+ affects other processes as well including the rapid release of DA from vesicular stores [55-56]; depolymerization of microtubules [16, 57]; induction of autophagy [19, 58], and the rapid loss of mitochondrial membrane potential and reduction in mitochondrial motility in DA axons [19] . Since many of these effects involve mitochondrial function, conceivably the *Wld*^{S} gene product is involved in preserving mitochondrial health or maintaining homeostatic control. Recently, Barrientos *et al.* reported that *Wld*^{S} is able to regulate the mitochondrial permeability transition pore (PTP) preventing, amongst other things, calcium release, ATP loss, oxidative stress and release of proteins involved in axonal degeneration [59]. This is consistent with other studies from Wishart *et al.* showing that striatal synaptosomes isolated from *Wld*^{S} versus WT animals expressed higher levels of various mitochondrial proteins including the PTP protein, VDAC2 [60]. Barrientos *et al.* suggested that *Wld*^{S} is part of a regulatory cascade that also involves JNK activation upstream of PTP opening [59]. Although JNK is a known regulator of axon degeneration [61], recently we showed that the JNK inhibitor, SP600125, did not prevent MPP^+ effects on DA mitochondria [19]. Thus diverse, unknown, regulatory steps appear to mediate *Wld*^{S} effects in DA axons.

Given its role as a ubiquitous cofactor, NAD^+ influences many cellular decisions such as DNA damage repair [62] and transcriptional regulation and

differentiation [63]. Earlier studies suggested that increased NAD^+ levels led to SIRT activation which, in turn, activated a transcription factor that induced genes involved in neuroprotection [30, 37]. Although an attractive hypothesis, subsequent studies using SIRT1 knock out animals did not support this notion for DRG neurons [64], or as in the present study, for DA neurons (Fig 2.8).

Why are results in DA neurons different than other systems? Because many of the studies published have been performed in peripheral model systems with dramatically over-expressed protein, there may be neuronal-specific or expression level-related effects that might account for the differences. For example, *Wld*^{S} has shown protection in several central nervous system models, but few have been further tested with only Nmnat1 even in dissociated neuronal models. Then too, DA axons may have intrinsic differences that contribute to the *Wld*^{S} effect. For instance, DA neurons have fewer [65], smaller and slower mitochondria than non-DA neurons [19]. Moreover, DA neurons produce a neurotransmitter prone to oxidation [66], exhibit a greater dependence on L-type Ca^{2+} channels with subunits that result in deleterious amounts of intracellular calcium and ensuing mitochondrial dysfunction [67], and extend long, thin lightly-myelinated processes which are selectively vulnerable in PD [68]. These unique characteristics in DA neurons may require higher levels and/or different forms of a neuroprotective agent in order to be effective.

In support of our previous *in vivo* study showing that *Wld*^{S} protects DA terminal fields from MPTP [23], the current results demonstrate in dissociated DA cultures that the entire *Wld*^{S} sequence is needed for axonal protection,

regardless of its NAD^+-synthesizing activity. Indeed, NAD^+ and *Wld*^{S} act through separate, possibly parallel, mechanisms to protect DA axons. As MPP^+ is thought to impair mitochondrial function, these results suggest that *Wld*^{S} might be involved in preserving mitochondrial health or maintaining cellular metabolism. Given that Parkinson's disease is the second most common neurodegenerative disease, our findings support the idea that studies expanding therapeutic efforts towards maintaining connections as well as saving the cell body will help in developing better interventions for PD.

2.5 Acknowledgements

This work was supported by National Institutes of Health Grants NS39084 (K.L.O.) and National Institutes of Health Neuroscience Blueprint Core Grant NS057105 to Washington University. This work was also supported by the Bakewell Family Foundation. We thank Steven K. Harmon for technical support and Drs. Michael Coleman, Jeffrey Milbrandt, Christian Sheline, Indra Chandrasekar, Paul Bridgman, and Valeria Cavalli for materials and helpful discussions.

References:

1. Dauer W, Przedborski S: **Parkinson's disease: mechanisms and models.** *Neuron* 2003, **39:**889-909.
2. Blum D, Torch S, Lambeng N, Nissou M, Benabid AL, Sadoul R, Verna JM: **Molecular pathways involved in the neurotoxicity of 6-OHDA, dopamine and MPTP: contribution to the apoptotic theory in Parkinson's disease.** *Prog Neurobiol* 2001, **65:**135-172.
3. Braak H, Ghebremedhin E, Rub U, Bratzke H, Del Tredici K: **Stages in the development of Parkinson's disease-related pathology.** *Cell Tissue Res* 2004, **318:**121-134.
4. Bernheimer H, Birkmayer W, Hornykiewicz O, Jellinger K, Seitelberger F: **Brain dopamine and the syndromes of Parkinson and Huntington. Clinical, morphological and neurochemical correlations.** *J Neurol Sci* 1973, **20:**415-455.
5. Scherman D, Desnos C, Darchen F, Pollak P, Javoy-Agid F, Agid Y: **Striatal dopamine deficiency in Parkinson's disease: role of aging.** *Ann Neurol* 1989, **26:**551-557.
6. Riederer P, Wuketich S: **Time course of nigrostriatal degeneration in parkinson's disease. A detailed study of influential factors in human brain amine analysis.** *J Neural Transm* 1976, **38:**277-301.
7. Cheng HC, Ulane CM, Burke RE: **Clinical progression in Parkinson disease and the neurobiology of axons.** *Ann Neurol* 2010, **67:**715-725.
8. Fearnley JM, Lees AJ: **Ageing and Parkinson's disease: substantia nigra regional selectivity.** *Brain* 1991, **114 (Pt 5):**2283-2301.
9. Kramer ML, Schulz-Schaeffer WJ: **Presynaptic alpha-synuclein aggregates, not Lewy bodies, cause neurodegeneration in dementia with Lewy bodies.** *J Neurosci* 2007, **27:**1405-1410.
10. Saha AR, Hill J, Utton MA, Asuni AA, Ackerley S, Grierson AJ, Miller CC, Davies AM, Buchman VL, Anderton BH, Hanger DP: **Parkinson's disease alpha-synuclein mutations exhibit defective axonal transport in cultured neurons.** *J Cell Sci* 2004, **117:**1017-1024.
11. Li Y, Liu W, Oo TF, Wang L, Tang Y, Jackson-Lewis V, Zhou C, Geghman K, Bogdanov M, Przedborski S, et al: **Mutant LRRK2(R1441G) BAC transgenic mice recapitulate cardinal features of Parkinson's disease.** *Nat Neurosci* 2009, **12:**826-828.
12. Kitada T, Asakawa S, Hattori N, Matsumine H, Yamamura Y, Minoshima S, Yokochi M, Mizuno Y, Shimizu N: **Mutations in the parkin gene cause autosomal recessive juvenile parkinsonism.** *Nature* 1998, **392:**605-608.
13. Weihofen A, Thomas KJ, Ostaszewski BL, Cookson MR, Selkoe DJ: **Pink1 forms a multiprotein complex with Miro and Milton, linking Pink1 function to mitochondrial trafficking.** *Biochemistry* 2009, **48:**2045-2052.
14. Mortiboys H, Thomas KJ, Koopman WJ, Klaffke S, Abou-Sleiman P, Olpin S, Wood NW, Willems PH, Smeitink JA, Cookson MR, Bandmann O:

Mitochondrial function and morphology are impaired in parkin-mutant fibroblasts. *Ann Neurol* 2008, **64:**555-565.
15. Ren Y, Liu W, Jiang H, Jiang Q, Feng J: **Selective vulnerability of dopaminergic neurons to microtubule depolymerization.** *J Biol Chem* 2005, **280:**34105-34112.
16. Cappelletti G, Pedrotti B, Maggioni MG, Maci R: **Microtubule assembly is directly affected by MPP(+)in vitro.** *Cell Biol Int* 2001, **25:**981-984.
17. Cartelli D, Ronchi C, Maggioni MG, Rodighiero S, Giavini E, Cappelletti G: **Microtubule dysfunction precedes transport impairment and mitochondria damage in MPP+ -induced neurodegeneration.** *J Neurochem* 2010, **115:**247-258.
18. Morfini G, Pigino G, Opalach K, Serulle Y, Moreira JE, Sugimori M, Llinas RR, Brady ST: **1-Methyl-4-phenylpyridinium affects fast axonal transport by activation of caspase and protein kinase C.** *Proc Natl Acad Sci U S A* 2007, **104:**2442-2447.
19. Kim-Han JS, Antenor-Dorsey JA, O'Malley KL: **The Parkinsonian Mimetic, MPP+, Specifically Impairs Mitochondrial Transport in Dopamine Axons.** *J Neurosci* 2011, **31:**7212-7221.
20. Coleman MP, Freeman MR: **Wallerian degeneration, wld(s), and nmnat.** *Annu Rev Neurosci* 2010, **33:**245-267.
21. Mi W, Beirowski B, Gillingwater TH, Adalbert R, Wagner D, Grumme D, Osaka H, Conforti L, Arnhold S, Addicks K, et al: **The slow Wallerian degeneration gene, WldS, inhibits axonal spheroid pathology in gracile axonal dystrophy mice.** *Brain* 2005, **128:**405-416.
22. Sajadi A, Schneider BL, Aebischer P: **Wlds-mediated protection of dopaminergic fibers in an animal model of Parkinson disease.** *Curr Biol* 2004, **14:**326-330.
23. Hasbani DM, O'Malley KL: **Wld(S) mice are protected against the Parkinsonian mimetic MPTP.** *Exp Neurol* 2006, **202:**93-99.
24. Conforti L, Wilbrey A, Morreale G, Janeckova L, Beirowski B, Adalbert R, Mazzola F, Di Stefano M, Hartley R, Babetto E, et al: **Wld S protein requires Nmnat activity and a short N-terminal sequence to protect axons in mice.** *J Cell Biol* 2009, **184:**491-500.
25. Sasaki Y, Vohra BP, Lund FE, Milbrandt J: **Nicotinamide mononucleotide adenylyl transferase-mediated axonal protection requires enzymatic activity but not increased levels of neuronal nicotinamide adenine dinucleotide.** *J Neurosci* 2009, **29:**5525-5535.
26. Sasaki Y, Araki T, Milbrandt J: **Stimulation of nicotinamide adenine dinucleotide biosynthetic pathways delays axonal degeneration after axotomy.** *J Neurosci* 2006, **26:**8484-8491.
27. Avery MA, Sheehan AE, Kerr KS, Wang J, Freeman MR: **Wld S requires Nmnat1 enzymatic activity and N16-VCP interactions to suppress Wallerian degeneration.** *J Cell Biol* 2009, **184:**501-513.
28. Zhai RG, Zhang F, Hiesinger PR, Cao Y, Haueter CM, Bellen HJ: **NAD synthase NMNAT acts as a chaperone to protect against neurodegeneration.** *Nature* 2008, **452:**887-891.

29. Wen Y, Parrish JZ, He R, Zhai RG, Kim MD: **Nmnat exerts neuroprotective effects in dendrites and axons.** *Mol Cell Neurosci* 2011.
30. Zhai RG, Cao Y, Hiesinger PR, Zhou Y, Mehta SQ, Schulze KL, Verstreken P, Bellen HJ: **Drosophila NMNAT maintains neural integrity independent of its NAD synthesis activity.** *PLoS Biol* 2006, **4:**e416.
31. Lotharius J, Dugan LL, O'Malley KL: **Distinct mechanisms underlie neurotoxin-mediated cell death in cultured dopaminergic neurons.** *J Neurosci* 1999, **19:**1284-1293.
32. Bernstein AI, Garrison SP, Zambetti GP, O'Malley KL: **6-OHDA generated ROS induces DNA damage and p53- and PUMA-dependent cell death.** *Mol Neurodegener* 2011, **6:**2.
33. Brown JA, Wysolmerski RB, Bridgman PC: **Dorsal root ganglion neurons react to semaphorin 3A application through a biphasic response that requires multiple myosin II isoforms.** *Mol Biol Cell* 2009, **20:**1167-1179.
34. Beirowski B, Babetto E, Gilley J, Mazzola F, Conforti L, Janeckova L, Magni G, Ribchester RR, Coleman MP: **Non-nuclear Wld(S) determines its neuroprotective efficacy for axons and synapses in vivo.** *J Neurosci* 2009, **29:**653-668.
35. Sasaki Y, Milbrandt J: **Axonal degeneration is blocked by nicotinamide mononucleotide adenylyltransferase (Nmnat) protein transduction into transected axons.** *J Biol Chem* 2010, **285:**41211-41215.
36. Press C, Milbrandt J: **Nmnat delays axonal degeneration caused by mitochondrial and oxidative stress.** *J Neurosci* 2008, **28:**4861-4871.
37. Araki T, Sasaki Y, Milbrandt J: **Increased nuclear NAD biosynthesis and SIRT1 activation prevent axonal degeneration.** *Science* 2004, **305:**1010-1013.
38. Sasaki Y, Vohra BP, Baloh RH, Milbrandt J: **Transgenic mice expressing the Nmnat1 protein manifest robust delay in axonal degeneration in vivo.** *J Neurosci* 2009, **29:**6526-6534.
39. Babetto E, Beirowski B, Janeckova L, Brown R, Gilley J, Thomson D, Ribchester RR, Coleman MP: **Targeting NMNAT1 to axons and synapses transforms its neuroprotective potency in vivo.** *J Neurosci* 2010, **30:**13291-13304.
40. Yan T, Feng Y, Zheng J, Ge X, Zhang Y, Wu D, Zhao J, Zhai Q: **Nmnat2 delays axon degeneration in superior cervical ganglia dependent on its NAD synthesis activity.** *Neurochem Int* 2010, **56:**101-106.
41. Conforti L, Fang G, Beirowski B, Wang MS, Sorci L, Asress S, Adalbert R, Silva A, Bridge K, Huang XP, et al: **NAD(+) and axon degeneration revisited: Nmnat1 cannot substitute for Wld(S) to delay Wallerian degeneration.** *Cell Death Differ* 2007, **14:**116-127.
42. Yahata N, Yuasa S, Araki T: **Nicotinamide mononucleotide adenylyltransferase expression in mitochondrial matrix delays Wallerian degeneration.** *J Neurosci* 2009, **29:**6276-6284.

43. Kaneko S, Wang J, Kaneko M, Yiu G, Hurrell JM, Chitnis T, Khoury SJ, He Z: **Protecting axonal degeneration by increasing nicotinamide adenine dinucleotide levels in experimental autoimmune encephalomyelitis models.** *J Neurosci* 2006, **26:**9794-9804.
44. Yang J, Klaidman LK, Chang ML, Kem S, Sugawara T, Chan P, Adams JD: **Nicotinamide therapy protects against both necrosis and apoptosis in a stroke model.** *Pharmacol Biochem Behav* 2002, **73:**901-910.
45. Sakakibara Y, Mitha AP, Ayoub IA, Ogilvy CS, Maynard KI: **Delayed treatment with nicotinamide (vitamin B3) reduces the infarct volume following focal cerebral ischemia in spontaneously hypertensive rats, diabetic and non-diabetic Fischer 344 rats.** *Brain Res* 2002, **931:**68-73.
46. Demarin V, Podobnik SS, Storga-Tomic D, Kay G: **Treatment of Alzheimer's disease with stabilized oral nicotinamide adenine dinucleotide: a randomized, double-blind study.** *Drugs Exp Clin Res* 2004, **30:**27-33.
47. Birkmayer JG, Vrecko C, Volc D, Birkmayer W: **Nicotinamide adenine dinucleotide (NADH)--a new therapeutic approach to Parkinson's disease. Comparison of oral and parenteral application.** *Acta Neurol Scand Suppl* 1993, **146:**32-35.
48. Birkmayer JG: **Coenzyme nicotinamide adenine dinucleotide: new therapeutic approach for improving dementia of the Alzheimer type.** *Ann Clin Lab Sci* 1996, **26:**1-9.
49. Kuhn W, Muller T, Winkel R, Danielczik S, Gerstner A, Hacker R, Mattern C, Przuntek H: **Parenteral application of NADH in Parkinson's disease: clinical improvement partially due to stimulation of endogenous levodopa biosynthesis.** *J Neural Transm* 1996, **103:**1187-1193.
50. Zhai RG, Rizzi M, Garavaglia S: **Nicotinamide/nicotinic acid mononucleotide adenylyltransferase, new insights into an ancient enzyme.** *Cell Mol Life Sci* 2009, **66:**2805-2818.
51. Ali YO, McCormack R, Darr A, Zhai RG: **Nicotinamide Mononucleotide Adenylyltransferase Is a Stress Response Protein Regulated by the Heat Shock Factor/Hypoxia-inducible Factor 1{alpha} Pathway.** *J Biol Chem* 2011, **286:**19089-19099.
52. Nicklas WJ, Vyas I, Heikkila RE: **Inhibition of NADH-linked oxidation in brain mitochondria by 1-methyl-4-phenyl-pyridine, a metabolite of the neurotoxin, 1-methyl-4-phenyl-1,2,5,6-tetrahydropyridine.** *Life Sci* 1985, **36:**2503-2508.
53. Ramsay RR, Krueger MJ, Youngster SK, Gluck MR, Casida JE, Singer TP: **Interaction of 1-methyl-4-phenylpyridinium ion (MPP+) and its analogs with the rotenone/piericidin binding site of NADH dehydrogenase.** *J Neurochem* 1991, **56:**1184-1190.
54. Ramsay RR, Salach JI, Singer TP: **Uptake of the neurotoxin 1-methyl-4-phenylpyridine (MPP+) by mitochondria and its relation to the**

inhibition of the mitochondrial oxidation of NAD+-linked substrates by MPP+. *Biochem Biophys Res Commun* 1986, **134:**743-748.
55. Lotharius J, O'Malley KL: **The parkinsonism-inducing drug 1-methyl-4-phenylpyridinium triggers intracellular dopamine oxidation. A novel mechanism of toxicity.** *J Biol Chem* 2000, **275:**38581-38588.
56. Chang GD, Ramirez VD: **The mechanism of action of MPTP and MPP+ on endogenous dopamine release from the rat corpus striatum superfused in vitro.** *Brain Res* 1986, **368:**134-140.
57. Cappelletti G, Surrey T, Maci R: **The parkinsonism producing neurotoxin MPP+ affects microtubule dynamics by acting as a destabilising factor.** *FEBS Lett* 2005, **579:**4781-4786.
58. Zhu JH, Horbinski C, Guo F, Watkins S, Uchiyama Y, Chu CT: **Regulation of autophagy by extracellular signal-regulated protein kinases during 1-methyl-4-phenylpyridinium-induced cell death.** *Am J Pathol* 2007, **170:**75-86.
59. Barrientos SA, Martinez NW, Yoo S, Jara JS, Zamorano S, Hetz C, Twiss JL, Alvarez J, Court FA: **Axonal degeneration is mediated by the mitochondrial permeability transition pore.** *J Neurosci* 2011, **31:**966-978.
60. Wishart TM, Paterson JM, Short DM, Meredith S, Robertson KA, Sutherland C, Cousin MA, Dutia MB, Gillingwater TH: **Differential proteomics analysis of synaptic proteins identifies potential cellular targets and protein mediators of synaptic neuroprotection conferred by the slow Wallerian degeneration (Wlds) gene.** *Mol Cell Proteomics* 2007, **6:**1318-1330.
61. Miller BR, Press C, Daniels RW, Sasaki Y, Milbrandt J, DiAntonio A: **A dual leucine kinase-dependent axon self-destruction program promotes Wallerian degeneration.** *Nat Neurosci* 2009, **12:**387-389.
62. Surjana D, Halliday GM, Damian DL: **Role of nicotinamide in DNA damage, mutagenesis, and DNA repair.** *J Nucleic Acids* 2010, **2010**.
63. Hisahara S, Chiba S, Matsumoto H, Horio Y: **Transcriptional regulation of neuronal genes and its effect on neural functions: NAD-dependent histone deacetylase SIRT1 (Sir2alpha).** *J Pharmacol Sci* 2005, **98:**200-204.
64. Wang J, Zhai Q, Chen Y, Lin E, Gu W, McBurney MW, He Z: **A local mechanism mediates NAD-dependent protection of axon degeneration.** *J Cell Biol* 2005, **170:**349-355.
65. Liang CL, Wang TT, Luby-Phelps K, German DC: **Mitochondria mass is low in mouse substantia nigra dopamine neurons: implications for Parkinson's disease.** *Exp Neurol* 2007, **203:**370-380.
66. Hastings TG: **The role of dopamine oxidation in mitochondrial dysfunction: implications for Parkinson's disease.** *J Bioenerg Biomembr* 2009, **41:**469-472.
67. Surmeier DJ, Guzman JN, Sanchez-Padilla J, Goldberg JA: **What causes the death of dopaminergic neurons in Parkinson's disease?** *Prog Brain Res* 2010, **183:**59-77.

68. Dickson DW, Fujishiro H, Orr C, DelleDonne A, Josephs KA, Frigerio R, Burnett M, Parisi JE, Klos KJ, Ahlskog JE: **Neuropathology of non-motor features of Parkinson disease.** *Parkinsonism Relat Disord* 2009, **15 Suppl 3:**S1-5.
69. Magni G, Amici A, Emanuelli M, Orsomando G, Raffaelli N, Ruggieri S: **Enzymology of NAD+ homeostasis in man.** *Cell Mol Life Sci* 2004, **61:**19-34.

Figure 2.1 - ***Wld*^{S} protects DA neurons from MPP^{+} toxicity**. (A) Dissociated DA cultures from both WT and *Wld*^{S} mice were treated with 2 μm MPP^{+} for 48 hours, and processed for TH immunoreactivity. (B) Quantification of TH+ cell bodies and (C) TH+ neurites was done using unbiased stereology. Data are normalized to control cultures and denote the mean ± SEM of representative determinations made in three separate cultures. *p<0.01; **p<0.001.

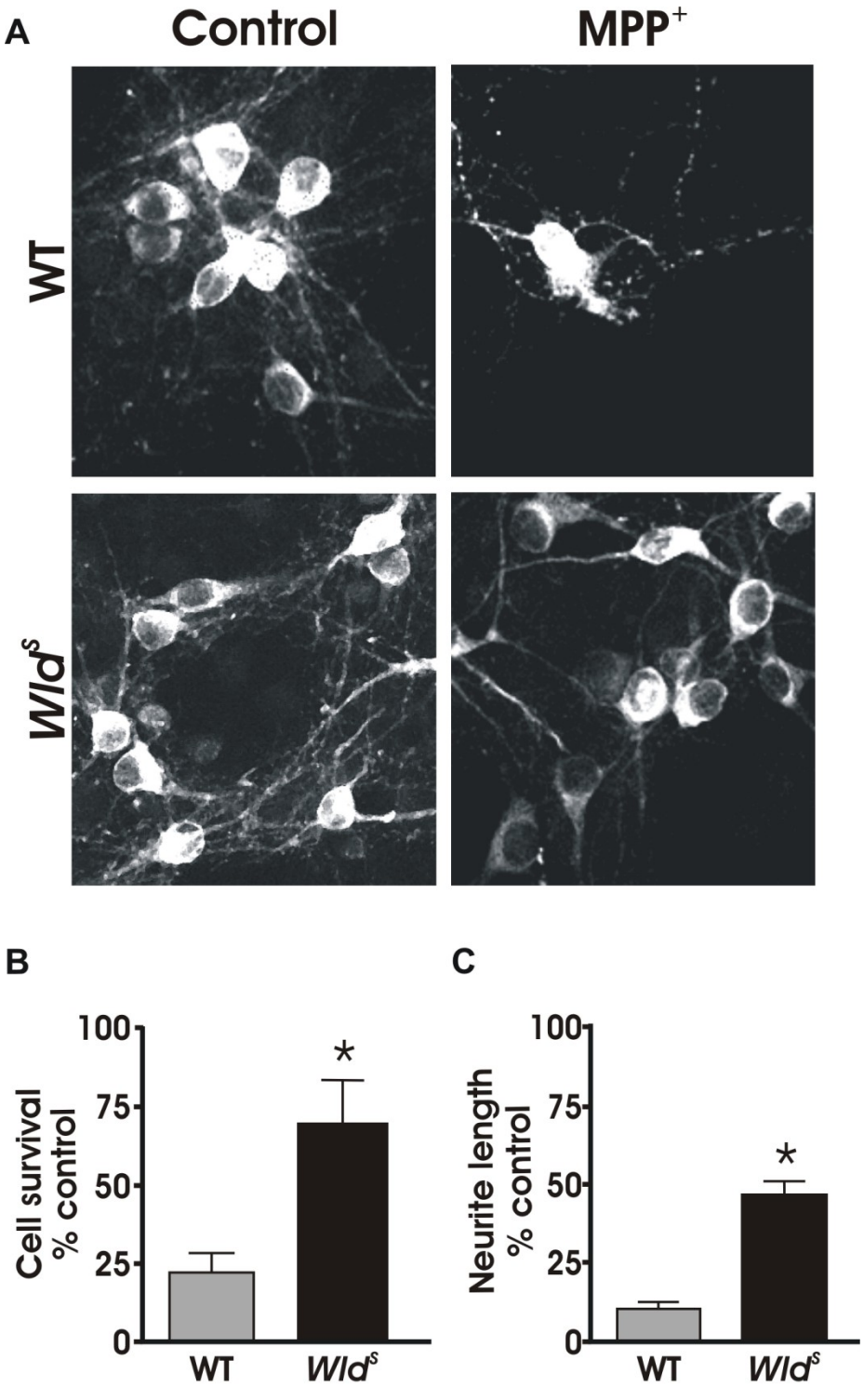
A
Control
MPP+
WT
Wlds
B
Cell survival
% control
100
75
50
25
0
*
WT
Wlds
C
Neurite length
% control
100
75
50
25
0
*
WT
Wlds

Fig.2.1

Figure 2.2 - **Cytoplasmic *Wld*^{S} protects DA neurons from MPP^{+} toxicity**. (A) Dissociated DA cultures from both WT and cyto *Wld*^{S} mice were co-stained with TH and *Wld*^{S} antibodies to confirm the subcellular localization of *Wld*^{S}. (B) Cultures were treated with 2 μm MPP^{+} for 48 hours prior to fixing and staining. (C) Quantification of TH+ cell bodies and (D) TH+ neurites shows that cytoplasmic *Wld*^{S} protected both cell bodies and neurites against MPP^{+}. Data are normalized to control cultures and denote the mean ± SEM of representative determinations made in three separate cultures. *$p<0.05$.

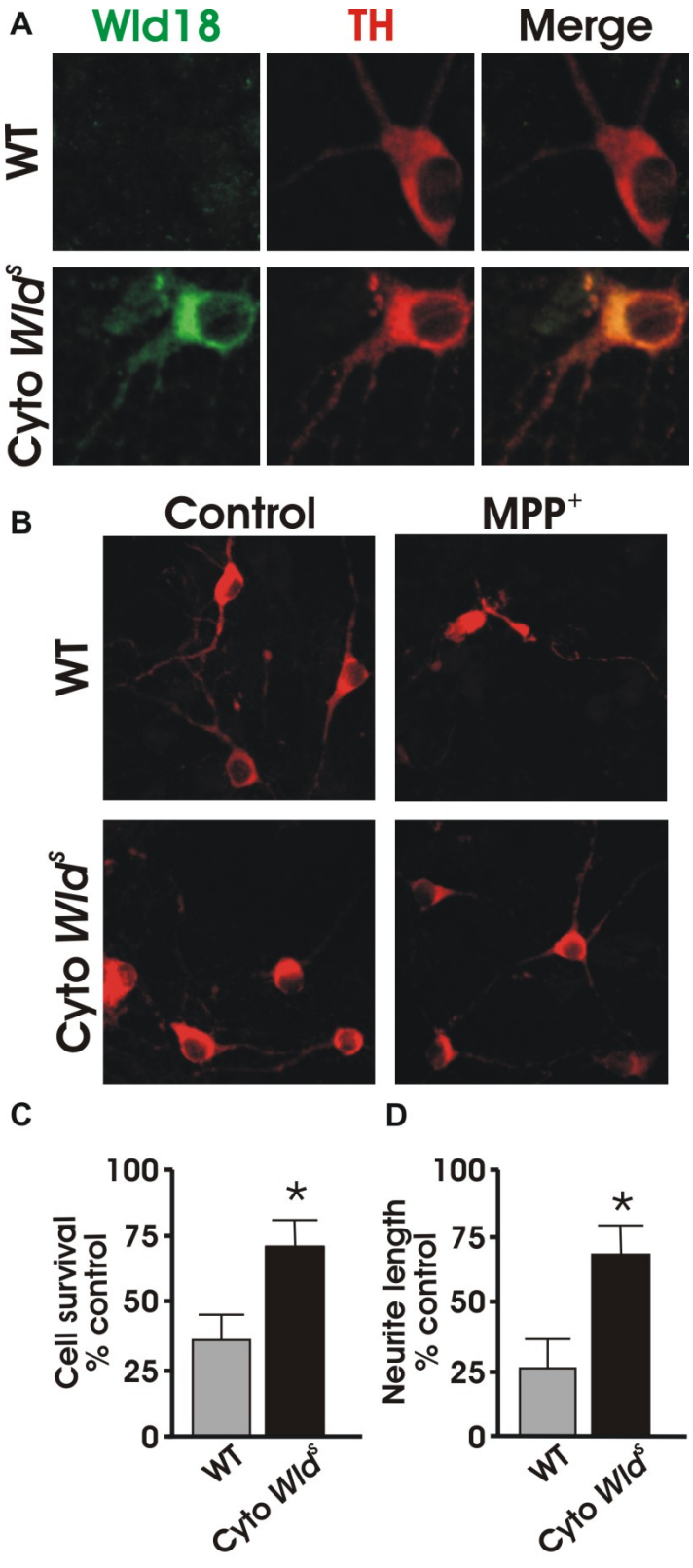
A
Wld18
TH
Merge
WT
Cyto Wld^S
B
Control
MPP+
WT
Cyto Wld^S
C
Cell survival % control
100
75
50
25
0
*
WT
Cyto Wld^S
D
Neurite length % control
100
75
50
25
0
*
WT
Cyto Wld^S

Fig.2.2

Figure 2.3 - **Nmnat by itself does not protect DA neurons from MPP^+ toxicity.** (A) Diagram of the lentiviral constructs used to transduce WT dissociated DA neurons. (B-D) Quantification of the western blots illustrates that all the transduced transgenes exhibit similar levels of expression. (E) Quantification of TH+ cell bodies and (F) TH+ neurites show that only *Wld*^{S}-transduced cultures protected neurites against MPP^+. Data are normalized to control cultures and denote the mean ± SEM of representative determinations made in three separate cultures. *p<0.001.

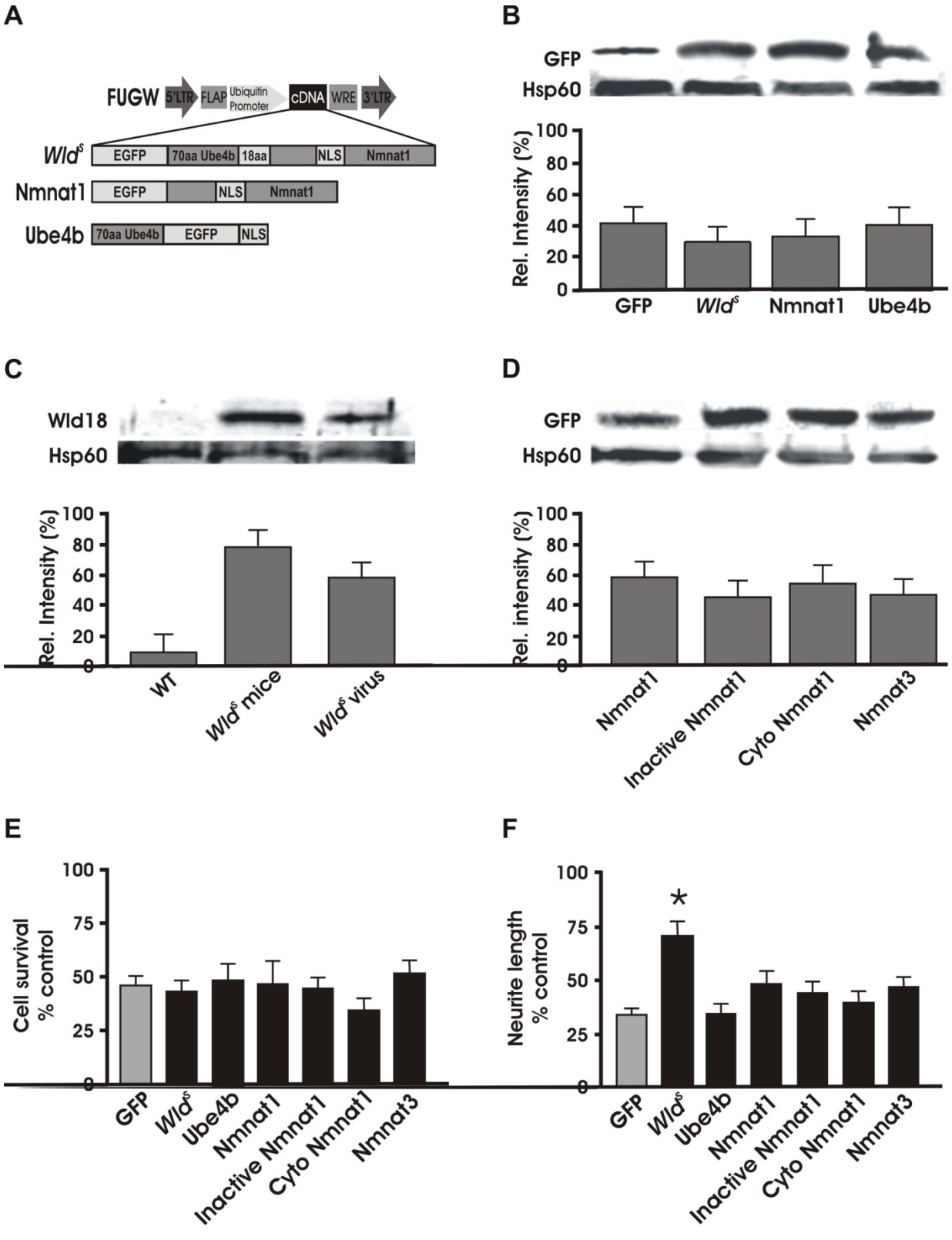
A
FUGW
5'LTR
FLAP
Ubiquitin Promoter
cDNA
WRE
3'LTR
Wlds
EGFP
70aa Ube4b
18aa
NLS
Nmnat1
Nmnat1
EGFP
NLS
Nmnat1
Ube4b
70aa Ube4b
EGFP
NLS
B
GFP
Hsp60
Rel. Intensity (%)
100
80
60
40
20
0
GFP
Wlds
Nmnat1
Ube4b
C
Wld18
Hsp60
Rel. Intensity (%)
100
80
60
40
20
0
WT
Wlds mice
Wlds virus
D
GFP
Hsp60
Rel. intensity (%)
100
80
60
40
20
0
Nmnat1
Inactive Nmnat1
Cyto Nmnat1
Nmnat3
E
Cell survival % control
100
75
50
25
0
GFP
Wlds
Ube4b
Nmnat1
Inactive Nmnat1
Cyto Nmnat1
Nmnat3
F
Neurite length % control
100
75
50
25
0
*
GFP
Wlds
Ube4b
Nmnat1
Inactive Nmnat1
Cyto Nmnat1
Nmnat3

Fig.2.3

Figure 2.4 - *Wld*^{S} and cytoplasmic Nmnat1 protect DRG axons from vincristine toxicity. (A) DRG cultures from E14 mice transduced with GFP, *Wld*^{S}, cyto Nmnat1, or inactive *Wld*^{S} were processed for acetylated tubulin immunoreactivity 24 hours after vincristine treatment. (B) Quantification of neurites shows that both *Wld*^{S} and cyto Nmnat1 protects DRG neurites from vincristine toxicity. Data are normalized to control cultures and denote the mean ± SEM of representative determinations made in three separate cultures. *p<0.05.

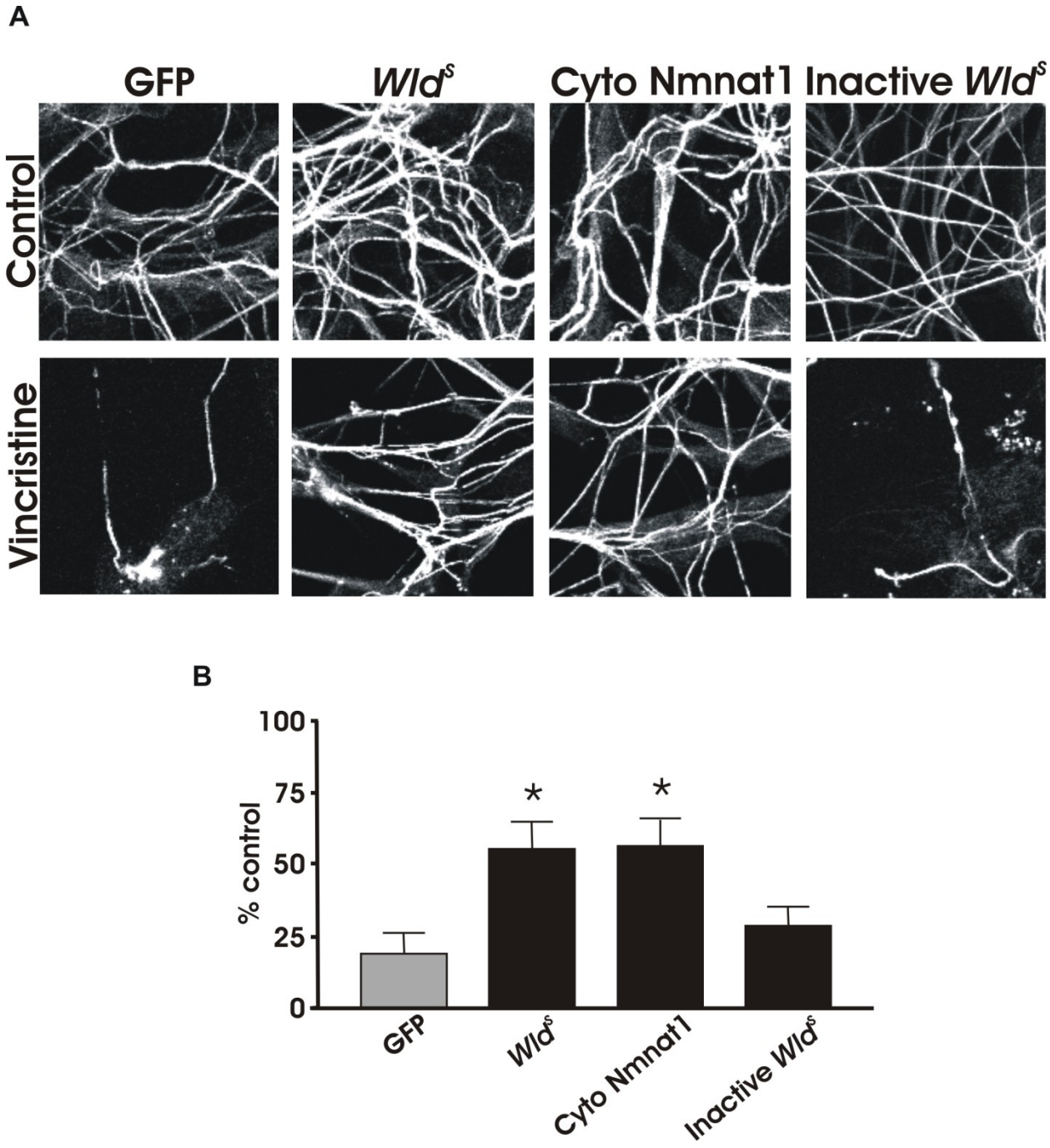
A
GFP
Wld^S
Cyto Nmnat1
Inactive Wld^S
Control
Vincristine
B
100
75
50
25
0
% control
*
*
GFP
Wld^S
Cyto Nmnat1
Inactive Wld^S

Fig.2.4

Figure 2.5 - **Inactive *Wld*^{S} also protects DA neurons from MPP^{+} toxicity.** (A) Dissociated DA neurons transduced with GFP or inactive *Wld*^{S} were treated and processed as described. (B) Quantification of TH+ cell bodies and (C) TH+ neurites. Data are normalized to control cultures and denote the mean ± SEM of representative determinations made in three separate cultures. *$p<0.05$.

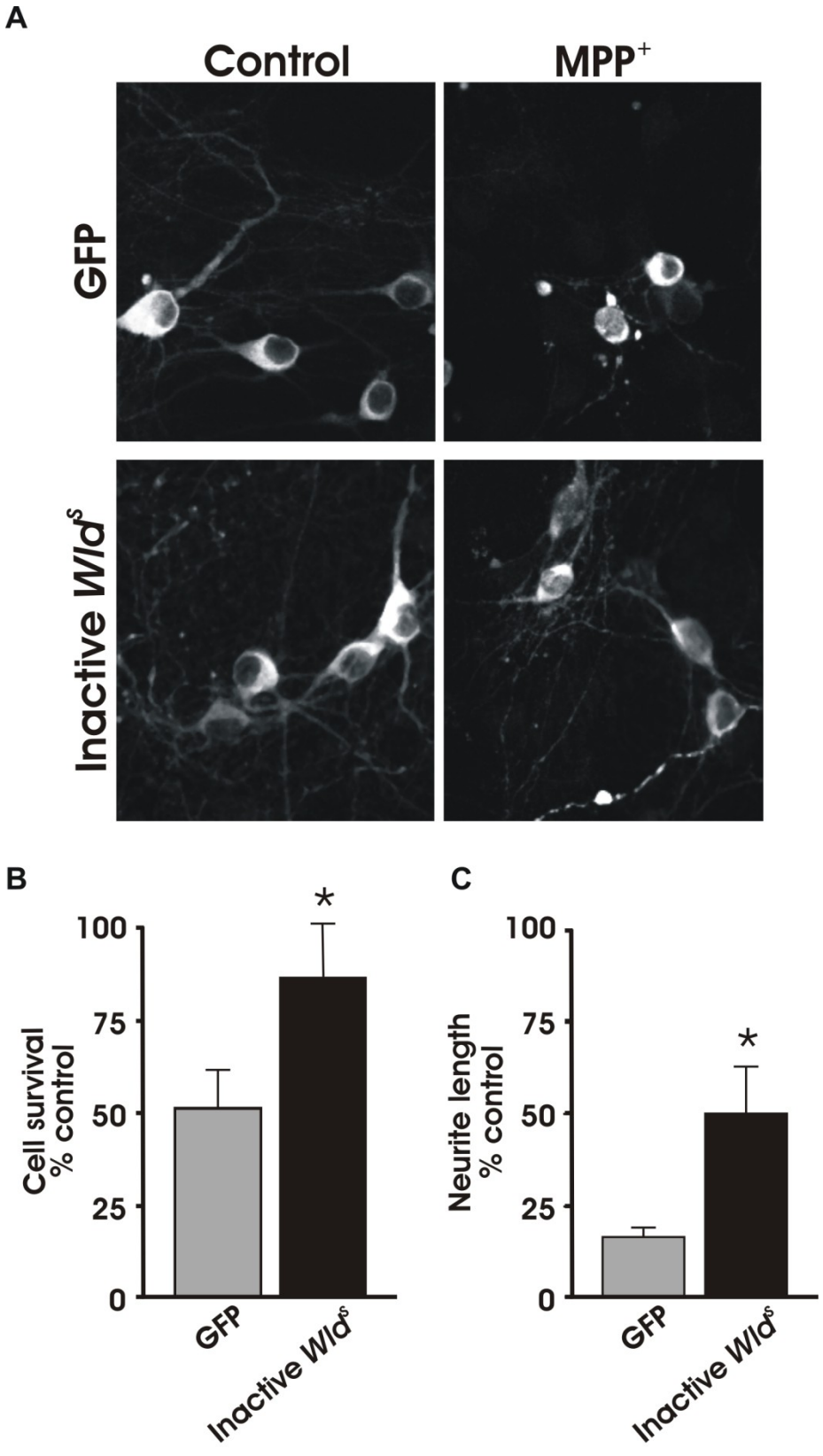
A
Control
MPP+
GFP
Inactive Wlds
B
Cell survival
% control
100
75
50
25
0
*
GFP
Inactive Wlds
C
Neurite length
% control
100
75
50
25
0
*
GFP
Inactive Wlds

Fig.2.5

Figure 2.6 - NAD^+ protects DA cells and neurites from MPP^+ toxicity. (A) NAD^+ biosynthetic pathway [69]. (B) Dissociated WT DA cultures were pretreated with NAD^+, NMN, or NaMN 24 hours before addition of 2 μm MPP^+. Quantification of TH+ cell bodies and (C) TH+ neurites show that NAD^+ and NMN, but not NaMN, protected cells and neurites from MPP^+. Data are normalized to control cultures and denote the mean ± SEM of representative determinations made in three separate cultures. *p<0.05, **p<0.01, ***p<0.001.

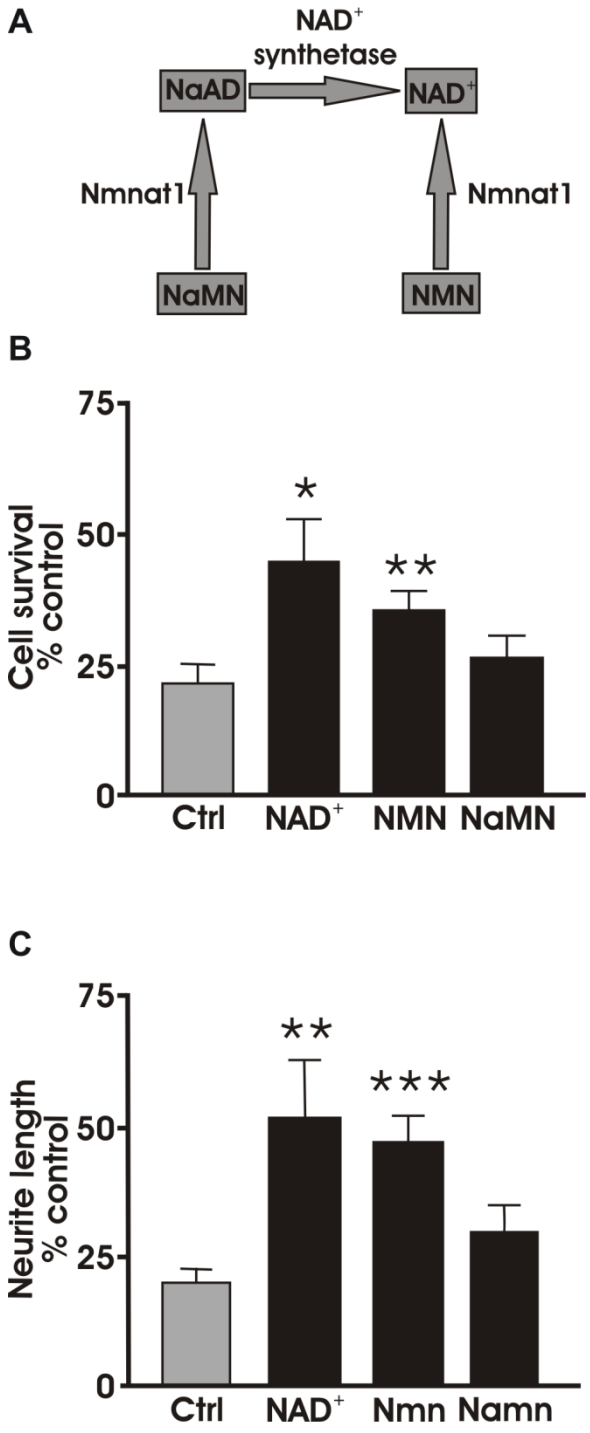
A
NAD+
synthetase
NaAD
NAD+
Nmnat1
Nmnat1
NaMN
NMN
B
Cell survival
% control
75
50
25
0
*
**
Ctrl
NAD+
NMN
NaMN
C
Neurite length
% control
75
50
25
0
**
***
Ctrl
NAD+
Nmn
Namn

Fig.2.6

Figure 2.7 - NAD^+ does not protect DA neurons through the Sirt1 pathway. (A) Dissociated midbrain cultures from both WT and Sirt1 KO mice were pretreated with NAD^+ 24 hours before addition of 2 μm MPP^+. (B) Quantification of TH+ cell bodies and (C) TH+ neurites show that NAD^+ protects cells and neurites from MPP^+ in both WT and Sirt1 KO cultures. Data are normalized to control cultures and denote the mean ± SEM of representative determinations made in three separate cultures. *$p<0.05$.

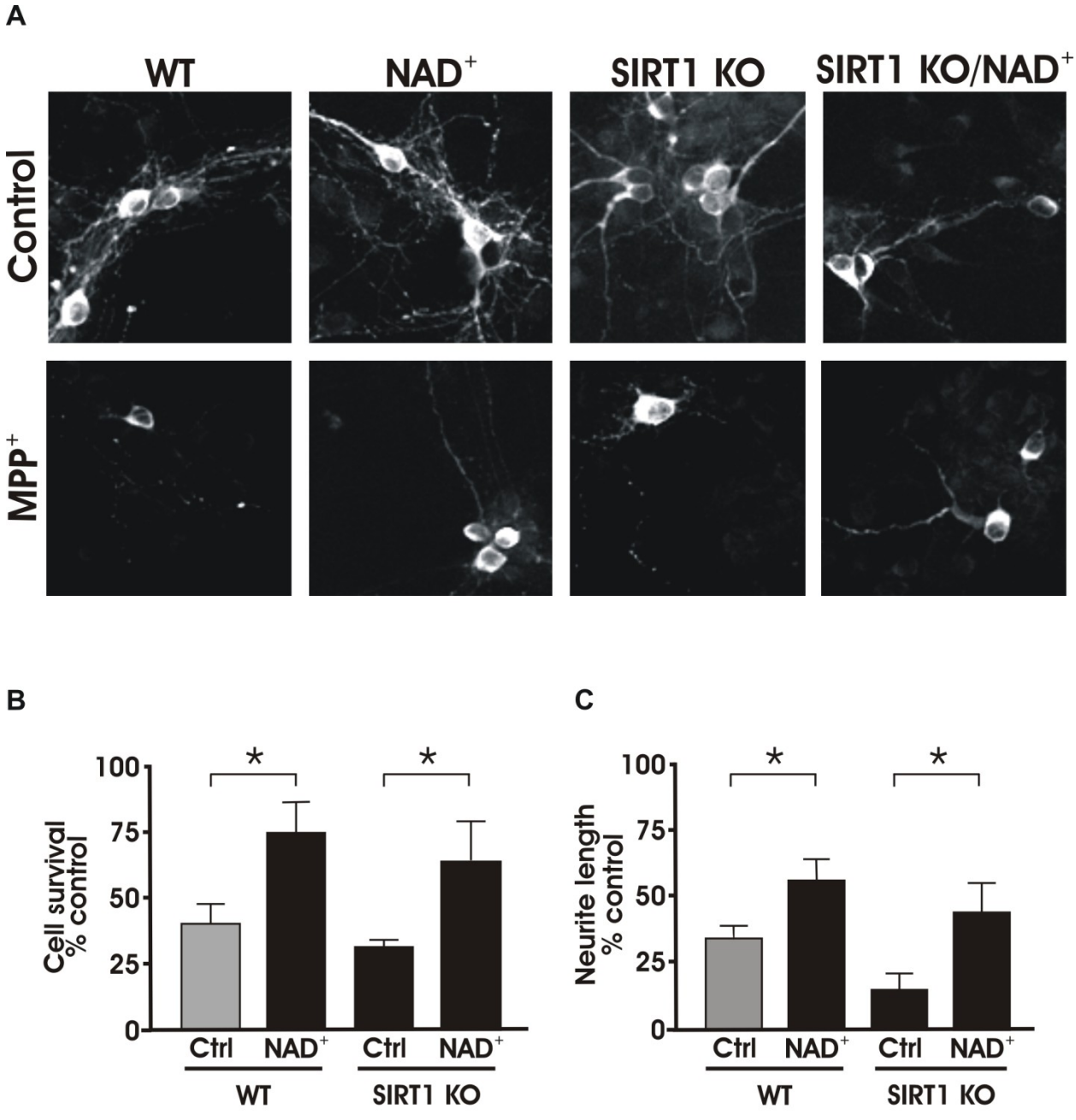
A
WT
NAD+
SIRT1 KO
SIRT1 KO/NAD+
Control
MPP+
B
Cell survival
% control
100
75
50
25
0
*
*
Ctrl
NAD+
Ctrl
NAD+
WT
SIRT1 KO
C
Neurite length
% control
100
75
50
25
0
*
*
Ctrl
NAD+
Ctrl
NAD+
WT
SIRT1 KO

Fig.2.7

Figure 2.8 - The protective effect of NAD^+ and *Wld*^{S} are additive. (A) Dissociated midbrain cultures from both WT and *Wld*^{S} mice were pretreated with NAD^+ 24 hours before addition of 2 μm MPP^+. (B) Quantification of TH+ cell bodies and (C) TH+ neurites show that NAD^+ pretreatment was more effective in protecting *Wld*^{S} neurites from MPP^+ versus untreated *Wld*^{S} cultures. (D) NAD^+ dose response curve showing that the protection seen with 1 mM NAD^+ is maximal. Addition of 10 mM NAD^+ before MPP^+ treatment induced 50% cell death in DA neurons (data not shown). Data are normalized to control cultures and denote the mean ± SEM of representative determinations made in three separate cultures. *$p<0.05$; **$p<0.001$.

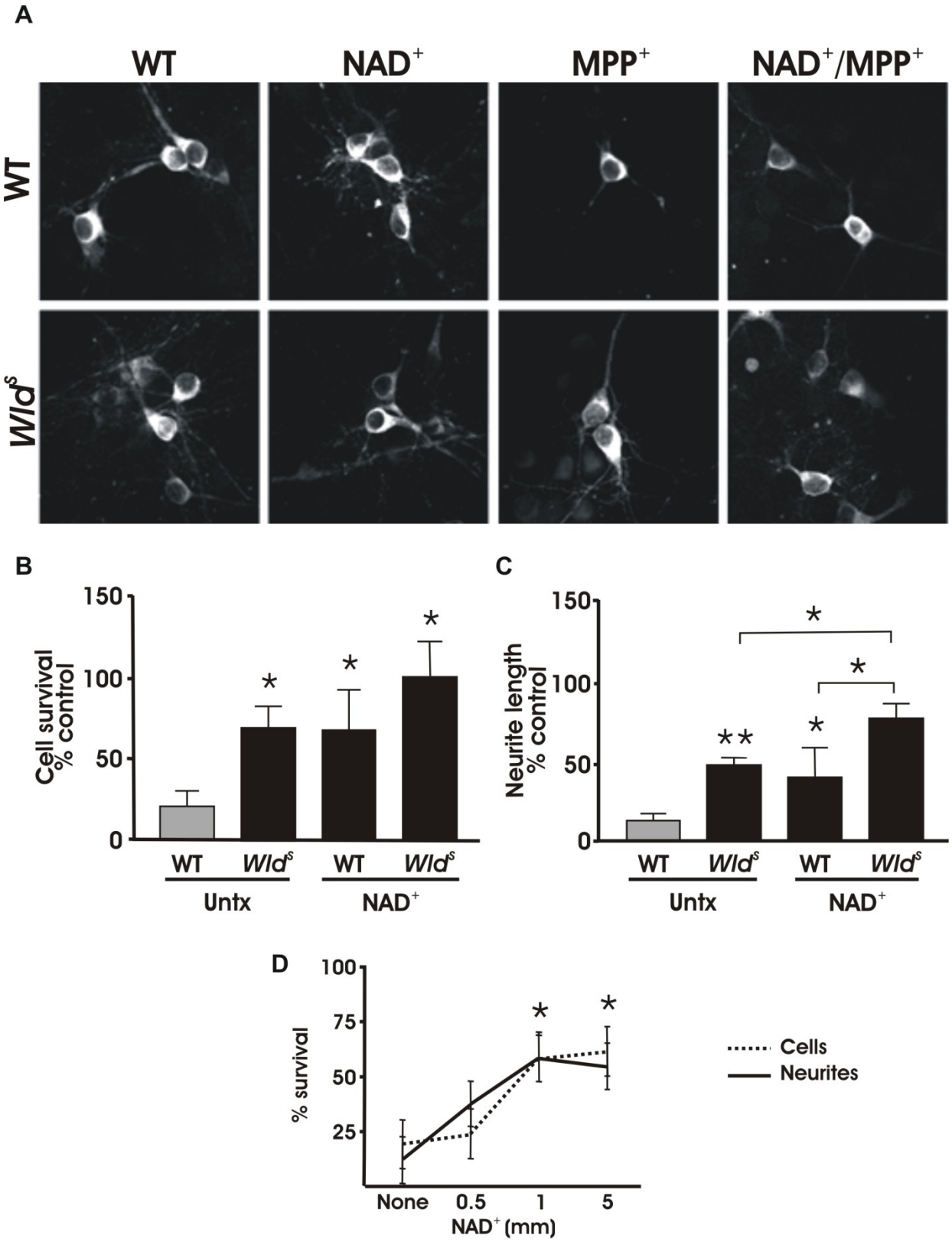
A
WT
NAD+
MPP+
NAD+/MPP+
WT
Wlds
B
Cell survival
% control
150
100
50
0
WT
Wlds
WT
Wlds
Untx
NAD+
C
Neurite length
% control
150
100
50
0
WT
Wlds
WT
Wlds
Untx
NAD+
D
% survival
100
75
50
25
None
0.5
1
5
NAD+ (mm)
Cells
Neurites

Fig.2.8

Chapter 3

Wld^{S} but not Nmnat1 protects dopaminergic neurites from 6-OHDA neurotoxicity

This manuscript is in preparation for publication

Abstract:

The *Wld*^{S} mouse mutant ("Wallerian degeneration-slow") delays axonal degeneration in a variety of disorders including *in vivo* models of Parkinson's disease. The mechanisms underlying *Wld*^{S}-mediated axonal protection are unclear, although many studies have attributed *Wld*^{S} neuroprotection to the NAD^+-synthesizing Nmnat1 portion of the fusion protein. We used dissociated dopaminergic (DA) cultures to test the hypothesis that catalytically active Nmnat1 protects DA neurons from the parkinsonian mimetic 6-hydroxydopamine-(6-OHDA). Using mutant mice and transduced DA neurons, the present study demonstrates that the entire *Wld*^{S} protein, but not Nmnat1 or cytoplasmically-targeted Nmnat1, protects DA axons from 6-OHDA. Additionally, exogenous NAD^+ was not able to protect DA axons against 6-OHDA. Our data suggest that *Wld*^{S} protects DA axons against 6-OHDA independent of its NAD^+-synthesizing ability. Therefore, *Wld*^{S} may induce a novel gain of function that counteracts the effects of 6-OHDA such as the generation of reactive oxygen species and/or mitochondrial dysfunction.

3.1 Introduction

Parkinson's disease (PD) is a late onset and progressive neurodegenerative disorder that affects 1-2% of people over the age of 55 in the United States. PD is caused by the death of DA neurons in the substantia nigra (SN) [1-2] and characterized by the occurrence of resting tremor, bradykinesia, rigidity, and abnormal gait in patients [3-4]. Interestingly, symptoms of PD manifest after 50-70% [5-6] of striatal dopamine (DA) has been depleted and 30-50% [7-8] of the nigral DA cells have died. These data are consistent with the hypothesis that PD severity correlates better with the extent of striatal DA depletion than with the loss of DA neurons in the SN [7].

PD-linked genetic mutations provide further evidence that axonal degeneration occurs prior to DA cell body loss. For example, α-synuclein inclusions have been reported to be present in neurites prior to the appearance of inclusions in neuronal cell bodies [3, 9]. Transgenic models expressing the PD-linked mutant gene leucine rich repeat kinase 2 (LRRK2) also exhibit decreased DA terminal fields and increased dystrophic processes with abnormal axonal swellings [10]. In addition, overexpression of PD-linked LRRK2 mutations lead to dramatic reductions in neurite length and branching yet only slight changes in cell soma diameter in primary neuronal cultures [11].

Environmental toxins known to induce Parkinson-like symptoms in animals such as 1-methyl-4-phenyl-1,2,3,6-tetrahydropyridine (MPTP) and 6-hydroxydopamine (6-OHDA) also exhibit terminal field changes prior to cell body loss. For example, MPTP administration in primates leads to marked reductions

of DA axons prior to the loss of nigral cell bodies [12]. In mice, Serra and colleagues showed that one day after MPTP treatment, striatal DA levels were diminished by 60% whereas at this same time point no tyrosine hydroxylase (TH) immunoreactive cell bodies were lost in the SN [13]. Other studies using 6-OHDA showed that striatal DA levels in the 6-OHDA-lesioned side of rodents were decreased by 64% whereas DA was reduced by only 43% in the lesioned SN. [14]. Similarly, Ebert *et al.* demonstrated that four days after 6-OHDA treatment, TH levels were significantly reduced in the striatum whereas there was very little loss of TH staining in the SN [15]. Finally, studies by Rosenblad *et al.* showed that even one day after 6-OHDA injection, axons already exhibited damaged pathology and retraction from the striatum whereas cell death was only observed weeks after toxin treatment [16-18].

Taken together, studies from PD patients as well as evidence from both genetic and toxin models of PD support the idea that nigral neurons degenerate through a “dying back” axonopathy in which degeneration begins in the distal axon and proceeds over weeks or months towards the cell body [19-20]. Hence, interventions that can halt or delay the progression of axonal degeneration may play an important role in designing therapeutics for PD.

Mice with the Wallerian degeneration slow (*Wld*^{S}) mutation exhibit dramatically delayed axonal degeneration in response to a wide range of genetic and toxin-inducing stimuli in both peripheral nervous system (PNS) [21] and central nervous system (CNS) models of degeneration [22-25]. In fact, *Wld*^{S} provides axon protection in a model of anterograde degeneration induced by

injection of 6-OHDA into the medial forebrain bundle [23, 25]. Because no other mutation or drug protects axons as robustly as *Wld*^{S}, understanding the mechanism by which the *Wld*^{S} fusion protein is able to prevent axon degeneration is the first step towards developing an intervention that would leave axons intact.

Wld^S is a chimeric protein composed of the first 70 amino acids of the ubiquitination factor E4b (Ube4b) followed by an 18-amino acid linker region and the entire coding sequence for nicotinamide mononucleotide adenylyltransferase (Nmnat1), a nicotinamide adenine dinucleotide (NAD^+) synthesizing enzyme (Fig. 3.1A) [21, 26]. Most studies have attributed the neuroprotective effect of *Wld*^{S} to the Nmnat1 portion of the protein, since enzymatically inactive *Wld*^{S} or Nmnat1 does not recapitulate the neuroprotection seen with the native *Wld*^{S} protein in certain model systems [27-28]. In support of these studies, exogenous addition of NAD^+ delays Wallerian degeneration in response to axotomy in dorsal root ganglion (DRG) cells [29]. In *Drosophila*, however, there is evidence both for [36] and against [30] the role of Nmnat's enzymatic activity for neuroprotection. In the latter model [30], as well as in a new study demonstrating that Nmnat also protects dendrites [31], neuroprotection of axons and dendrites by Nmnat has been attributed to a separate chaperone-like activity [30, 32].

Because it has previously been reported that *Wld*^{S} protects DA terminal fields from 6-OHDA *in vivo* [23], we used a dissociated midbrain culture system to determine if Nmnat1 is responsible for the *Wld*^{S}-mediated neurite protection in DA neurons. We found that the entire *Wld*^{S} sequence is needed for the *Wld*^{S},

neuroprotective phenotype against 6-OHDA in DA neurons and present data showing that NAD^+ cannot protect against 6-OHDA-mediated toxicity.

3.2 Materials and methods:

All of the methods and materials for these set of experiments were performed exactly as described for Chapter 2 with the exception that cultures were treated with 20 μM 6-OHDA with ascorbic acid dissolved in N_2-bubbled water instead of MPP^+ on DIV 7.

3.3 Results

3.3.1 *Wld*^{S} protects DA cell bodies and neurites from 6-OHDA

DA terminal fields but not cell bodies are protected against 6-OHDA treatment in *Wld*^{S} mice [23]. To validate these observations in a more manipulable system, we utilized dissociated cultures of midbrain neurons in which 1-5% of the total cells plated are DA cells [33]. Cultures from *Wld*^{S} mice but not control animals exhibited significant protection of neurites after 6-OHDA treatment (Fig. 3.2A,C). In contrast to *in vivo* results [23], DA cell bodies were also protected from 6-OHDA treatment in *Wld*^{S} versus control cultures (Fig. 3.2A,B), demonstrating that *Wld*^{S} effectively protects neurites (dendrites and axons) as well as cell bodies from a known PD mimetic *in vitro*.

3.3.2 Nmnat1 does not protect DA neurons against 6-OHDA toxicity

Many studies done in PNS model systems have shown that Nmnat1 completely or partially mimics the effects of the entire fusion protein [28, 34]. To determine whether this is true in DA neurons, we transduced primary midbrain cultures from wild type (WT) animals with either GFP, the entire *Wld*^{S} coding region, the 70 amino acid fragment of Ube4b encoded within the *Wld*^{S} gene, Nmnat1, or cytoplasmically-targeted Nmnat1 (cyto Nmnat1) using lentiviral vectors expressing GFP [34] (Fig. 3.2). Western blotting was done to confirm that transductions led to similar expression levels in dissociated cultures (Fig 2.3). Despite equivalent levels of transgene expression, only cell bodies and neurites transduced with the entire coding sequence of *Wld*^{S} were protected from 6-OHDA injury (Fig. 3.2B,C). In addition, although cyto Nmnat1 protects dissociated DRG cultures from vincristine treatment in our studies (Fig 2.4) and in others [35], it was unable to protect DA neurons from 6-OHDA. These data confirm and extend the hypothesis that *Wld*^{S} has a cell type-specific effect in given neuronal populations.

3.3.3 NAD^+ does not protect DA cell bodies and neurites against 6-OHDA

It has been previously reported that exogenous application of NAD^+ on DRGs is neuroprotective [34]. Although transduced Nmnat1 did not rescue DA neurons from 6-OHDA treatment (Fig. 3.2), inadequate levels of viral transduction may have affected the outcome. Conversely, NAD^+ might act in a parallel fashion. Consequently, we tested whether exogenous addition of NAD^+

or one of its precursors (Fig. 3.3) could rescue cell bodies or neurites from 6-OHDA treatment. Dissociated primary midbrain WT cultures were pretreated with either 1 mM NAD^+, *nicotinamide* mononucleotide (NMN), or nicotinic acid mononucleotide (NaMN) 24 hours before addition of the toxin. None of these pretreatments protected against 6-OHDA toxicity (Fig. 3.3) suggesting that the NAD^+-synthesizing activity of *Wld*^{S} is not necessary for its neuroprotective effect against 6-OHDA toxicity.

3.4 Discussion

To date, no consistent hypothesis has emerged on the mechanism(s) underlying *Wld*^{S}-mediated axonal protection. PNS model studies have emphasized the role of Nmnat in protecting axons from various injuries whereas few CNS studies have confirmed this role. Using cellular, molecular and pharmacological tools, our study shows that the *Wld*^{S} protein plays a critical role in protecting DA processes, but not through its NAD^+-synthesizing activity. Specifically, Nmnat1, cyto Nmnat1 and NAD^+ are all able to protect peripheral model systems from toxicity [35,43] whereas none were able to do so in 6-OHDA-treated dissociated DA cultures. These data support the notion that *Wld*^{S} acts in a cell specific manner to rescue neurites from degeneration.

The importance of Nmnat's NAD^+ synthesizing ability is underscored in several studies in which Nmnat's active sites were disrupted and neuroprotection was subsequently lost [28, 34, 36-37]. Moreover, NAD^+ itself and/or some of its biosynthetic precursors, protect against axonal degeneration in different disease

model systems such as *autoimmune encephalomyelitis* [29, 38], ischemia [39-40], Alzheimer's disease [41], and PD [42-44]. In at least one study, addition of NAD^+ was not effective [45]. In addition, a study in *Drosophila* found that Nmnat's enzyme activity is not necessary for axon protection following mechanical injury, excitotoxic or polyglutamine-induced dysfunction [32], suggesting that dNmnat may perform a chaperone-like function [30]. In fact, structural studies of the three different Nmnat isoforms have revealed characteristic similarities to known chaperones such as UspA and Hsp100 [46]. Consistent with this notion, dNmnat was recently shown to function as a stress protein in response to heat shock, hypoxia, and paraquat [47]. However, Nmnat1 does not seem to function as either an axonal protectant or a chaperone in DA neurons.

Our lab has shown that 6-OHDA-oxidized proteins cause ER stress and upregulation of the unfolded protein response (UPR), which regulates protein folding, protein degradation and protein translation leading to cell death of dopaminergic neurons [48]. Activation of UPR-associated proteins such as IRE1*α* was seen in axotomized motoneurons [49], implying a relationship between the UPR and axonal degeneration. More recently, Bernstein *et al*. has found that 6-OHDA-generated ROS induces DNA damage and causes cell death through a p53-dependent mechanism. Cultures from p53 knockout mice exhibited protection of both their cell bodies and neurites against 6-OHDA injury [50]. Thus, 6-OHDA may also cause axonal degeneration through its effect on p53. Finally, 6-OHDA causes rapid mitochondrial depolarization in both human neuroblastoma cell lines (SH-SY5Y) [51-52] and DA neurons [33] demonstrating a direct effect

on mitochondrial function. Since mitochondrial dysfunction can trigger axonal degeneration [53], loss of neurites following 6-OHDA treatment might be entirely due to direct changes in membrane potential.

Given the possible means by which 6-OHDA can cause axonal degeneration, *Wld*^{S} potentially preserves axons against 6-OHDA injury through different mechanisms. For instance, *Wld*^{S} may protect against 6-OHDA toxicity by working as an antioxidant. Mouse embryonic fibroblasts from *Wld*^{S} mice show protection against paraquat, a PD-linked toxin known to generate ROS [54]. Therefore, similar to the case of paraquat, *Wld*^{S} can function as an antioxidant that protects DA axons against 6-OHDA-mediated neurite degeneration. As described before, Nmnat may also have chaperone activity based on studies in *Drosophila* and on structural similarities to identified chaperone proteins. Even though we found that Nmnat1 by itself could not protect DA axons against 6-OHDA, it is still possible that *Wld*^{S} itself has chaperone activity and that the 70 amino acid N-terminal fragment of *Wld*^{S} imparts some necessary function in the preservation of DA neurons. Although Nmnat1 has been linked to SIRT1 activation, an NAD^+-dependent histone deacetylase, which is in turn linked to p53 regulation [55], the fact that neither Nmnat nor NAD^+ rescued DA neurons from 6-OHDA toxicity would make this a less likely regulatory pathway.

In regards to 6-OHDA's effect on the mitochondria, a recent study has found that *Wld*^{S} is able to regulate the mitochondrial permeability transition pore (mPTP) [53], therefore affecting mitochondrial health. This is consistent with other studies showing that striatal synaptosomes isolated from *Wld*^{S} versus WT

animals expressed higher levels of various mitochondrial proteins including the mPTP associated protein, VDAC2 [56]. Therefore, the *Wld*^{S} protein may also protect against 6-OHDA-mediated injury by preserving mitochondrial integrity. Additional studies are underway to explore these possibilities.

In vivo, Wld^S provided remarkable axon protection in a model of anterograde degeneration induced by injection of 6-OHDA into the medial forebrain bundle. But surprisingly, *Wld*^{S} did not confer protection against a retrograde model of DA axon degeneration by injection of 6-OHDA into the striatum [23]. These findings were confirmed by Cheng *et al.* in transgenic mice that express green fluorescent protein using the TH promoter to visualize and quantify DA axons following injury [25]. These results identify a definitive, fundamental difference between mechanisms of anterograde and retrograde degeneration in DA axons. It will be interesting to see whether these findings are recapitulated in vitro using our microchamber devices (Chapter 4).

In support of previous *in vivo* work showing that *Wld*^{S} protects DA terminal fields from 6-OHDA, our study demonstrates that the entire *Wld*^{S} sequence is needed for axonal protection against 6-OHDA-mediated toxicity in dissociated DA cultures. We also show that NAD^+ by itself is not able to confer protection of DA neurons against 6-OHDA. This suggests that the *Wld*^{S} protein may produce a novel gain of function that counteracts the effects of 6-OHDA such as the generation of ROS, activation of UPR, p53 upregulation, and/or mitochondrial dysfunction. Given that PD is the second most common neurodegenerative disorder, our findings support the idea that studies expanding therapeutic efforts

towards maintaining connections as well as saving the cell body will help in developing better interventions for PD.

3.5 Acknowledgements:

This work was supported by National Institutes of Health Grants NS39084 (K.L.O.) and National Institutes of Health Neuroscience Blueprint Core Grant NS057105 to Washington University. This work was also supported by the Bakewell Family Foundation. We thank Steven K. Harmon for technical support and Drs. Michael Coleman, Jeffrey Milbrandt, and Valeria Cavalli for materials and helpful discussions.

References:

1. Dauer W, Przedborski S: **Parkinson's disease: mechanisms and models.** *Neuron* 2003, **39:**889-909.
2. Blum D, Torch S, Lambeng N, Nissou M, Benabid AL, Sadoul R, Verna JM: **Molecular pathways involved in the neurotoxicity of 6-OHDA, dopamine and MPTP: contribution to the apoptotic theory in Parkinson's disease.** *Prog Neurobiol* 2001, **65:**135-172.
3. Braak H, Ghebremedhin E, Rub U, Bratzke H, Del Tredici K: **Stages in the development of Parkinson's disease-related pathology.** *Cell Tissue Res* 2004, **318:**121-134.
4. Bernheimer H, Birkmayer W, Hornykiewicz O, Jellinger K, Seitelberger F: **Brain dopamine and the syndromes of Parkinson and Huntington. Clinical, morphological and neurochemical correlations.** *J Neurol Sci* 1973, **20:**415-455.
5. Scherman D, Desnos C, Darchen F, Pollak P, Javoy-Agid F, Agid Y: **Striatal dopamine deficiency in Parkinson's disease: role of aging.** *Ann Neurol* 1989, **26:**551-557.
6. Riederer P, Wuketich S: **Time course of nigrostriatal degeneration in parkinson's disease. A detailed study of influential factors in human brain amine analysis.** *J Neural Transm* 1976, **38:**277-301.
7. Cheng HC, Ulane CM, Burke RE: **Clinical progression in Parkinson disease and the neurobiology of axons.** *Ann Neurol* 2010, **67:**715-725.
8. Fearnley JM, Lees AJ: **Ageing and Parkinson's disease: substantia nigra regional selectivity.** *Brain* 1991, **114 (Pt 5):**2283-2301.
9. Kramer ML, Schulz-Schaeffer WJ: **Presynaptic alpha-synuclein aggregates, not Lewy bodies, cause neurodegeneration in dementia with Lewy bodies.** *J Neurosci* 2007, **27:**1405-1410.
10. Li Y, Liu W, Oo TF, Wang L, Tang Y, Jackson-Lewis V, Zhou C, Geghman K, Bogdanov M, Przedborski S, et al: **Mutant LRRK2(R1441G) BAC transgenic mice recapitulate cardinal features of Parkinson's disease.** *Nat Neurosci* 2009, **12:**826-828.
11. MacLeod D, Dowman J, Hammond R, Leete T, Inoue K, Abeliovich A: **The familial Parkinsonism gene LRRK2 regulates neurite process morphology.** *Neuron* 2006, **52:**587-593.
12. Herkenham M, Little MD, Bankiewicz K, Yang SC, Markey SP, Johannessen JN: **Selective retention of MPP+ within the monoaminergic systems of the primate brain following MPTP administration: an in vivo autoradiographic study.** *Neuroscience* 1991, **40:**133-158.
13. Serra PA, Sciola L, Delogu MR, Spano A, Monaco G, Miele E, Rocchitta G, Miele M, Migheli R, Desole MS: **The neurotoxin 1-methyl-4-phenyl-1,2,3,6-tetrahydropyridine induces apoptosis in mouse nigrostriatal glia. Relevance to nigral neuronal death and striatal neurochemical changes.** *J Biol Chem* 2002, **277:**34451-34461.

14. Kearns CM, Cass WA, Smoot K, Kryscio R, Gash DM: **GDNF protection against 6-OHDA: time dependence and requirement for protein synthesis.** *J Neurosci* 1997, **17:**7111-7118.
15. Ebert AD, Hann HJ, Bohn MC: **Progressive degeneration of dopamine neurons in 6-hydroxydopamine rat model of Parkinson's disease does not involve activation of caspase-9 and caspase-3.** *J Neurosci Res* 2008, **86:**317-325.
16. Rosenblad C, Kirik D, Bjorklund A: **Sequential administration of GDNF into the substantia nigra and striatum promotes dopamine neuron survival and axonal sprouting but not striatal reinnervation or functional recovery in the partial 6-OHDA lesion model.** *Exp Neurol* 2000, **161:**503-516.
17. Kirik D, Rosenblad C, Bjorklund A: **Preservation of a functional nigrostriatal dopamine pathway by GDNF in the intrastriatal 6-OHDA lesion model depends on the site of administration of the trophic factor.** *Eur J Neurosci* 2000, **12:**3871-3882.
18. Kirik D, Georgievska B, Bjorklund A: **Localized striatal delivery of GDNF as a treatment for Parkinson disease.** *Nat Neurosci* 2004, **7:**105-110.
19. Raff MC, Whitmore AV, Finn JT: **Axonal self-destruction and neurodegeneration.** *Science* 2002, **296:**868-871.
20. Iseki E, Kato M, Marui W, Ueda K, Kosaka K: **A neuropathological study of the disturbance of the nigro-amygdaloid connections in brains from patients with dementia with Lewy bodies.** *J Neurol Sci* 2001, **185:**129-134.
21. Coleman MP, Freeman MR: **Wallerian degeneration, wld(s), and nmnat.** *Annu Rev Neurosci* 2010, **33:**245-267.
22. Mi W, Beirowski B, Gillingwater TH, Adalbert R, Wagner D, Grumme D, Osaka H, Conforti L, Arnhold S, Addicks K, et al: **The slow Wallerian degeneration gene, WldS, inhibits axonal spheroid pathology in gracile axonal dystrophy mice.** *Brain* 2005, **128:**405-416.
23. Sajadi A, Schneider BL, Aebischer P: **Wlds-mediated protection of dopaminergic fibers in an animal model of Parkinson disease.** *Curr Biol* 2004, **14:**326-330.
24. Hasbani DM, O'Malley KL: **Wld(S) mice are protected against the Parkinsonian mimetic MPTP.** *Exp Neurol* 2006, **202:**93-99.
25. Cheng HC, Burke RE: **The Wld(S) mutation delays anterograde, but not retrograde, axonal degeneration of the dopaminergic nigro-striatal pathway in vivo.** *J Neurochem* 2010, **113:**683-691.
26. Fainzilber M, Twiss JL: **Tracking in the Wlds--the hunting of the SIRT and the luring of the Draper.** *Neuron* 2006, **50:**819-821.
27. Sasaki Y, Vohra BP, Lund FE, Milbrandt J: **Nicotinamide mononucleotide adenylyl transferase-mediated axonal protection requires enzymatic activity but not increased levels of neuronal nicotinamide adenine dinucleotide.** *J Neurosci* 2009, **29:**5525-5535.
28. Conforti L, Wilbrey A, Morreale G, Janeckova L, Beirowski B, Adalbert R, Mazzola F, Di Stefano M, Hartley R, Babetto E, et al: **Wld S protein**

requires Nmnat activity and a short N-terminal sequence to protect axons in mice. *J Cell Biol* 2009, **184:**491-500.
29. Sasaki Y, Araki T, Milbrandt J: **Stimulation of nicotinamide adenine dinucleotide biosynthetic pathways delays axonal degeneration after axotomy.** *J Neurosci* 2006, **26:**8484-8491.
30. Zhai RG, Zhang F, Hiesinger PR, Cao Y, Haueter CM, Bellen HJ: **NAD synthase NMNAT acts as a chaperone to protect against neurodegeneration.** *Nature* 2008, **452:**887-891.
31. Wen Y, Parrish JZ, He R, Zhai RG, Kim MD: **Nmnat exerts neuroprotective effects in dendrites and axons.** *Mol Cell Neurosci* 2011.
32. Zhai RG, Cao Y, Hiesinger PR, Zhou Y, Mehta SQ, Schulze KL, Verstreken P, Bellen HJ: **Drosophila NMNAT maintains neural integrity independent of its NAD synthesis activity.** *PLoS Biol* 2006, **4:**e416.
33. Lotharius J, Dugan LL, O'Malley KL: **Distinct mechanisms underlie neurotoxin-mediated cell death in cultured dopaminergic neurons.** *J Neurosci* 1999, **19:**1284-1293.
34. Araki T, Sasaki Y, Milbrandt J: **Increased nuclear NAD biosynthesis and SIRT1 activation prevent axonal degeneration.** *Science* 2004, **305:**1010-1013.
35. Sasaki Y, Vohra BP, Baloh RH, Milbrandt J: **Transgenic mice expressing the Nmnat1 protein manifest robust delay in axonal degeneration in vivo.** *J Neurosci* 2009, **29:**6526-6534.
36. Avery MA, Sheehan AE, Kerr KS, Wang J, Freeman MR: **Wld S requires Nmnat1 enzymatic activity and N16-VCP interactions to suppress Wallerian degeneration.** *J Cell Biol* 2009, **184:**501-513.
37. Yahata N, Yuasa S, Araki T: **Nicotinamide mononucleotide adenylyltransferase expression in mitochondrial matrix delays Wallerian degeneration.** *J Neurosci* 2009, **29:**6276-6284.
38. Kaneko S, Wang J, Kaneko M, Yiu G, Hurrell JM, Chitnis T, Khoury SJ, He Z: **Protecting axonal degeneration by increasing nicotinamide adenine dinucleotide levels in experimental autoimmune encephalomyelitis models.** *J Neurosci* 2006, **26:**9794-9804.
39. Yang J, Klaidman LK, Chang ML, Kem S, Sugawara T, Chan P, Adams JD: **Nicotinamide therapy protects against both necrosis and apoptosis in a stroke model.** *Pharmacol Biochem Behav* 2002, **73:**901-910.
40. Sakakibara Y, Mitha AP, Ayoub IA, Ogilvy CS, Maynard KI: **Delayed treatment with nicotinamide (vitamin B3) reduces the infarct volume following focal cerebral ischemia in spontaneously hypertensive rats, diabetic and non-diabetic Fischer 344 rats.** *Brain Res* 2002, **931:**68-73.
41. Demarin V, Podobnik SS, Storga-Tomic D, Kay G: **Treatment of Alzheimer's disease with stabilized oral nicotinamide adenine dinucleotide: a randomized, double-blind study.** *Drugs Exp Clin Res* 2004, **30:**27-33.

42. Birkmayer JG, Vrecko C, Volc D, Birkmayer W: **Nicotinamide adenine dinucleotide (NADH)--a new therapeutic approach to Parkinson's disease. Comparison of oral and parenteral application.** *Acta Neurol Scand Suppl* 1993, **146:**32-35.
43. Birkmayer JG: **Coenzyme nicotinamide adenine dinucleotide: new therapeutic approach for improving dementia of the Alzheimer type.** *Ann Clin Lab Sci* 1996, **26:**1-9.
44. Kuhn W, Muller T, Winkel R, Danielczik S, Gerstner A, Hacker R, Mattern C, Przuntek H: **Parenteral application of NADH in Parkinson's disease: clinical improvement partially due to stimulation of endogenous levodopa biosynthesis.** *J Neural Transm* 1996, **103:**1187-1193.
45. Conforti L, Fang G, Beirowski B, Wang MS, Sorci L, Asress S, Adalbert R, Silva A, Bridge K, Huang XP, et al: **NAD(+) and axon degeneration revisited: Nmnat1 cannot substitute for Wld(S) to delay Wallerian degeneration.** *Cell Death Differ* 2007, **14:**116-127.
46. Zhai RG, Rizzi M, Garavaglia S: **Nicotinamide/nicotinic acid mononucleotide adenylyltransferase, new insights into an ancient enzyme.** *Cell Mol Life Sci* 2009, **66:**2805-2818.
47. Ali YO, McCormack R, Darr A, Zhai RG: **Nicotinamide Mononucleotide Adenylyltransferase Is a Stress Response Protein Regulated by the Heat Shock Factor/Hypoxia-inducible Factor 1{alpha} Pathway.** *J Biol Chem* 2011, **286:**19089-19099.
48. Holtz WA, O'Malley KL: **Parkinsonian mimetics induce aspects of unfolded protein response in death of dopaminergic neurons.** *J Biol Chem* 2003, **278:**19367-19377.
49. Penas C, Font-Nieves M, Fores J, Petegnief V, Planas A, Navarro X, Casas C: **Autophagy, and BiP level decrease are early key events in retrograde degeneration of motoneurons.** *Cell Death Differ* 2011.
50. Bernstein AI, Garrison SP, Zambetti GP, O'Malley KL: **6-OHDA generated ROS induces DNA damage and p53- and PUMA-dependent cell death.** *Mol Neurodegener* 2011, **6:**2.
51. Gomez-Lazaro M, Bonekamp NA, Galindo MF, Jordan J, Schrader M: **6-Hydroxydopamine (6-OHDA) induces Drp1-dependent mitochondrial fragmentation in SH-SY5Y cells.** *Free Radic Biol Med* 2008, **44:**1960-1969.
52. Tirmenstein MA, Hu CX, Scicchitano MS, Narayanan PK, McFarland DC, Thomas HC, Schwartz LW: **Effects of 6-hydroxydopamine on mitochondrial function and glutathione status in SH-SY5Y human neuroblastoma cells.** *Toxicol In Vitro* 2005, **19:**471-479.
53. Barrientos SA, Martinez NW, Yoo S, Jara JS, Zamorano S, Hetz C, Twiss JL, Alvarez J, Court FA: **Axonal degeneration is mediated by the mitochondrial permeability transition pore.** *J Neurosci* 2011, **31:**966-978.
54. Yu Q, Wang T, Zhou X, Wu J, Chen X, Liu Y, Wu D, Zhai Q: **Wld Reduces Paraquat-Induced Cytotoxicity via SIRT1 in Non-Neuronal Cells by Attenuating the Depletion of NAD.** *PLoS One* 2011, **6:**e21770.

55. Luo J, Nikolaev AY, Imai S, Chen D, Su F, Shiloh A, Guarente L, Gu W: **Negative control of p53 by Sir2alpha promotes cell survival under stress.** *Cell* 2001, **107:**137-148.
56. Wishart TM, Paterson JM, Short DM, Meredith S, Robertson KA, Sutherland C, Cousin MA, Dutia MB, Gillingwater TH: **Differential proteomics analysis of synaptic proteins identifies potential cellular targets and protein mediators of synaptic neuroprotection conferred by the slow Wallerian degeneration (Wlds) gene.** *Mol Cell Proteomics* 2007, **6:**1318-1330.
57. Coleman M: **Axon degeneration mechanisms: commonality amid diversity.** *Nat Rev Neurosci* 2005, **6:**889-898.

Figure 3.1 - *Wld*^{S} protects DA neurons from 6-OHDA toxicity. (A) Schematic of mouse *Wld*^{S} fusion protein structure. GenBank accession number AAG17285, adapted from Coleman (2005). Amino acid residue numbers relative to Ube4b and NMNAT1 are shown [57]. (B) Dissociated DA cultures from both WT and *Wld*^{S} mice were treated with 20 μm 6-OHDA for 24 hours, and processed for TH immunoreactivity. (C) Quantification of TH+ cell bodies and (D) TH+ neurites was done using unbiased stereology. Data are normalized to control cultures and denote the mean ± SEM of representative determinations made in three separate cultures. *p<0.01; **p<0.001.

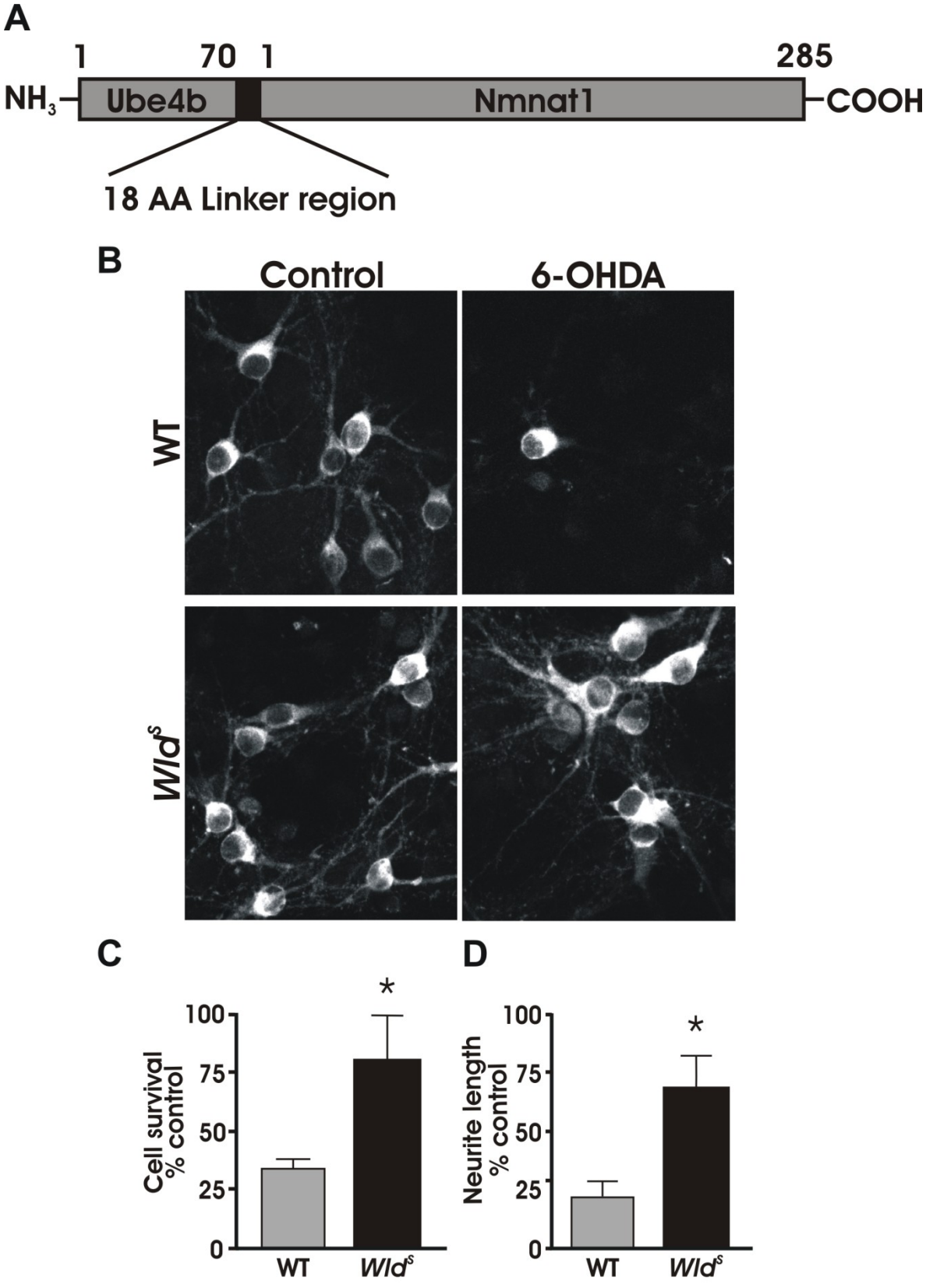
A
1
70
1
285
NH3
Ube4b
Nmnat1
COOH
18 AA Linker region
B
Control
6-OHDA
WT
Wlds
C
D
Cell survival % control
Neurite length % control
100
75
50
25
0
*
WT
Wlds

Fig.3.1

Figure 3.2 - **Nmnat1 by itself does not protect DA neurons from 6-OHDA toxicity.** (A) Dissociated DA cultures from WT mice were transduced with transgenes for GFP, *Wld*^{S}, 70AA-Ube4b, Nmnat1, and cyto Nmnat1 at DIV2 then treated at DIV7 with 20 μm 6-OHDA for 24 hours, and processed for TH immunoreactivity. (B) Quantification of TH+ cell bodies and (C) TH+ neurites show that only *Wld*^{S}-transduced cultures protected cells and neurites against 6-OHDA. Data are normalized to control cultures and denote the mean ± SEM of representative determinations made in three separate cultures. *$p<0.001$.

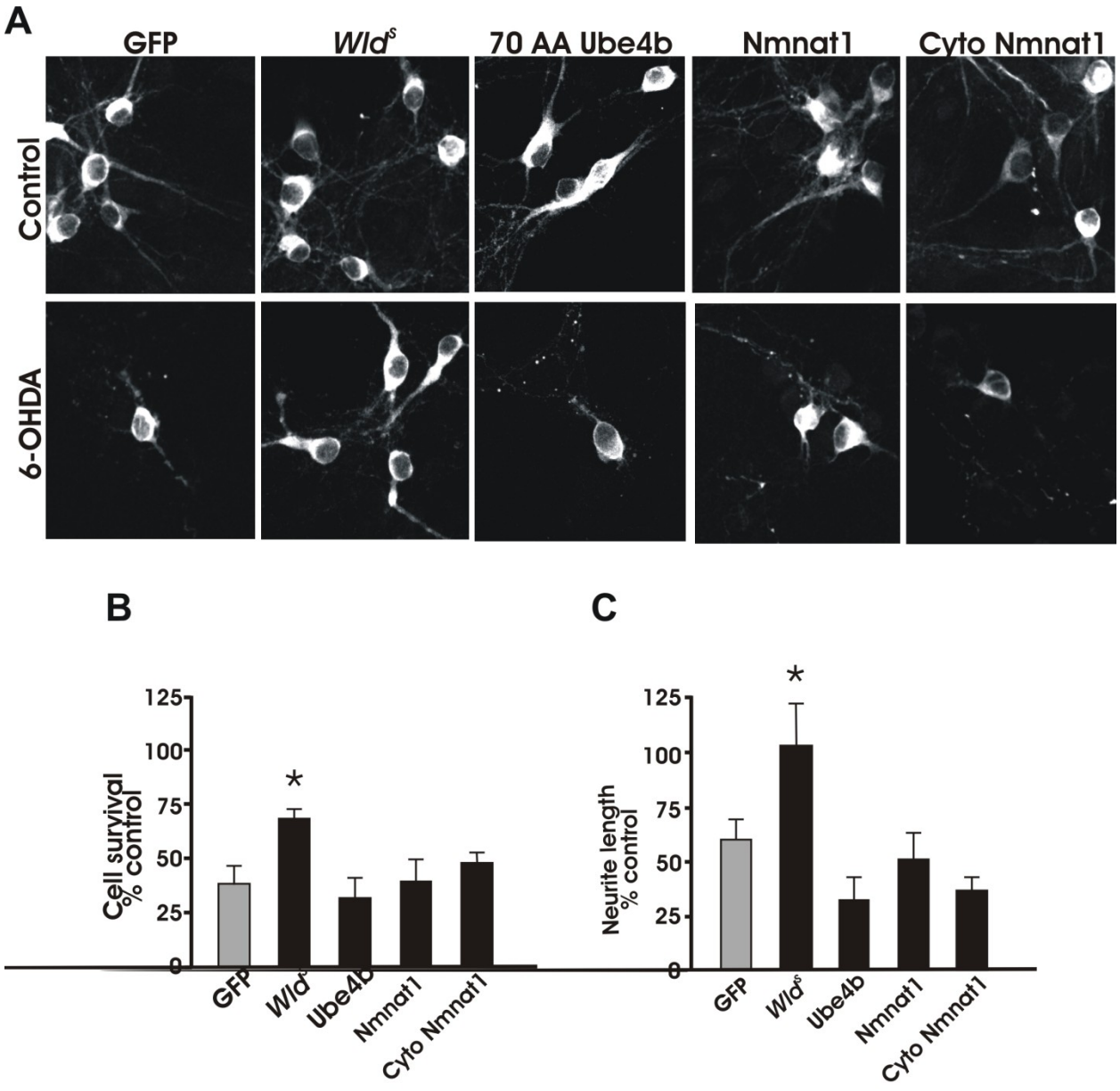
A
GFP
Wld^S
70 AA Ube4b
Nmnat1
Cyto Nmnat1
Control
6-OHDA
B
Cell survival
% control
125
100
75
50
25
0
*
GFP
Wld^S
Ube4b
Nmnat1
Cyto Nmnat1
C
Neurite length
% control
125
100
75
50
25
0
*
GFP
Wld^S
Ube4b
Nmnat1
Cyto Nmnat1

Fig.3.2

Figure 3.3 - NAD^+ does not protect DA cells and neurites from 6-OHDA toxicity. (A) Dissociated WT DA cultures were pretreated with NAD^+, Nmn, or Namn 24 hours before addition of 20 μm 6-OHDA. (B) Quantification of TH+ cell bodies and (C) TH+ neurites show that none of the pretreatments protected cells and neurites from 6-OHDA. Data are normalized to control cultures and denote the mean ± SEM of representative determinations made in three separate cultures.

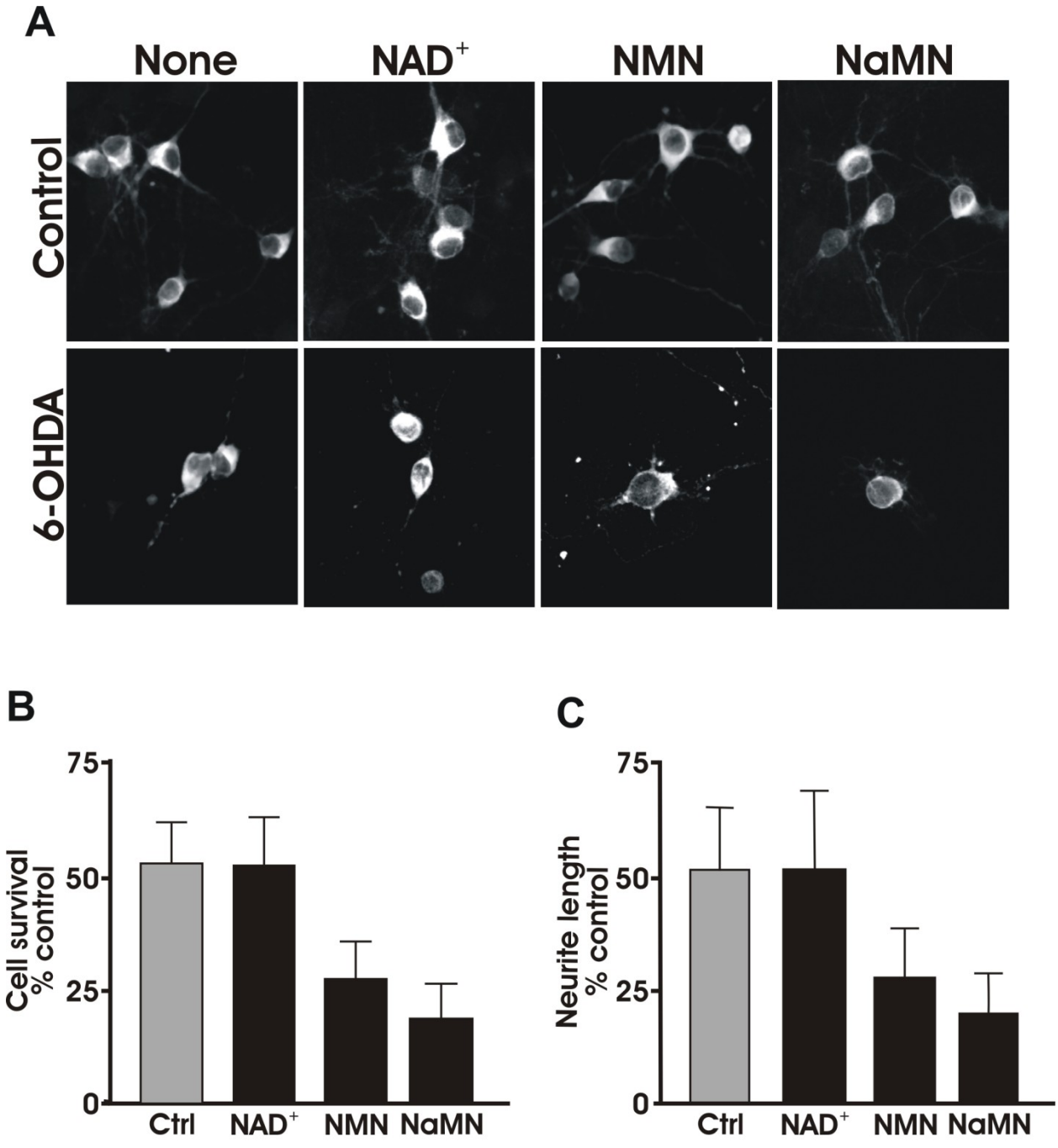
A
None
NAD+
NMN
NaMN
Control
6-OHDA
B
Cell survival
% control
75
50
25
0
Ctrl
NAD+
NMN
NaMN
C
Neurite length
% control
75
50
25
0
Ctrl
NAD+
NMN
NaMN

Fig.3.3

Chapter 4

The Parkinsonian Mimetic, MPP^+, Specifically Impairs Mitochondrial Transport in Dopamine Axons

This manuscript has been published as:

Kim-Han JS*, **Antenor-Dorsey JA***, O'Malley KL. The Parkinsonian Mimetic, MPP^+, Specifically Impairs Mitochondrial Transport in Dopamine Axons. J Neurosci. 2011 May 11;31(19):7212-21.

*J.S.K.-H. and J.A.A.-D. contributed equally to this work.

Abstract

Impaired axonal transport may play a key role in Parkinson's disease. To test this notion, a microchamber system was adapted to segregate axons from cell bodies using green fluorescent protein-labeled mouse dopamine (DA) neurons. Transport was examined in axons challenged with the DA neurotoxin, 1-methyl-4-phenylpyridinium ion (MPP^+). MPP^+ rapidly reduced overall mitochondrial motility in DA axons; among motile mitochondria, anterograde transport was slower yet retrograde transport was increased. Transport effects were specific for DA mitochondria, which were smaller and transported more slowly than their non-DA counterparts. MPP^+ did not affect synaptophysin-tagged vesicles or any other measureable moving particle. Toxin effects on DA mitochondria were not dependent upon ATP, calcium, free radical species, JNK, or caspase3/PKC pathways but were completely blocked by the thiol-anti-oxidant *N*-acetyl-cysteine or membrane-permeable glutathione. Since these drugs also rescued processes from degeneration, these findings emphasize the need to develop therapeutics aimed at axons as well as cell bodies to preserve "normal" circuitry and function as long as possible.

4.1 Introduction

Impaired axonal transport plays an important role in a variety of neurodegenerative disorders, including Parkinson disease (PD) [1]. Postmortem studies on PD patients show widespread axonal pathology that appears to precede the loss of cell bodies [2], supporting the notion that nigral neurons degenerate through a “dying back” axonopathy [3]. Animal models of PD-linked genes also point to axonal impairment as being a critical factor. For example, transgenic mice expressing the PD-linked R1441G LRRK2 mutation exhibit decreased dopamine (DA) terminal fields together with increased dystrophic processes and abnormal axonal swellings, findings consistent with DA axonopathy [4]. Reduced axonal transport is also seen with α-synuclein mutants, which accumulate in the cell soma when overexpressed in cortical neurons [5]. Moreover, vesicle-associated α-synuclein binds to microtubule motor proteins like kinesin and dynein, underscoring a potential role in microtubule-dependent axonal transport [6]. In addition, genetic mutations in Parkin, an E3 ligase, and PINK1, a mitochondrially targeted kinase, lead to impaired mitochondrial dynamics, resulting in altered transport and distribution of mitochondria as well as loss of synaptic function [7]. PINK1 can also form a complex with Miro and Milton [8], proteins known to recruit kinesin to the mitochondria and promote motility along microtubule tracks [9]. Thus, these PD-linked mutations are consistent with the idea that axonal dysfunction plays an early and significant role in the disorder. Environmental toxins mimicking PD such as *N*-methyl-4-phenyl-1,2,3,6-tetrahydropyridine (MPTP) or its active derivative, 1-methyl-4-

phenylpyridinium ion (MPP^+), also disrupt axonal function. MPTP-treated monkeys [10] or mice [11] first lose DA terminal fields and then exhibit cell body loss. Moreover, Wallerian degeneration slow (*WldS*) mutant mice rescue DA projections in MPTP-treated animals but not cell bodies, emphasizing the independence of cell body function versus axon specialization [12]. In addition, MPP^+ can directly inhibit axon transport in the squid axoplasm [13]. Although the mechanisms underlying the latter response are unclear, in vertebrate models MPP^+ depolymerizes microtubules, leading to axon fragmentation and decreased synaptic function [14-15]. Difficulty in assessing real-time changes in DA axons has precluded testing models of structural or trafficking impairment. Although much can be learned from the squid giant axon, this system as well as studies in vertebrate peripheral, cortical, or other non-DA cell types [15], may be unrepresentative of a bona fide DA neuron. Recently, we have adapted a microchamber system in which axons are segregated to one side, leaving cell bodies and dendrites on the other. When used with GFP-labeled DA neurons derived from genetically engineered mice, DA axons can be examined using targeted fluorescent markers and time lapse imaging. Using these chambers, here we show that MPP^+ specifically decreases mitochondrial movement in DA axons. We also explore potential mechanisms underlying the effect of MPP^+ on mitochondrial transport in DA axons.

4.2 Materials and Methods

4.2.1 Cell culture and microchamber devices

Murine mesencephalic cultures were prepared, treated with toxin for indicated time periods, then fixed and stained for tyrosine hydroxylase (TH) as described previously [16]. TH-positive cell bodies and neurites were counted using Stereo Investigator (MBF Bioscience). DA/GFP cultures were prepared from embryonic day 14 Tg(TH-EGFP)DJ76GSAT transgenic mice (Gene Expression Nervous System Atlas, National Institutes of Health, Bethesda, MD). Typically DA/GFP males were mated with wild-type females. Brains isolated from the resulting embryos were screened for GFP fluorescence before midbrain dissection. GFP-positive tissue was pooled and plated. Microchamber devices were modified from Ivins *et al.* [17]. Briefly, 20mmglass bottom culture dishes (MatTek) were coated with 100 μg/ml Matrigel (BD Bioscience), rinsed with DMEM/F-12, and dried. A polytetrafluoroethylene Teflon tubing [17 (outside diameter) x 13 (inside diameter) x 2 (wall thickness) x 5 mm (length)] was cut in half and attached to the bottom of the dish using sterile vacuum grease. A rectangular glass coverslip (9 x 18 mm) was sandwiched between both pieces of Teflon and sealed in place with a Matrigel/collagen complex (1 mg/ml collagen type I, 3 mg/ml Matrigel, DMEM). Isolated neurons (250,000 cells/cm 2) were plated on one side of the chamber in DMEM/F-12, 5% FBS, supplemented with B-27 (Invitrogen) and penicillin/ streptomycin. Axonal chambers were supplemented with 300 μg/ml NetrinI (R&D Systems) to direct axonal outgrowth

under the coverslip. Transport was assessed between days *in vitro* (DIV) 12 and 14.

4.2.2 Determination of cell viability

To determine DA cell viability following MPP^+ treatment both in cell bodies and neurites, mesencephalic cultures were processed for TH immunoreactivity and counted using Stereo Investigator (MBF Bioscience). Briefly, 50 fields were assayed per dish leading to the quantification of 200–300 TH neurons and 2000–5000 neurites/dish. Experiments were repeated 3–5 times using cultures isolated from independent dissections.

4.2.3 Quantification of tubulin

The tubulin-mCherry construct was prepared by replacing the EGFP sequence of pEGFP-tubulin (Invitrogen) with mCherry (Dr. Mike Nonet, Washington University, St. Louis, MO). Neurons were transfected using Lipofectamine 2000 (Invitrogen) at DIV5-6 and imaged 1 d later. Live images were taken at 1, 3, 6, and 24 h after MPP^+ treatment. Tubulin integrity was also measured by immunostaining with antibodies against tyrosine hydroxylase (Pel-Freez Biologicals) and acetylated tubulin (AcTub; Sigma) on the axonal side of microchamber devices. TH-positive axons with at least three AcTub breaks per 40 μm of axon were considered damaged and calculated as the percentage total of all TH-positive axons.

4.2.4 Autophagy

Cells were transfected with a GFP-tagged LC3 expression vector (kindly provided by Dr. Chris Weihl, Washington University) at DIV5-6 as previously reported(Kumaet al., 2007). A day later, cells were treated with 2 μM MPP^+ for the indicated time, fixed, and immunostained with a rabbit anti-TH antibody (Pel-Freez Biologicals). Cy3-conjugated secondary antibodies (Jackson ImmunoResearch Laboratories) were used for visualization. TH-positive neurons with LC3-GFP granules were counted using Stereo Investigator (MBF Bioscience).

4.2.5 Optical imaging

At DIV12–14, mitochondria on the axonal chamber side were labeled with 25 nM MitoTracker Red (MTR; Invitrogen). Plasmids containing mitochondrially targeted Dendra2 and synaptophysin fused in frame with cerulean (Syn-Cer) were provided by Evrogen and Dr. Rachel Wong (University of Washington, Seattle, WA), respectively. Subsequently, mitochondrially targeted Dendra2 and Syn-Cer were inserted into the FUGW lentiviral expression vector provided by Dr. Jeffrey Milbrandt (Washington University). Lentiviral preparations were generated using HEK 293T cells as described previously (Araki et al., 2004). DA/GFP cultures were inoculated with virus at DIV2 for 4–6 h and imaged at DIV12–13. Images were taken using a Zeiss LSM510 Meta NLO Multiphoton System (Carl Zeiss) on Axiovert 200M inverted microscope with 40x water objective [C-Apochromat 40x/1.2W Corr.1.2 numerical aperture, collar correction (0.14–0.18)]

equipped with a 5% CO2/37°C controlled chamber. Filter sets used for visualizing a given fluorescent marker included 488 nm argon laser and 505 long pass emission filter (GFP and Dendra2), 543 nm HeNe laser and 560 long pass emission filter [MTR, tetramethylrhodamine ethyl ester (TMRE), or tubulin-mCherry], and 458 nm argon laser and 466–514 meta emission filter (Syn-Cer). Sixty images at 5 sec intervals were acquired before addition of toxin and then again 30 min after 2 μM MPP^+ treatment.

4.2.6 Image analysis

Kymographs were created using ImageJ/Multiple Kymograph (NIH, Bethesda, MD). In all cases, direction was determined by identifying the axonal terminal from tile scanned images. To calculate particle speed in each direction, the following approach was adopted. Diagonal lines were drawn for each moving particle on a kymograph. Angle and length information were collected for each particle's diagonal line. Distance and time were calculated using the following equations in which 112.5 μm was the frame length, 512 the pixel size, and 5 sec the interval of time-lapse images:

Distance (μm) = (112.5 * {Length * COS[RADIANS(Angle)]})/ 512 (1)

Time (s) = 5 * {-Length * SIN[RADIANS(Angle)]} (2)

Total numbers of particles were obtained using particle analysis with a threshold image. Only particles moving a minimum of 5 μm in length for at least 15 sec

within the imaging time were counted. Particle size was assessed using ImageJ/Particle analysis. Anterograde movements are expressed as positive integers whereas retrograde movement is expressed by negative integers.

4.2.7 [3H]Dopamine release

DA release on the microchamber devices was measured as described previously [18](Lotharius and O'Malley, 2000). Briefly, cells were loaded in both somal and axonal sides with 2.4 μCi/ml [^{3}H]DA/Krebs–Ringer solution for 20 min at 37°C and washed 3 times for 3 min. Radioactive counts from a wash sample were measured using a Beckman scintillation counter and used as a control for basal levels of [^{3}H]DA release. Cells were then treated with MPP^+ for 10 min, and the amount of [^{3}H]DA released during this time period was counted. Cultures were then washed extensively and maintained in [^{3}H]DA-free Krebs–Ringer solution. Following medium collection, cells were lysed in 0.1 N perchloric acid by freeze thawing, and residual, intracellular [^{3}H]DA was measured. Total counts and percentages were calculated.

4.2.8 Mitochondrial membrane potential and size

Cells were loaded with either 50 nM TMRE (Invitrogen) or MTR for 15 min and medium was subsequently added for a final concentration of 25 nM. Mitochondrial potential was assessed based on changes in TMRE fluorescence before and after toxin treatment as described by Ward [19]. The cross area of

axonal mitochondria was estimated by MTR fluorescence using ImageJ/ particle analysis.

4.2.9 Statistical analysis

One-way ANOVA and unpaired two-tailed Student's *t* test were used for statistical analysis (SAS, GraphPad Software).

4.3 Results

4.3.1 MPP^+ causes neuritic degeneration and autophagy before cell body loss

Because MPP^+ serves as a substrate for the plasma membrane DA transporter [20], its toxic effects are highly selective for DA neurons versus the non-DA interneurons that predominate dissociated mesencephalic cultures. Consistent with *in vivo* results showing that loss of DA terminal fields occurs earlier and is more pronounced than cell body loss [10-11], MPP^+ leads to a significant loss of neurites in dissociated DA cultures before cell bodies are affected. As early as 12 hours post-MPP^+ treatment, neurite loss was apparent (Fig. 4.1A). It should be noted that most of the "neurites" measured here have morphological features of proximal dendrites in that they exhibit a wide diameter that tapers away from the cell body. When compartmentalized axons (Fig. 4.2A,B) were assessed for fragmentation at 12 hours, significantly more fragmentation was observed (70.3 $\pm$ 8.9% nontreated axon control versus 50.4 $\pm$

8.4% nontreated dendritic control, p 0.05). These data suggest that axons are more vulnerable than dendrites in the presence of MPP^+. In contrast, TH-positive cell bodies were not significantly reduced until 24 hours later and then by only ~40% (Fig. 4.1B). Because DA uptake sites vary among DA neurons from the substantia nigra pars compacta (SNpc) and ventral tegmental area (VTA) [20] and that the described dissociated DA cultures would contain neurons from both populations, some variability among MPP^+ effects is to be expected. Thus, a 40% death level might represent all of the DA SNpc neurons, yet only a small fraction of DA neurons arising from the VTA.

Since MPP^+ is thought to depolymerize microtubules [14](Cappelletti et al., 2005), we stained DA/GFP cultures with antibodies directed against acetylated α-tubulin, a marker of stable microtubules, and examined DA axons for the presence of beading and/or fragmentation. “Beading” was first observed by 6 h (Fig. 4.1C, arrowheads), although no significant fragmentation was observed at this time point (Fig. 4.1D). To confirm and extend this result, the integrity of tubulin was also assessed by introducing a tubulin-mCherry construct into dissociated DA cultures. The mCherry-positive axons were examined for breaks in DA (GFP+) and non-DA (GFP-) processes at various time points following MPP^+ treatment. Consistent with MPP^+ effects on acetylated α-tubulin, significant axonal disintegration in DA neurons was not seen until 6 hours posttreatment, which exceeded 80% by 24 hours (Fig. 4.1E,F). Together, these data indicate that MPP^+ affects one important component of axonal structure, namely the microtubule tracks, 12–18 hours before significant cell body loss is observed.

MPP^+ has been shown to induce autophagy, a catabolic system to degrade and recycle damaged proteins and/or organelles [21] within 24 hours in DA neurons [22]. To determine whether the disruption of microtubule tracks preceded the induction of autophagic markers such as LC3 (microtubule-associated protein 1, light chain 3; also known as ATG8) [23], we transfected an LC3-GFP clone into DA cultures and measured the appearance of autophagic granules. Under normal conditions, LC3-GFP fluorescence exhibits a diffuse cytoplasmic distribution (Fig. 4.1G). As early as 3 hours after toxin treatment, LC3 takes on a punctuated appearance as it localizes to the inner membrane of forming autophagosomes (Fig. 4.1G,H). This observation confirms and accelerates the timeframe reported by Zhu *et al.* [22]. Moreover, these results suggest that even before damaged microtubules are apparent, other toxin-induced molecular events induce hallmarks of autophagy.

4.3.2 MPP^+ disrupts mitochondrial axonal transport

MPP^+ also inhibits complex I, leading to mitochondrial dysfunction [24]. To analyze mitochondrial movement, size, and membrane potential ($\Delta\Psi_m$) in DA processes, we initially used a microfluidic strategy [25]. However, DA neurons attached poorly and were highly susceptible to shear stress resulting from plating, media changes, and/or toxin addition. Using a simplified chamber design [17], we established compartmented cultures such that: (1) axons were segregated from cell bodies and dendrites; (2) transport direction was easily discerned, imaged, and quantified; and (3) cell bodies or axons could be

independently exposed to drugs, toxins, DNA, etc. (Fig. 4.2A). When we used dissociated cultures from DA/GFP mice, DA axon terminals could be identified via GFP fluorescence (Fig. 4.2B). Immunostaining with the dendritic marker MAP2 (microtubule-associated protein 2) or axon-preferring tau verified that processes that grew under the glass coverslip were axons, not dendrites (Fig. 4.2C). To avoid overlapping fluorescent emissions in analyzing mitochondrial movement, we considered several approaches. These included: (1) lipid-based transfections with mitochondrially targeted DsRed2 (mtDsRed2) and/or the photoactivatable fluorescent protein Dendra2 (mtDendra2); (2) transductions with the same constructs packaged as lentiviral particles; and (3) mitochondrial dyes such as MTR and TMRE. In the first scenario, finding fluorescently labeled mitochondria in DA/GFP axons for live imaging is hampered by the low numbers of DA neurons typically isolated (2–5% of the total) and low transfection efficiencies in these cultures (5%). The second scenario, lentiviral transduction of fluorescent proteins targeted to the mitochondria (mtDsRed2; mtDendra2), was more efficient and, at least with mtDendra2, provided the option of following particles after photoconversion. Caveats associated with the third scenario include the notion that mitochondrial dyes might interfere with mobility [26-27]. Thus we started these studies using a targeted mtDendra2 lentivirus. Although Dendra normally emits at the same wavelength as GFP before excitation, it is easy to discern mitochondrially targeted Dendra in DA axons because the latter typically exhibit a smooth, homogenous pattern of GFP expression distinct from the tubulovesicular appearance of mtDendra2 (Fig. 4.2D). That these structures

represent mitochondria can be shown by colocalization with the fluorescent lipophilic cation TMRE, which rapidly accumulates in mitochondria (Fig. 4.2D). Unfortunately, in our system mtDendra2 did not photoconvert with the efficiency or at the wavelength originally claimed [28]; nonetheless, analysis of nonconverted mtDendra2 particles showed that MPP^+ decreased total numbers of moving mitochondria (Fig. 4.2E,F). Moreover, MPP^+ treatment decreased mitochondrial speeds in the anterograde direction but increased them in the retrograde direction (Fig. 4.2G).

Despite the usefulness of mtDendra2, the small number of DA neurons and variability associated with transduction still made acquiring sufficient data in multiple experimental paradigms logistically challenging. In contrast, mitochondrial dyes have the benefit of labeling all mitochondria within a chamber, ensuring adequate numbers for analysis despite potential limitations such as diffusion of fluorescence, quenching, and interference with bioenergetic states [26]. At least some of these limitations can be overcome when low concentrations (50 nM) of MitoTrackers such as MTR are used [26, 29-31]. In our studies, excellent loading and labeling of mitochondria was achieved using even lower concentrations of MTR (25 nM). At this concentration, MTR labeled exactly the same structures that TMRE did (data not shown). More importantly, when an identical experimental protocol was used to measure MTR-labeled mitochondria, essentially the same results as those for mtDendra2 were produced (Fig. 4.3). In either case, we observed that like other neurons [32], >70% of all axonal mitochondria were stationary [32]. Of those mitochondria that were moving, over

50% had stopped after only 30 min of MPP^+ treatment (Figs. 4.2F, 4.3B). Moreover, the number of moving mitochondria was reduced in either the anterograde or retrograde direction (Figs. 4.2G, 4.3C). In agreement with previously published values [33], motile DA mitochondria moved with an average speed of 0.32 μm/s in the anterograde direction, whereas a slower rate was observed in the retrograde direction (0.26 μm/s) (Figs. 4.2G; 4.3C). Following MPP^+ treatment these rates were reversed: anterograde velocity was reduced whereas retrograde speed was accelerated (Figs. 4.2G, 4.3C). Thus, MPP^+ rapidly affects both the fraction of motile DA mitochondria and the speed at which they travel. These data suggest that in this cell system and at this concentration MTR is a reliable measure of mitochondrial mobility. Importantly, using two different approaches essentially the same results were observed: MPP^+ rapidly reduced overall mitochondrial motility in DA axons; among motile mitochondria, anterograde transport was slower yet retrograde transport was increased.

4.3.3 MPP^+ does not affect vesicular transport

To determine whether MPP^+ affects all cargo movement or just that of mitochondria, DA/GFP cultures in microchamber devices were transduced with a lentivirus expressing Syn-Cer (Fig. 4.4A,B). As shown by others [34], the synaptophysin sequence targets small, rapidly moving particles that do not colocalize with MTR (Fig. 4.4A). Despite inhibiting mitochondrial movement within 30 min, MPP^+ did not affect the number or speed of synaptophysin-tagged particles moving in either direction (Fig. 4.3B–D). Since numerous studies have

also shown that MPP^+ is taken up into vesicular compartments where it rapidly (10 min) leads to the displacement of DA [18], which was reproduced in our microchamber devices (Fig. 4.5), these results emphasize that the presence of a neurotransmitter is not a requirement for transport. As synaptophysin labels only synaptic vesicles, we also examined all moving particles using transmitted light images. After subtracting out mitochondria from MTR-colabeled axons, the remaining particles showed no significant difference in movement following toxin treatment (data not shown). These data underscore the specificity of the MPP^+ effect on mitochondria versus general axonal cargos and also rule out damaged microtubules as a contributing factor in decreased mitochondrial motility.

4.3.4 MPP^+ rapidly depolarizes axonal mitochondria

MPP^+ inhibition of complex I leads to ROS, loss of $\Delta\Psi_m$, and eventually loss of ATP [35]. Previously we showed that MPP^+-induced ROS changes occurred within 15 min in DA cell bodies using dihydrorhodamine and dihydroethidium [16, 36]. Although we could confirm our cell body results, we could not quantitate ROS changes in DA axons with these reagents (data not shown). To determine whether $\Delta\Psi_m$ was altered over the same time period that movement was reduced, segregated DA/GFP axons were labeled with the sensitive $\Delta\Psi_m$ indicator TMRE before acquiring baseline images. After 30 min of toxin treatment, $\Delta\Psi_m$ was significantly reduced in DA (79.8 $\pm$ 7.23% decrease in TMRE fluorescence) (Fig. 4.6B) but not non-DA axonal mitochondria ($\leq$ 12.9 $\pm$ 7.34% TMRE fluorescent decrease) (Fig. 4.6B), highlighting the DA-specific

nature of the MPP^+ effects. Because bioenergetic declines are thought to shift fusion/fission dynamics toward fission, resulting in smaller mitochondria [37], we measured mitochondrial size. Although TMRE-labeled mitochondria appeared to undergo a decrease in size (Fig. 4.6A), this was due to the loss of TMRE fluorescence since MPP^+ treatment did not decrease the size of MTR-labeled axonal mitochondria (Fig. 4.6C). Thus, MPP^+ rapidly depolarized DA mitochondria but did not reduce their size, at least in the time frame tested. Collectively, these results are consistent with recent work in hippocampal neurons showing that depolarized mitochondria travel more rapidly in a retrograde direction [38].

4.3.5 Thiol-based reagents rescue disrupted transport, neurites, and cells

What are the underlying mechanisms associated with MPP^+-mediated alterations in transport? Conceivably, MPP^+-compromised mitochondria block transport due to the ATP dependency of the molecular motors. In the squid axoplasm preparation, however, MPP^+ effects on fast axonal transport were independent of ATP production. Rather, MPP^+ treatment led to axonal activation of caspase-3, which in turn cleaved PKC_δ into its catalytically active fragment [13]. Like the squid preparation, increasing ATP levels in bona fide DA axons via glucose preincubation (ATP levels increased from $3.93 \pm 0.20 \times 10^{-12}$ to $4.88 \pm 0.11 \times 10^{-12}$ mole/μg of protein, p-value = 0.002) did not rescue MPP^+ effects on mitochondrial motility (Table 4.1). One caveat to this finding is that there are no methodologies to measure ATP levels *in situ*. Thus, we cannot rule

out the possibility that regional variations in ATP levels might underlie the loss of mitochondrial movement. Unlike the invertebrate preparation, neither the PKC (Go¨6976) nor the caspase inhibitor, Csp3I-II, blocked MPP^+ effects in DA axons (Table 4.1) although both inhibitors significantly blocked 6-OHDA-induced DA cell death (Go¨6976: 45.94 $\pm$ 11.48% and Csp3I-II: 50.70 $\pm$ 11.58% protection). We also tested whether Ca^{2+} chelators would affect mitochondrial transport since Ca^{2+} plays a role in axonal loss [39] and is also implicated in DA neurodegeneration [40]. Neither EGTA nor BAPTA-AM prevented MPP^+-disrupted mitochondrial transport at concentrations showing intracellular Ca^{2+} changes in axons using Oregon Green (data not shown). Because axonal injury induces activation of the c-Jun N-terminal kinase (JNK) family in the peripheral nervous system [41], we examined whether the general JNK inhibitor SP600125 could rescue toxin-blocked mitochondrial motility in segregated DA axons. SP600125 did not affect mitochondrial trafficking (Table 4.1) nor did it prevent MPP^+-mediated DA cell death at a concentration that was effective for blocking *t*-butylhydroperoxide induced DA cell death (64.08 $\pm$ 2.18% protection). Given that MPP^+ generates ROS via inhibition of complex I or via release of vesicular DA followed by its cytoplasmic oxidation [16, 42], we tested *N* acetylcysteine (NAC; precursor of glutathione), Mn(III)tetrakis(4-benzoic acid) porphyrin (MnTBAP, a superoxide dismutase mimetic), and glutathione monoethyl ester (GSHEE; membrane-permeable GSH) as axonal protectants. Remarkably, pretreatment with the redox-sensitive neuroprotectants NAC and GSHEE completely rescued MPP^+-induced changes in numbers of motile mitochondria, whereas the anti-

oxidant, MnTBAP was ineffective at a concentration of 100 μM (Table 4.1). Moreover, NAC pretreatment not only rescued mitochondrial motility but also MPP^+-induced neurite and cell body loss (Fig. 4.7). Thus, NAC or similar drugs can potentially be useful therapeutic tools. Although these differences may simply reflect extruded axoplasm responses versus an intact axon, they may also reflect clear differences between vertebrate and invertebrate mitochondrial trafficking systems and indicate that redox equilibria may play a critical role in at least the mammalian processes.

4.3.6 DA mitochondria are smaller and slower than non-DA mitochondria

Recent studies show that nigral DA neurons have lower numbers of mitochondria in their cell bodies and dendrites than non-DA neurons [43]. To determine whether differences exist in organelle size or movement between DA and non-DA axons, we measured various critical attributes of axonal mitochondria and synaptophysin-tagged vesicles (Table 4.2). Consistent with the *in vivo* study [43], DA mitochondria are about half the size of non-DA mitochondria and are transported almost three times slower. Although the density of mitochondria along the axon is the same, there are fewer moving mitochondria in DA versus non-DA axons. Mitochondrial membrane potential is the same. Similarly, the number of moving vesicles per unit length axon is reduced in DA versus non-DA axons, but their speed is not (Table 4.2). No difference was found in other general moving particles. Importantly, non DA mitochondria were not affected by MPP^+ in terms of size, mobility, or speed (Table 4.3). Given that

these data were acquired from the same experiments in which DA axons were analyzed, they serve as useful internal controls showing that the loss of signal or change in parameter is not due to bleaching caused by imaging or other non-specific effects. Together, these data suggest that DA axons may be more susceptible to dysfunction than non-DA axons due to innate differences in axonal mitochondrial characteristics.

4.4 Discussion

Mounting evidence suggests that axonal dysfunction precedes the death of cell bodies in many neurodegenerative disorders, especially PD. The present study uses cellular, optical, and pharmacological techniques to provide new insights into the biological changes underlying toxin-mediated DA axonal impairment. Results demonstrate: (1) that the PD-mimetic MPP^+ affects DA neuritic processes and microtubule tracks 12–18 hours before cell bodies appear altered, and neuritic autophagic puncta are visible by 3 hours; (2) MPP^+ halts mitochondrial trafficking in DA but not non-DA axons within 30 min, an event which precedes autophagy and loss of microtubules; (3) remaining motile mitochondria exhibit decreased anterograde movement but increased retrograde trafficking; (4) MPP^+ effects are specific for mitochondria, as synaptophysin tagged vesicles and other detectable moving particles continue normal movements in either direction; (5) decreased mitochondrial trafficking is accompanied by a loss of $\Delta\Psi_m$; (6) loss of mitochondrial movement is not associated with ATP loss but rather redox changes; (7) DA mitochondria are

smaller and slower than non-DA organelles, suggesting cell type-specific differences exist for axonal mitochondria.

Although widely used as an animal model of PD, the mechanism by which MPP^+ kills DA neurons remains equivocal. Previously we have shown that MPP^+ induces a protein synthesis-dependent yet caspase-independent cell death in DA neurons that is partially mediated by ROS [16]. In those studies and this one, DA cell bodies die over a period of 48 hours following toxin treatment, although early loss of neurites is consistently observed [16] (Fig. 4.1). Increased free radical species such as mitochondrial superoxide have been proposed as an important mechanism underlying the neurotoxicity of MPP^+ [44]. Previously, however, we have shown that MPP^+-induced ROS are primarily derived from toxin-released vesicular DA [18] (Fig. 4.5). Since redistributed, cytoplasmic DA is thought to form a number of oxidized toxic metabolites, including DA quinones [45], it is perhaps not surprising that MnTBAP, a cell permeable SOD mimetic, did not show a protective effect. Conceivably, other types of ROS, including hydroxyl radicals and/or nitric oxide [44, 46-47], might also play a role in MPP^+-mediated neurotoxicity. What role, if any, these factors play in axonal transport awaits future study.

Recently, Cartelli et al. [15] also reported that MPP^+ affects mitochondrial trafficking in the pheochromocytoma cell line PC12. In this study, however, MPP^+ led to microtubule impairment before transport dysfunction. In contrast, the present findings show that mitochondrial dysfunction (30 min) (Figs. 4.2, 4.3, 4.6) precedes microtubule fragmentation in DA axons (Fig. 4.1). Although microtubule

polymerization is a GTP dependent process [48], it is also controlled by ATP dependent pathways. For example, the energy-sensing AMP activated protein kinase is required for microtubule stabilization [49]. Conceivably, MPP^+-mediated energy deprivation over the course of 6 h may underlie microtubule fragmentation (Fig. 4.1).

A direct effect of MPP^+ on axonal transport was first seen in the isolated squid axoplasm [13]. Despite the evolutionary distance between the squid and mouse, in both cases MPP^+ decreased anterograde trafficking while increasing retrograde movement. However, in the squid axoplasm, MPP^+ affected all organelles and vesicles moving via fast axonal transport, whereas in *bona fide* DA neurons, toxin-mediated effects were specific for mitochondria. Although model preparations such as the squid axoplasm and/or the noradrenergic peripheral tumor cell line can yield valuable insights, our results underscore the uniqueness of a midbrain DA neuron. Indeed, the rapidity and specificity of MPP^+ actions on DA axons are striking: toxin effects on mitochondria occur hours before microtubule tracks fall apart and before cell bodies are lost (Fig. 4.1). Moreover, neither non-DA mitochondria nor any other detectable type of moving particle is affected by toxin treatment, confirming the integrity of the microtubule tracks (Table 4.2). Together, these data point to an early and profound toxin-mediated block of mitochondrial trafficking those results in mitochondrial redistribution away from the synapse back to the soma. Conceivably, damaged mitochondria moving toward the soma could deliver signals from the axon to the cell body, leading to the initiation of cell death.

Mitochondria undergo complex yet continual processes of fusion and fission that are critical for the exchange of organelle contents, repolarization, or degradation by autophagy [50]. Two PD-linked genes that are ubiquitously expressed have also been implicated in this process. Current data indicate that PINK1 is selectively stabilized on depolarized mitochondrial membranes [51]. This in turn acts as a signal for Parkin recruitment, which tags Pink-positive depolarized mitochondria for destruction via autophagy [51-53]. The latter studies would predict that following MPP^+ treatment and bioenergetic declines, PINK1 will be stabilized and Parkin will then be recruited to the PINK-tagged organelles before the appearance of autophagic puncta in DA axons. One caveat to this model, however, is that the previous studies were conducted in cell lines. A recent report examining PINK1 recruitment of Parkin in bona fide neurons did not see depolarization-mediated Parkin recruitment or autophagy [54]. Thus, other mechanisms may also contribute to the induction of these processes in neurons.

In addition to its role in monitoring mitochondrial dynamics [7], PINK1 might directly affect mitochondrial motility since it also forms a complex with Miro and Milton [8]. The latter proteins are known to recruit kinesin to the mitochondria and promote motility along microtubule tracks [9]. Recently, an ROS-independent, redox dependentprotein termed HUMMR (hypoxia upregulated mitochondrial movement regulator) was discovered that also interacts with Milton and Miro to influence mitochondrial movement and direction [55]. Knockdown of HUMMR decreased anterograde movement of mitochondria and increased retrograde movement [55]. Given that MPP^+-disrupted mitochondria exhibited

decreased anterograde and increased retrograde movement and that only the redox protectants NAC and GSHEE prevented these axonal effects, it may be possible that HUMMR, in conjunction with PINK1/Milton and Miro, plays a role in this process. Although MPP^+-decreased $\Delta\Psi_m$ may be sufficient to reduce and alter mitochondrial movement, whether these or other transport-associated proteins play ancillary roles awaits future studies.

A recent study suggests that somal and dendritic DA mitochondria occupy only 40% of the area of non-DA mitochondria [43]. Our cross-sectional measurements of mitochondria in DA axons versus non-DA axons mirror these results, with DA mitochondria being only 40% of the size of their non-DA counterparts (Table 4.2). Most importantly, axonal DA mitochondria exhibit an instantaneous velocity that is almost three times slower than non-DA mitochondria (Table 4.2). The validity of these observations is underscored by the use of two different mechanisms to measure mitochondrial properties (MTR and mtDendra2) (Table 4.2) with essentially the same results. Moreover, since all measurements were taken from within the same axonal fields, even if absolute numbers were affected by experimental conditions, the actual results are relative to each other. Presumably, this reflects inherent differences in DA axonal mitochondria themselves; perhaps a unique outer membrane protein interacts with a scaffolding protein that, in turn, binds to a slower motor. Alternatively, DA axons might be slightly narrower, slowing larger organelles and potentially contributing to their smaller size. Thus, in addition to producing a transmitter prone to oxidation [45] and reliance upon L-type Ca^{2+} channels that appear to

drain ATP resources [56], DA neurons might also be less effective at delivering mitochondria to sites of high energy usage such as synapses.

Redistribution of mitochondria away from sites of high ATP usage would lead to axonal impairment, loss of synaptic connectivity, and hence loss of function. Although mitochondrial redistribution may not be the sole trigger of axonal dysfunction, it occurs early and is consistent with increased mitochondrial staining in the cell body (data not shown). This study, together with the large amount of evidence suggesting that PD is associated with axonal "dying-back," underscores the necessity of developing therapeutics aimed at axons as well as cell bodies so as to preserve circuitry and function. Because NAC pretreatment not only prevented mitochondrial dysfunction but also preserved neurites and cell bodies, NAC or drugs like it may serve a future therapeutic role.

4.5 Acknowledgements

This work was supported by National Institutes of Health Grants NS39084 (K.L.O.) and National Institutes of Health Neuroscience Blueprint Core Grant NS057105 to Washington University. This work was also supported by the Bakewell Family Foundation. We thank Steven K. Harmon, Manouela Valtcheva, Diane Ma, and Scott Elman for technical support and data analysis and Drs. Mike Nonet, Rachel Wong, Jeffrey Milbrandt, and Chris Weihl for plasmid constructs. We also thank Drs. Paul Bridgman and Valeria Cavalli for helpful discussions.

References:

1. De Vos KJ, Grierson AJ, Ackerley S, Miller CC: **Role of axonal transport in neurodegenerative diseases.** *Annu Rev Neurosci* 2008, **31:**151-173.
2. Orimo S, Uchihara T, Nakamura A, Mori F, Ikeuchi T, Onodera O, Nishizawa M, Ishikawa A, Kakita A, Wakabayashi K, Takahashi H: **Cardiac sympathetic denervation in Parkinson's disease linked to SNCA duplication.** *Acta Neuropathol* 2008, **116:**575-577.
3. Raff MC, Whitmore AV, Finn JT: **Axonal self-destruction and neurodegeneration.** *Science* 2002, **296:**868-871.
4. Li Y, Liu W, Oo TF, Wang L, Tang Y, Jackson-Lewis V, Zhou C, Geghman K, Bogdanov M, Przedborski S, et al: **Mutant LRRK2(R1441G) BAC transgenic mice recapitulate cardinal features of Parkinson's disease.** *Nat Neurosci* 2009, **12:**826-828.
5. Saha AR, Hill J, Utton MA, Asuni AA, Ackerley S, Grierson AJ, Miller CC, Davies AM, Buchman VL, Anderton BH, Hanger DP: **Parkinson's disease alpha-synuclein mutations exhibit defective axonal transport in cultured neurons.** *J Cell Sci* 2004, **117:**1017-1024.
6. Yang ML, Hasadsri L, Woods WS, George JM: **Dynamic transport and localization of alpha-synuclein in primary hippocampal neurons.** *Mol Neurodegener* 2010, **5:**9.
7. Bueler H: **Impaired mitochondrial dynamics and function in the pathogenesis of Parkinson's disease.** *Exp Neurol* 2009, **218:**235-246.
8. Weihofen A, Thomas KJ, Ostaszewski BL, Cookson MR, Selkoe DJ: **Pink1 forms a multiprotein complex with Miro and Milton, linking Pink1 function to mitochondrial trafficking.** *Biochemistry* 2009, **48:**2045-2052.
9. Reis K, Fransson A, Aspenstrom P: **The Miro GTPases: at the heart of the mitochondrial transport machinery.** *FEBS Lett* 2009, **583:**1391-1398.
10. Meissner W, Prunier C, Guilloteau D, Chalon S, Gross CE, Bezard E: **Time-course of nigrostriatal degeneration in a progressive MPTP-lesioned macaque model of Parkinson's disease.** *Mol Neurobiol* 2003, **28:**209-218.
11. Serra PA, Sciola L, Delogu MR, Spano A, Monaco G, Miele E, Rocchitta G, Miele M, Migheli R, Desole MS: **The neurotoxin 1-methyl-4-phenyl-1,2,3,6-tetrahydropyridine induces apoptosis in mouse nigrostriatal glia. Relevance to nigral neuronal death and striatal neurochemical changes.** *J Biol Chem* 2002, **277:**34451-34461.
12. Hasbani DM, O'Malley KL: **Wld(S) mice are protected against the Parkinsonian mimetic MPTP.** *Exp Neurol* 2006, **202:**93-99.
13. Morfini G, Pigino G, Opalach K, Serulle Y, Moreira JE, Sugimori M, Llinas RR, Brady ST: **1-Methyl-4-phenylpyridinium affects fast axonal transport by activation of caspase and protein kinase C.** *Proc Natl Acad Sci U S A* 2007, **104:**2442-2447.

14. Cappelletti G, Surrey T, Maci R: **The parkinsonism producing neurotoxin MPP+ affects microtubule dynamics by acting as a destabilising factor.** *FEBS Lett* 2005, **579:**4781-4786.
15. Cartelli D, Ronchi C, Maggioni MG, Rodighiero S, Giavini E, Cappelletti G: **Microtubule dysfunction precedes transport impairment and mitochondria damage in MPP+ -induced neurodegeneration.** *J Neurochem* 2010, **115:**247-258.
16. Lotharius J, Dugan LL, O'Malley KL: **Distinct mechanisms underlie neurotoxin-mediated cell death in cultured dopaminergic neurons.** *J Neurosci* 1999, **19:**1284-1293.
17. Ivins KJ, Bui ET, Cotman CW: **Beta-amyloid induces local neurite degeneration in cultured hippocampal neurons: evidence for neuritic apoptosis.** *Neurobiol Dis* 1998, **5:**365-378.
18. Lotharius J, O'Malley KL: **The parkinsonism-inducing drug 1-methyl-4-phenylpyridinium triggers intracellular dopamine oxidation. A novel mechanism of toxicity.** *J Biol Chem* 2000, **275:**38581-38588.
19. Ward MW: **Quantitative analysis of membrane potentials.** *Methods Mol Biol* 2010, **591:**335-351.
20. Storch A, Ludolph AC, Schwarz J: **Dopamine transporter: involvement in selective dopaminergic neurotoxicity and degeneration.** *J Neural Transm* 2004, **111:**1267-1286.
21. Yang Z, Klionsky DJ: **Mammalian autophagy: core molecular machinery and signaling regulation.** *Curr Opin Cell Biol* 2010, **22:**124-131.
22. Zhu JH, Horbinski C, Guo F, Watkins S, Uchiyama Y, Chu CT: **Regulation of autophagy by extracellular signal-regulated protein kinases during 1-methyl-4-phenylpyridinium-induced cell death.** *Am J Pathol* 2007, **170:**75-86.
23. Kadowaki M, Karim MR: **Cytosolic LC3 ratio as a quantitative index of macroautophagy.** *Methods Enzymol* 2009, **452:**199-213.
24. Murphy MP, Krueger MJ, Sablin SO, Ramsay RR, Singer TP: **Inhibition of complex I by hydrophobic analogues of N-methyl-4-phenylpyridinium (MPP+) and the use of an ion-selective electrode to measure their accumulation by mitochondria and electron-transport particles.** *Biochem J* 1995, **306 (Pt 2):**359-365.
25. Taylor AM, Blurton-Jones M, Rhee SW, Cribbs DH, Cotman CW, Jeon NL: **A microfluidic culture platform for CNS axonal injury, regeneration and transport.** *Nat Methods* 2005, **2:**599-605.
26. Buckman JF, Hernandez H, Kress GJ, Votyakova TV, Pal S, Reynolds IJ: **MitoTracker labeling in primary neuronal and astrocytic cultures: influence of mitochondrial membrane potential and oxidants.** *J Neurosci Methods* 2001, **104:**165-176.
27. Wang X, Schwarz TL: **Imaging axonal transport of mitochondria.** *Methods Enzymol* 2009, **457:**319-333.
28. Gurskaya NG, Verkhusha VV, Shcheglov AS, Staroverov DB, Chepurnykh TV, Fradkov AF, Lukyanov S, Lukyanov KA: **Engineering of a**

monomeric green-to-red photoactivatable fluorescent protein induced by blue light. *Nat Biotechnol* 2006, **24:**461-465.
29. Rui Y, Tiwari P, Xie Z, Zheng JQ: **Acute impairment of mitochondrial trafficking by beta-amyloid peptides in hippocampal neurons.** *J Neurosci* 2006, **26:**10480-10487.
30. Konzack S, Thies E, Marx A, Mandelkow EM, Mandelkow E: **Swimming against the tide: mobility of the microtubule-associated protein tau in neurons.** *J Neurosci* 2007, **27:**9916-9927.
31. Trimmer PA, Schwartz KM, Borland MK, De Taboada L, Streeter J, Oron U: **Reduced axonal transport in Parkinson's disease cybrid neurites is restored by light therapy.** *Mol Neurodegener* 2009, **4:**26.
32. Kang JS, Tian JH, Pan PY, Zald P, Li C, Deng C, Sheng ZH: **Docking of axonal mitochondria by syntaphilin controls their mobility and affects short-term facilitation.** *Cell* 2008, **132:**137-148.
33. Brown A: **Axonal transport of membranous and nonmembranous cargoes: a unified perspective.** *J Cell Biol* 2003, **160:**817-821.
34. Nakata T, Terada S, Hirokawa N: **Visualization of the dynamics of synaptic vesicle and plasma membrane proteins in living axons.** *J Cell Biol* 1998, **140:**659-674.
35. Ali SF, David SN, Newport GD, Cadet JL, Slikker W, Jr.: **MPTP-induced oxidative stress and neurotoxicity are age-dependent: evidence from measures of reactive oxygen species and striatal dopamine levels.** *Synapse* 1994, **18:**27-34.
36. Lotharius J, O'Malley KL: **Role of mitochondrial dysfunction and dopamine-dependent oxidative stress in amphetamine-induced toxicity.** *Ann Neurol* 2001, **49:**79-89.
37. Benard G, Bellance N, James D, Parrone P, Fernandez H, Letellier T, Rossignol R: **Mitochondrial bioenergetics and structural network organization.** *J Cell Sci* 2007, **120:**838-848.
38. Gerencser AA, Nicholls DG: **Measurement of instantaneous velocity vectors of organelle transport: mitochondrial transport and bioenergetics in hippocampal neurons.** *Biophys J* 2008, **95:**3079-3099.
39. Stirling DP, Stys PK: **Mechanisms of axonal injury: internodal nanocomplexes and calcium deregulation.** *Trends Mol Med*, **16:**160-170.
40. Surmeier DJ: **Calcium, ageing, and neuronal vulnerability in Parkinson's disease.** *Lancet Neurol* 2007, **6:**933-938.
41. Abe N, Cavalli V: **Nerve injury signaling.** *Curr Opin Neurobiol* 2008, **18:**276-283.
42. Lotharius J, Brundin P: **Pathogenesis of Parkinson's disease: dopamine, vesicles and alpha-synuclein.** *Nat Rev Neurosci* 2002, **3:**932-942.
43. Liang CL, Wang TT, Luby-Phelps K, German DC: **Mitochondria mass is low in mouse substantia nigra dopamine neurons: implications for Parkinson's disease.** *Exp Neurol* 2007, **203:**370-380.

44. Jackson-Lewis V, Smeyne RJ: **MPTP and SNpc DA neuronal vulnerability: role of dopamine, superoxide and nitric oxide in neurotoxicity. Minireview.** *Neurotox Res* 2005, **7:**193-202.
45. Hastings TG: **The role of dopamine oxidation in mitochondrial dysfunction: implications for Parkinson's disease.** *J Bioenerg Biomembr* 2009, **41:**469-472.
46. Obata T: **Nitric oxide and MPP+-induced hydroxyl radical generation.** *J Neural Transm* 2006, **113:**1131-1144.
47. Yokoyama H, Kuroiwa H, Yano R, Araki T: **Targeting reactive oxygen species, reactive nitrogen species and inflammation in MPTP neurotoxicity and Parkinson's disease.** *Neurol Sci* 2008, **29:**293-301.
48. Carlier MF, Pantaloni D: **Kinetic analysis of guanosine 5'-triphosphate hydrolysis associated with tubulin polymerization.** *Biochemistry* 1981, **20:**1918-1924.
49. Nakano A, Kato H, Watanabe T, Min KD, Yamazaki S, Asano Y, Seguchi O, Higo S, Shintani Y, Asanuma H, et al: **AMPK controls the speed of microtubule polymerization and directional cell migration through CLIP-170 phosphorylation.** *Nat Cell Biol* 2010, **12:**583-590.
50. Chen H, Chan DC: **Mitochondrial dynamics--fusion, fission, movement, and mitophagy--in neurodegenerative diseases.** *Hum Mol Genet* 2009, **18:**R169-176.
51. Matsuda N, Sato S, Shiba K, Okatsu K, Saisho K, Gautier CA, Sou YS, Saiki S, Kawajiri S, Sato F, et al: **PINK1 stabilized by mitochondrial depolarization recruits Parkin to damaged mitochondria and activates latent Parkin for mitophagy.** *J Cell Biol*, **189:**211-221.
52. Narendra D, Tanaka A, Suen DF, Youle RJ: **Parkin is recruited selectively to impaired mitochondria and promotes their autophagy.** *J Cell Biol* 2008, **183:**795-803.
53. Narendra DP, Jin SM, Tanaka A, Suen DF, Gautier CA, Shen J, Cookson MR, Youle RJ: **PINK1 is selectively stabilized on impaired mitochondria to activate Parkin.** *PLoS Biol* 2010, **8:**e1000298.
54. Van Laar VS, Arnold B, Cassady SJ, Chu CT, Burton EA, Berman SB: **Bioenergetics of neurons inhibit the translocation response of Parkin following rapid mitochondrial depolarization.** *Hum Mol Genet* 2011, **20:**927-940.
55. Li Y, Lim S, Hoffman D, Aspenstrom P, Federoff HJ, Rempe DA: **HUMMR, a hypoxia- and HIF-1alpha-inducible protein, alters mitochondrial distribution and transport.** *J Cell Biol* 2009, **185:**1065-1081.
56. Chan CS, Gertler TS, Surmeier DJ: **A molecular basis for the increased vulnerability of substantia nigra dopamine neurons in aging and Parkinson's disease.** *Mov Disord* 2010, **25 Suppl 1:**S63-70.

Table 4.1 - Effects of substrates, inhibitors, and anti-oxidants on MPP^+-disrupted mitochondrial axonal transport.

	Motile mitochondria (%)
Control	18.41 ± 3.62
MPP^+	8.25 ± 1.34 [a]
+ Glucose	6.19 ± 1.26
+ Csp3I- II	10.96 ± 2.58
+ Gö6976	6.16 ± 3.42
+ EGTA	4.80 ± 2.70
+ SP600125	4.63 ± 0.63
+ MnTBAP	9.49 ± 1.51
+ NAC	18.62 ± 3.53[b]
+ GSHEE	15.49 ± 3.10[b]

Numbers are mean ± SEM, [a]$p<0.05$ compared to Control, [b]$p<0.05$ compared to MPP^+. Concentration: MPP^+ (2 μM), Glucose (20 mM), Csp3I-II (Caspase-3 inhibitor II, 5 μM), Gö6976 (500 nM), EGTA (2.5 mM), SP600125 (10 μM), MnTBAP(100 μM), NAC (N-acetylcysteine, 2.5 mM), GSHEE (5 mM).

Table 4.2 - DA axons exhibit unique mitochondrial and vesicular characteristics

		DA	non-DA
Density‡		8.89 ± 0.86	9.50 ± 0.82
Moving particles‡		1.93 ± 0.22	2.49 ± 0.24*
Speed (μm/s)			
	MTR	0.28 ± 0.05	0.79 ± 0.07**
	mtDendra2	0.30 ± 0.02	0.61 ± 0.11**
Cross area (μm^2)			
	MTR	1.07 ± 0.12	2.52 ± 0.11**
	mtDendra2	0.94 ± 0.06	2.17 ± 0.47*
Ψ_m (AU)		58.5 ± 3.22	65.2 ± 4.08
Synaptic vesicles			
Moving particles‡		3.93 ± 0.30	5.71 ± 0.63*
Speed (μm/s)		0.56 ± 0.05	0.52 ± 0.03
All particles			
Moving particles‡		6.35 ± 1.22	6.79 ± 0.48
Speed (μm/s)		0.12 ± 0.01	0.14 ± 0.01

‡ (#/100 μm). Numbers are mean ± SEM, *p<0.05, **p<0.001 compared to DA neurons. For MTR studies, 33 dishes from 11 independent experiments were evaluated; for mtDendra2 studies, eight dishes from four independent experiments were assessed. For synaptic vesicles, three dishes from three independent experiments were assessed. When measuring all particles, seven dishes from seven independent experiments were measured. In all cases 3-5 axons per dish were analyzed.

Table 4.3 - MPP^+ did not affect mitochondrial number, speed or size in non-DA axons

		Control	MPP^+
Moving particles (#/100 μm)			
	MTR	2.49 ± 0.24	2.01 ± 0.23
	mtDendra2	1.92 ± 0.61	2.48 ± 0.14
Speed (μm/s)			
	MTR	0.79 ± 0.07	0.71 ± 0.09
	mtDendra2	0.61 ± 0.11	0.65 ± 0.19
Cross area (μm^2)			
	MTR	2.52 ± 0.11	2.36 ± 0.19
	mtDendra2	2.17 ± 0.47	2.57 ±0.46

Numbers are mean ± SEM. For MTR studies, 33 dishes from 11 independent experiments were evaluated; for mtDendra2 studies, eight dishes from four independent experiments were assessed. In all cases 3-5 axons per dish were analyzed.

Figure 4.1 - Neurite degeneration, microtubule disruption, and autophagy precede DA cell death following MPP^+ treatment. (A) Dissociated DA neurons were treated with 1 μM MPP^+ for indicated times and then fixed and immunostained with rabbit polyclonal anti TH antibody. (B) Quantification of TH-positive cell bodies and neurites remaining after toxin treatment. Numbers of TH-positive cell bodies and neurites were counted using Stereo Investigator. Neurites were significantly reduced after 12 hours of treatment, whereas the number of cell bodies did not significantly change until 24 hours. Data denote the mean ± SEM of representative determinations made in three independent experiments. (C) Integrity of microtubule tracks was assessed by measuring tubulin fragmentation before and after MPP^+ treatment. Compartmented axons (described below) were fixed after 3, 6, and 24 hours of MPP^+ treatment and stained with antibodies directed against AcTub and TH. Beading is seen as early as 6 hours (insert, arrowheads) and fragmentation at 24 hours (arrow). (D) TH-positive axons with fragmented acetylated tubulin were quantified. One hundred to three hundred TH-positive axons were counted per dish and three dishes were counted per group. (E) Integrity of microtubule tracks was also assessed by transfecting tubulin-mCherry into DA/GFP cultures at DIV6. Following the addition of 2 mM MPP^+, live images were acquired at the indicated times. (F) Tubulin intensity was expressed as percentage control. Mean ± SEM made in three independent experiments, **p*0.05, ***p*0.001, compared to 0 hours; #*p*0.05, compared to DA at 24 hours. (G) Autophagy was assessed by introducing a GFP-tagged LC3 expression clone at DIV6 and treating DA neurons 1 day later

with 2 μM MPP^+.The formation of LC3-positive granules was measured as indicated by immunostaining. Lower panels show LC3 fluorescence within TH-positive axons before (top) and after (bottom) toxin treatment. For clarity, only LC3 fluorescence in axons is shown. (H) The number of TH-positive neurons with at least three LC3-GFP granules was counted and expressed as percentage of all neurons that were both TH positive and LC3-GFP positive, regardless of whether the LC3-GFP signal in these neurons was diffuse or punctuate. Mean + SEM in three independent experiments, **p*0.05. In all bar graphs, hatching indicates toxin treatment. Scale bars: (A,C,E) 10 μm (G) 1 μm.

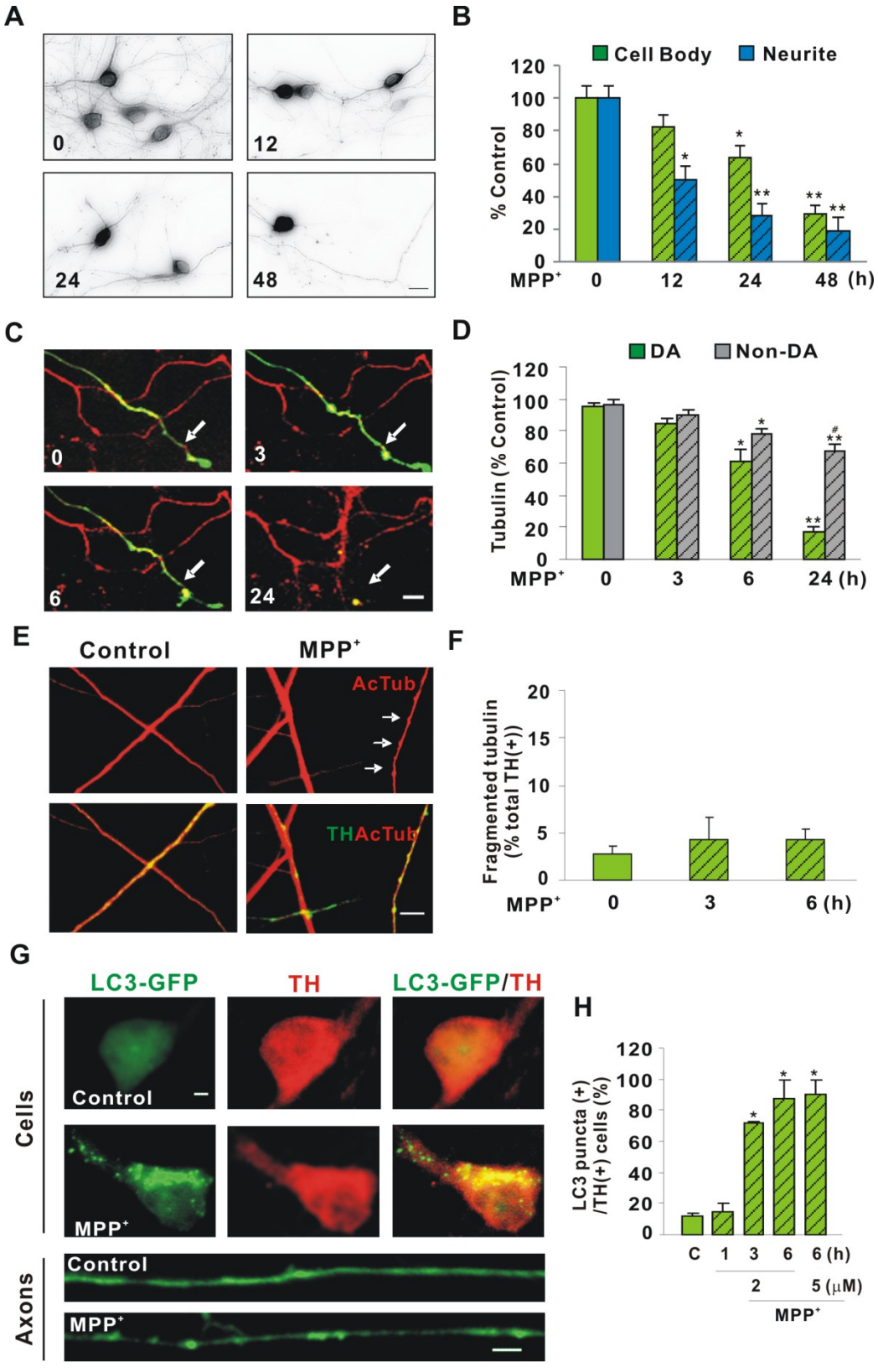
A
0
12
24
48
B
Cell Body
Neurite
% Control
120
100
80
60
40
20
0
MPP+ 0 12 24 48 (h)
C
0
3
6
24
D
DA
Non-DA
Tubulin (% Control)
120
100
80
60
40
20
0
MPP+ 0 3 6 24 (h)
E
Control
MPP+
AcTub
THAcTub
F
Fragmented tubulin (% total TH(+))
20
15
10
5
0
MPP+ 0 3 6 (h)
G
LC3-GFP
TH
LC3-GFP/TH
Cells
Control
MPP+
Axons
Control
MPP+
H
LC3 puncta (+) /TH(+) cells (%)
120
100
80
60
40
20
0
C 1 3 6 6 (h)
2 5 (μM)
MPP+

Fig.4.1

Figure 4.2 – MPP^+ rapidly decreases mitochondrial movement in DA axons as shown by mtDendra2. (A) Diagram of microchamber device. (B) Transmitted light image of segregated axons derived from DIV12 DA/GFP cultures in the top panel, GFP fluorescence in the middle panel, and the merged image in the bottom panel showing TH-positive and TH-negative axons in same field. (C) Immunostaining of the axonal side with TH, the axonal marker Tau, and the dendritic marker MAP2. Tau but not MAP2 positive processes is present on axonal side. Scale bar, 10 μm. (D) mtDendra2 colocalizes with TMRE. Despite presence of nonconverted mtDendra2, DA axon is easily identified. (E) Axonal movement of mitochondria. Mitochondria labeled with mtDendra2 were imaged for 5 min at 5 sec intervals after 30 min incubation with and without 2 μM MPP^+. For consistency, mitochondrial measurements were assessed near the axon terminal at least 2 mm away from the cell bodies. Resulting kymographs are shown below. (F) Number of moving mitochondria per 100 μm length of axon was calculated. (G) Speed was calculated as described in Materials and Methods. (F,G) Mean ± SEM, **p*0.05, total of 17 (control) and 14 (MPP^+-treated) axons derived from at least 7 dishes in 3 independent experiments. The anterograde speed (Antero) was decreased and the retrograde speed (Retro) increased as early as 30 min after MPP^+ treatment. Scale bars: (B-D) 10 μm. Hatching indicates toxin treatment.

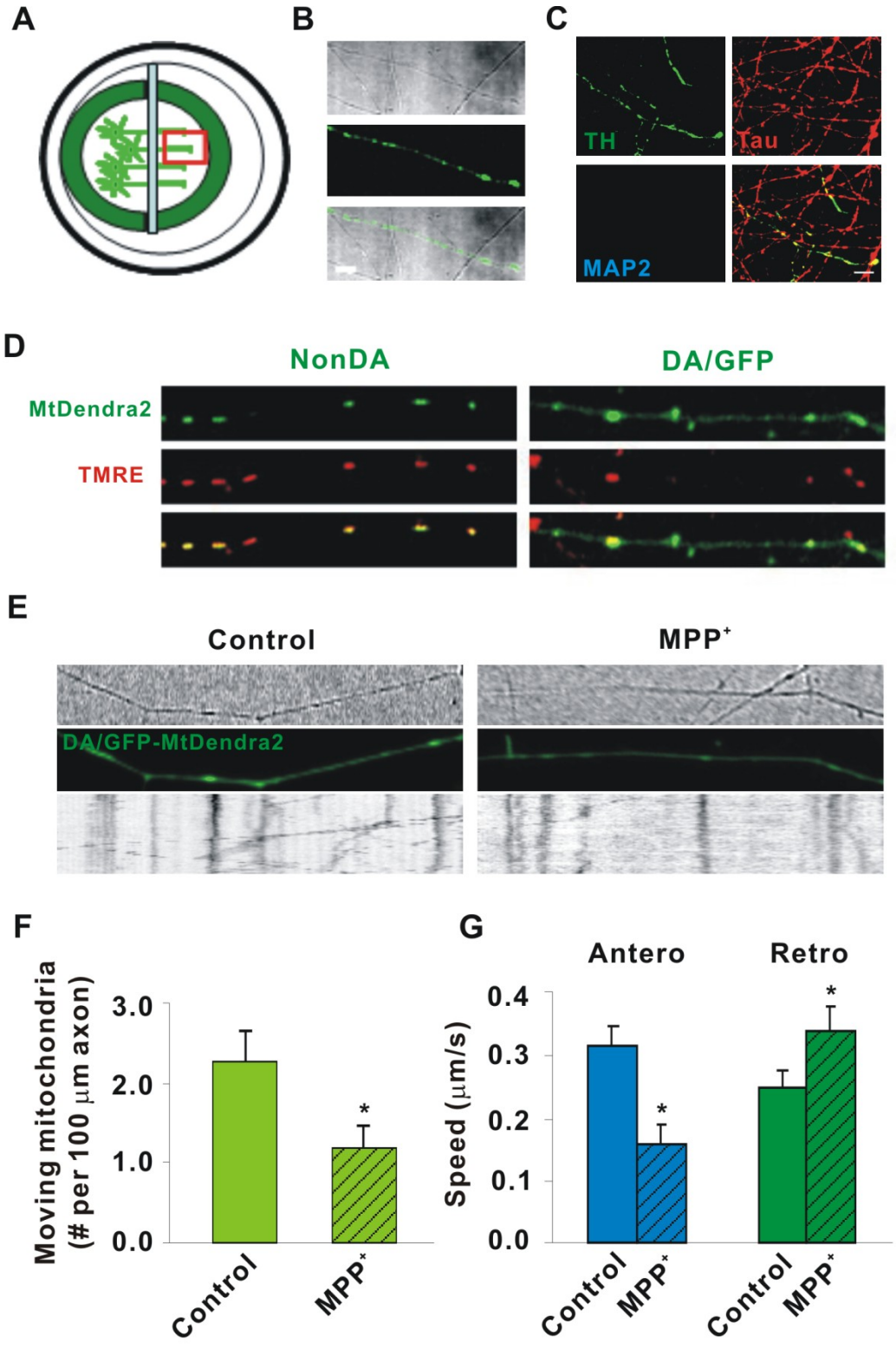
A
B
C
TH
Tau
MAP2
D
NonDA
DA/GFP
MtDendra2
TMRE
E
Control
MPP+
DA/GFP-MtDendra2
F
Moving mitochondria (# per 100 μm axon)
3.0
2.0
1.0
0.0
*
Control
MPP+
G
Antero
Retro
Speed (μm/s)
0.4
0.3
0.2
0.1
0.0
*
*
Control
MPP+
Control
MPP+

Fig.4.2

Figure 4.3 – MPP^+ rapidly decreases mitochondrial movement in DA axons as shown by MitoTracker Red. (A) Axonal movement of mitochondria. Mitochondria were labeled with 25 nM MTR and imaged for 5 min at 5 sec intervals after 30 min of incubation with and without 2 μM MPP^+. Mitochondrial measurements were assessed as described in Figure 2. Resulting kymographs are shown below. (B) Total and moving mitochondria were counted and the rate of motile mitochondria was calculated. (C) Speed was calculated as described in Materials and Methods. (B,C) Mean ± SEM, **p*0.05, total of 114 (control) and 175 (MPP^+-treated) axons from 15 and 28 dishes in 13 independent experiments. Total length of control and MPP^+-treated axons sampled were 10,716 and 16,732 μm, respectively, and the total numbers of mitochondria examined were 1762 and 2632, respectively. The anterograde speed (Antero) was decreased and the retrograde speed (Retro) increased as early as 30 min after MPP^+ treatment. Hatching indicates toxin treatment.

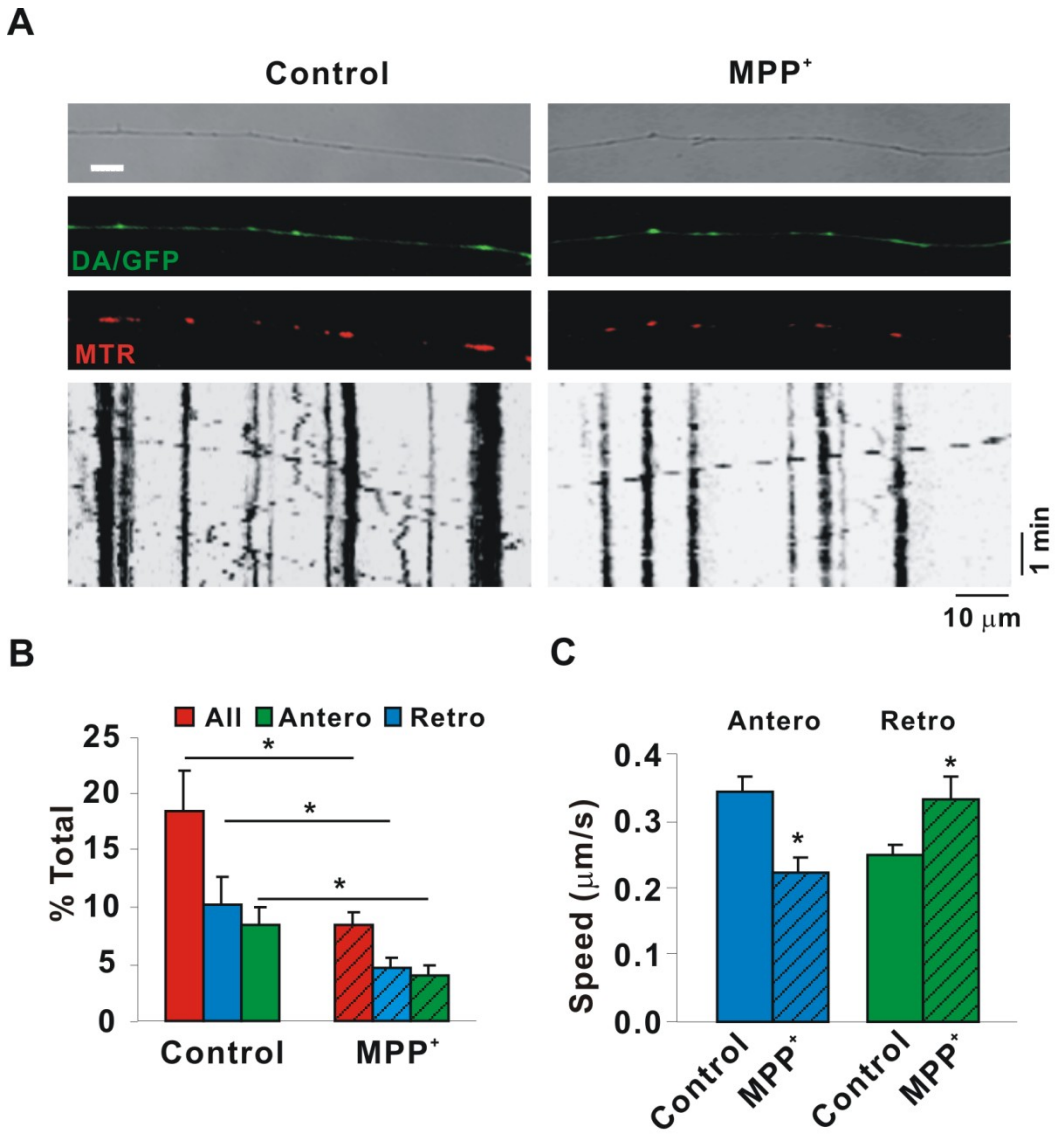
A
Control
MPP+
DA/GFP
MTR
1 min
10 μm
B
All
Antero
Retro
% Total
25
20
15
10
5
0
*
*
*
Control
MPP+
C
Antero
Retro
Speed (μm/s)
0.4
0.3
0.2
0.1
0.0
*
*
Control
MPP+
Control
MPP+

Fig.4.3

Figure 4.4 – MPP^+ does not affect axonal movement of synaptic vesicles. Dissociated DA/GFP cultures were transduced with Syn-Cer lentivirus at DIV2. Vesicular movement was assessed on DIV12–13 before and after toxin treatment. (A) Although some vesicles were clumped and appeared to overlap mitochondria, individual vesicles labeled with Syn-Cer (arrows) were also visualized adjacent to mitochondria labeled with MTR (arrowheads). (B) Vesicular movement was observed for 5 min before and after 30 min of incubation with and without 2 μM MPP^+. Because of the smaller size of vesicular particles and the relative "dimness" of the cerulean emission, tracks of moving particles are shown below for clarity. (C,D) Quantification of moving particles (C) and speed (D) were determined as described in Materials and Methods. Scale bar: 10 μm. Mean ± SEM, ns, nonsignificant, total of 25 (control) and 38 (MPP^+-treated) axons from 4 and 5 dishes in 4 independent experiments. Total lengths of control and MPP^+-treated axons sampled were 2247 and 3497 μm, respectively. Hatching indicates toxin treatment.

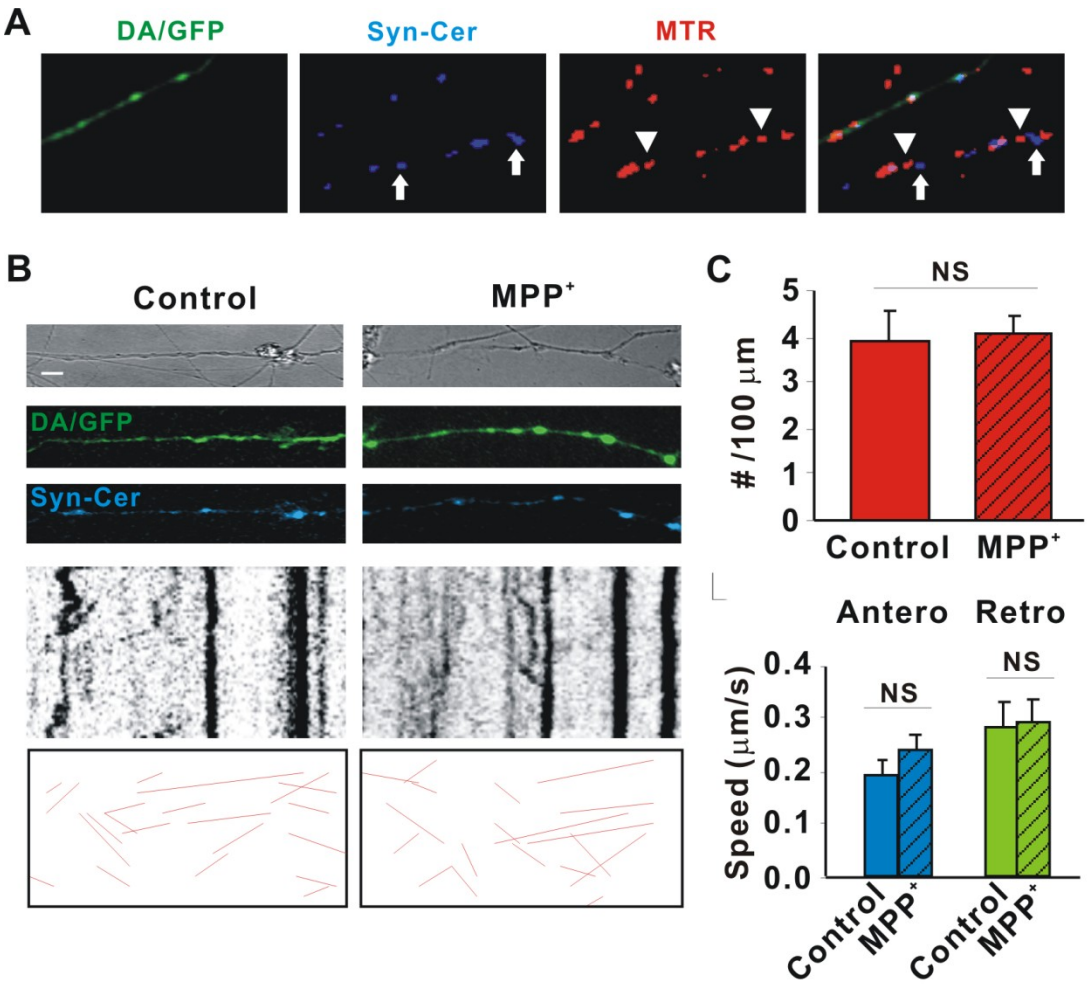
A
DA/GFP
Syn-Cer
MTR
B
Control
MPP+
DA/GFP
Syn-Cer
C
NS
/100 μm
5
4
3
2
1
0
Control
MPP+
Antero
Retro
Speed (μm/s)
0.4
0.3
0.2
0.1
0.0
NS
NS
Control
MPP+
Control
MPP+

Fig.4.4

Figure 4.5 - MPP^+ rapidly leads to DA efflux. ^{3}H-DA release assays were performed exactly as we have previously described except that 10 min treatment windows were used instead of 6 min [18]. (A) MPP^+ dose response curve; EC_{50} for DA release is 0.42 ± 0.04 μM (mean ± SEM). (B) MPP^+-mediated DA release can also be assessed in segregated axons. Each chamber was briefly incubated with ^{3}H-DA, washed extensively with PBS and then treated with or without 1 μM MPP^+ for 10 min. Chambers were washed and then treated with 60 mM K^+ to release vesicular contents and finally lysed to assess remaining DA levels [18]. Top panel, high K^+ releases 50-60% of intracellular DA levels in control cell bodies and axons whereas, 1 μM MPP^+ releases >95% (Bottom panel). Axon-only chamber represented about 25% of transmitter levels in cell body chamber.

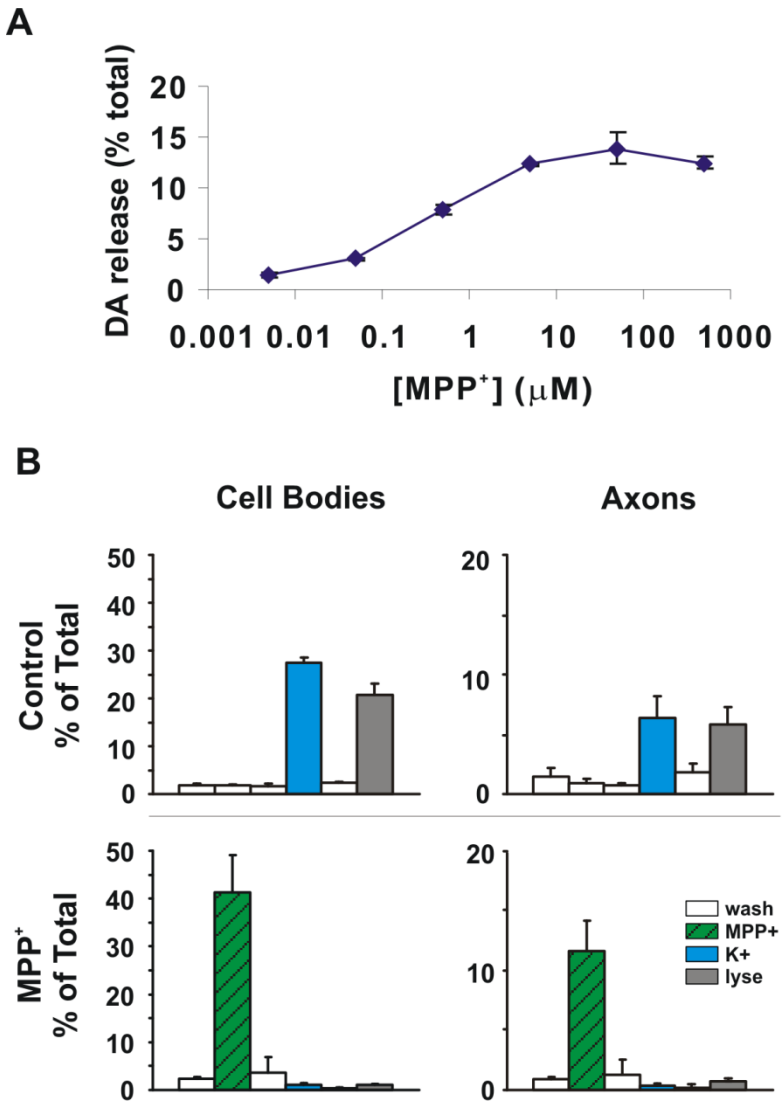
A
DA release (% total)
20
15
10
5
0
0.001 0.01 0.1 1 10 100 1000
[MPP+] (μM)
B
Cell Bodies
Axons
Control
% of Total
MPP+
% of Total
50
40
30
20
10
0
wash
MPP+
K+
lyse

Fig.4.5

Figure 4.6 - MPP^+ rapidly depolarizes DA mitochondria. (A) Mitochondria in axons from DA/GFP cultures were labeled with 25 nM TMRE and then assessed before and 30 min after MPP^+ treatment. Scale bar: 5 μm (B) MPP^+ led to significant differences in $\Delta\Psi_m$ as measured in arbitrary units (AU; arrows). (C) Cross sectional areas of mitochondria labeled with MTR were measured before and after toxin treatment using Image J particle analysis. Hatching indicates toxin treatment. (Mean ± SEM of representative determinations from three independent experiments, **p<0.001)

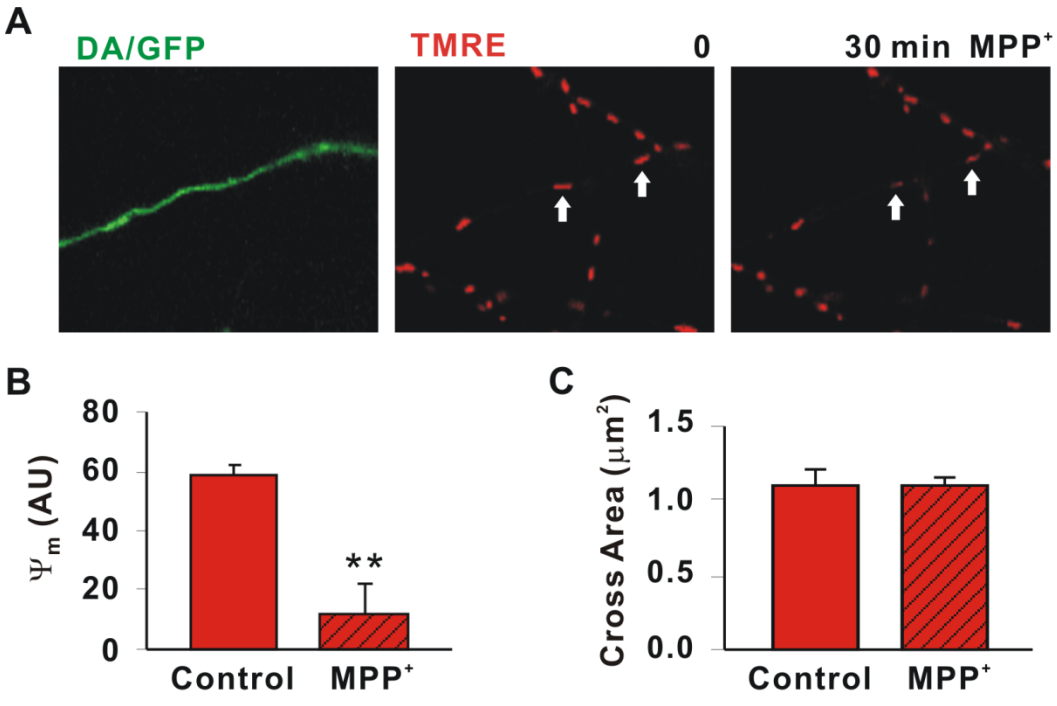
A
DA/GFP
TMRE
0
30 min MPP+
B
Ψm (AU)
80
60
40
20
0
**
Control
MPP+
C
Cross Area (μm2)
1.5
1.0
0.5
0.0
Control
MPP+

Fig.4.6

Figure 4.7 - NAC protects DA cell bodies and neurites from MPP^+-induced degeneration. (A) Dissociated DA neurons were pretreated with 2.5 mM NAC for 18 hours, treated with 2 μM MPP^+ for 24 hours and then fixed and immunostained with rabbit polyclonal anti-TH antibody. Scale bar: 10 μm (B) Quantification of TH-positive cell bodies and neurites. Cell bodies and neurites were significantly protected by NAC. (Mean ± SEM from three independent experiments, *$p<0.05$, compared to Control, #: $p<0.05$, ##: $p<0.001$, compared to MPP^+)

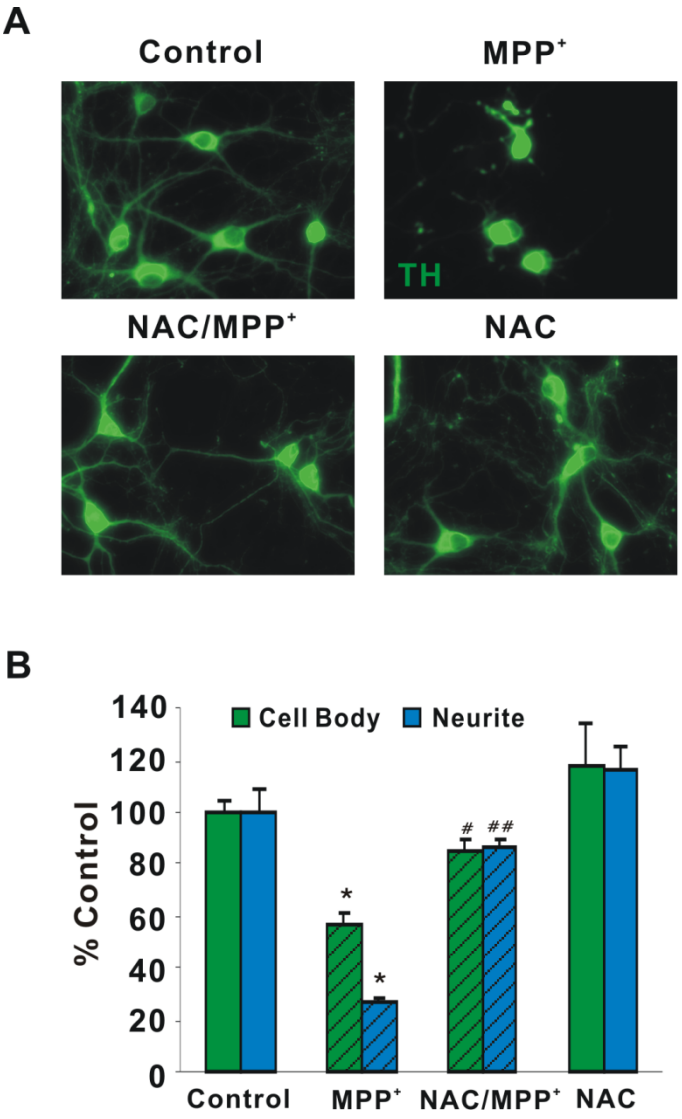
A
Control
MPP+
TH
NAC/MPP+
NAC
B
Cell Body
Neurite
% Control
140
120
100
80
60
40
20
0
*
*
#
##
Control
MPP+
NAC/MPP+
NAC

Fig.4.7

Chapter 5

Wld^{S} protects dopaminergic axons from MPP^{+}-induced changes in mitochondrial transport

This manuscript is in preparation for publication

Abstract

An emerging hypothesis in Parkinson's disease (PD) is that dopaminergic (DA) neurons degenerate through a "dying back" axonopathy wherein degeneration begins in the distal axon and progresses over time towards the cell body. Impaired axonal transport also appears to play an early, pivotal role in PD. Thus processes that delay axonal transport dysfunction and/or axonal degeneration might slow PD progression. Previously, our lab has found that the *Wld*^{S} mouse mutant ("Wallerian degeneration-slow"), which exhibits delayed axonal degeneration after peripheral axonopathy, also protects DA terminal fields from the PD-mimetic 1-methyl-4-phenyl-1,2,3,6-tetrahydropyridine (MPTP) *in vivo*. To understand the mechanisms underlying *Wld*^{S}-mediated axonal protection, we utilized compartmented chambers that enabled us to segregate axons from cell bodies and dendrites. Using these devices, we found that MPP^+ impaired mitochondrial in DA axons and that *Wld*^{S} rescued MPP^+-mediated impairment of mitochondrial transport in DA axons. Mechanistically, this appears to be the result of *Wld*^{S}-mediated protection from toxin-induced loss of mitochondrial membrane potential. These results extend *Wld*^{S} protection to CNS DA axons and suggest that *Wld*^{S} confers a gain-of-function phenotype that attenuates mitochondrial dysfunction. This study also underscores the necessity of developing therapeutics aimed at axons as well as cell bodies in order to preserve circuitry and function.

5.1 Introduction

Parkinson's disease (PD) is the second most common neurodegenerative disorder in the U.S. The cardinal motor symptoms of PD include resting tremor, bradykinesia, rigidity, and abnormal gait [1-2]. These symptoms appear after 50-70% [3-4] of striatal dopamine (DA) levels have been depleted and 30-50% [5-6] of the DA cells in the substantia nigra (SN) have died. Given that the severity of PD symptoms correlates better with loss of striatal DA [5] and because many postmortem studies show widespread axonal pathology [7,8], early axonal dysfunction may play a significant role in PD.

Data from animal models of PD support the notion that DA axons are compromised prior to cell body loss. For example, transgenic mice expressing the PD-linked R1441G leucine-rich repeat kinase2 (LRRK2) mutation exhibited decreased DA terminal fields and increased dystrophic processes yet only modest changes were seen in the number of their SN neurons. [7]. In addition, mutant α-synuclein proteins accumulate in the cell soma when overexpressed in cortical neurons suggesting that these mutants exhibit reduced axonal transport [8]. Support for this notion comes from data showing that vesicle-associated α-synuclein binds to the microtubule motor proteins kinesin and dynein [9], thereby affecting microtubule-dependent axonal transport. Another PD-linked gene, PINK1, a mitochondrially targeted kinase, can also form a complex with Miro and Milton [10], proteins known to recruit kinesin to the mitochondria and promote motility along microtubule tracks [11]. Finally, in some but not all model systems [12-13], the PD associated ubiquitin ligase, Parkin, is recruited to mitochondrial

membranes by stabilized PINK1. Through unknown mechanisms, Parkin then recruits autophagy machinery to the mitochondria [14] (mitophagy) presumably to clear dysfunctional organelles [15]. If the clearance system is overwhelmed, axonal degeneration may ensue [16].

Environmental toxins mimicking PD such as *N*-methyl-4-phenyl-1,2,3,6-tetrahydropyridine (MPTP) or its active derivative, 1-methyl-4-phenylpyridinium (MPP^+) have also been shown to disrupt axonal function. For example, Herkenham *et al*., observed marked reductions of dopaminergic axons prior to the loss of nigral cell bodies following acute MPTP administration in monkeys [17]. Similarly, Meissner *et al*. reported an 80% loss of both the dopamine plasma membrane transporter (DAT) and DA levels in the macaque striatum following chronic MPTP delivery whereas only a 43% loss of DA cells was observed in the SN [18]. DA terminal loss is also the earliest event in murine MPTP models [19]. Using both the acute and chronic MPTP paradigms, Li and colleagues observed ~25% cell body loss after treatment whereas DA terminals were decreased by ~65-70% in either model [20]. Finally, a recent study reported a profound decrease (73%) in striatal DA following MPTP treatment whereas only a 9% decline of SN cells was observed [21]. In this same study, the GDNF receptor, RET, rescued the cells but not the terminal fields, re-confirming the basic observation that axons and cell bodies constitute separate compartments. These findings support the hypothesis that nigral neurons degenerate through a “dying back” axonopathy in which degeneration begins in the distal axon and proceeds over time towards the cell body [22-23].

The question arises then as to what factor or signaling system might rescue axons from degeneration? One serendipitous protein is the spontaneous mouse mutant, Wallerian degeneration slow (*Wld*^{S}). *Wld*^{S} delays axonal degeneration about 10-fold from a wide variety of genetic and toxin-inducing stimuli in the peripheral nervous system (PNS) [24] and in several central nervous system (CNS) models of degeneration including animal models of PD [25-26]. For example, we have shown that *Wld*^{S} rescues 85% of DA axons for at least 7 days post MPTP treatment *in vivo* [27]. Not only does *Wld*^{S} protect DA terminal fields *in vivo*, the same holds true *in vitro* as demonstrated in Chapters 2 and 3. Specifically, dissociated DA neurons prepared from *Wld*^{S} mice were also significantly protected from MPP^+. *Wld*^{S} itself is a chimeric protein composed of the N-terminal 70 amino acids of the ubiquitination factor Ube4b followed by a 18 amino acid linker region and the entire sequence of Nmnat1, a key enzyme in the biosynthesis of NAD^+ [28]. In contrast to peripheral model systems [24], we saw that only the entire *Wld*^{S} fusion protein protected DA neurites, whereas Nmnat1, cytoplasmically targeted Nmnat1 or Nmnat3 did not (Fig. 2.3 and 3.2). Surprisingly, *Wld*^{S} constructs mutagenized for NAD^+ synthesizing activity were just as effective as non-mutagenized *Wld*^{S} constructs (Fig. 2.5). These data suggest that increased NAD^+ may not underlie the ability of *Wld*^{S} to rescue DA neurites from toxin effects. Given these significant attributes of *Wld*^{S}, understanding how the *Wld*^{S} fusion protein prevents axon degeneration is an important step towards identifying an intervention that would leave axons intact.

In order to more easily test the effects of *Wld*^{S} on DA axons we crossed *Wld*^{S} mice with genetically engineered mice expressing GFP in DA neurons (DA/GFP). The resulting *Wld*^{S}/DA/GFP mice were plated in microchamber devices that segregated DA axons from DA cell bodies. As shown previously [29], wild type mice rapidly lost mitochondrial motility in DA axons when challenged with MPP^+. In contrast, *Wld*^{S} protected DA axons from MPP^+-induced disruption in mitochondrial axonal transport, possibly through a direct action on the mitochondria.

5.2 Materials and methods

All of the methods and materials for making the cell cultures and microchamber devices, imaging and quantifying axonal transport, measuring dopamine uptake and release, quantifying mitochondrial membrane potential ($\Delta\Psi_m$) and length, measuring autophagy, and performing statistical analyses for these set of experiments were performed exactly as described for Chapter 4. Experiments were done on both DA/GFP and *Wld*^{S}-DA/GFP murine mesencephalic cultures prepared from embryonic day 14 Tg(TH-EGFP)DJ76GSAT and C57Bl/OlaHsd-WldS-Tg(TH-EGFP)DJ76GSAT mice, respectively (Gene Expression Nervous System Atlas, National Institutes of Health, Bethesda, MD and Harlan, Bichester, UK).

5.2.1 Western Blotting

Western blotting was done as described in Chapters 2 and 3, with the exception that PVDF membranes were probed with a mouse acetylated tubulin antibody (Sigma-Aldrich, Saint Louis, MO). As a loading control, PVDF membranes were also probed with mouse monoclonal anti-actin antibody (Sigma-Aldrich) followed by an HRP-linked mouse secondary antibody (Jackson Immunoresearch, West Grove, PA).

5.2.2 Immunohistochemistry

To determine where *Wld*^{S} is expressed in DA axons, *Wld*^{S} primary mesencephalic cultures were plated in microchamber devices, fixed and then stained with rabbit *Wld*^{S} antibody (1:500, gift of M.P. Coleman) and Alexa488 anti-rabbit antibody (1:500, Molecular Probes, Carlsbad, CA). In some cases, axons were incubated with 25 nM MitoTracker Red (MTR; Invitrogen, Carlsbad, CA) prior to fixation. To determine acetylated tubulin levels specifically in DA axons, primary midbrain cultures plated in microchamber devices were fixed and stained with mouse acetylated tubulin (1:1000, Sigma-Aldrich) and Cy3 anti-mouse antibodies (1:500, Molecular Probes, Carlsbad, CA).

5.2.3 Fragmentation of axons

Fragmentation of axons was assessed by sampling five non-overlapping fields in the axonal part of the chamber. The number of DA/GFP axons was

counted using an unbiased grid system in ImageJ. The degree of change in axon structure was quantified as: (Number of fragmented axons) / (Number of total axons).

5.3 Results

5.3.1 *Wld*^{S} prevents MPP$^+$-induced changes in axonal structure

We have previously reported that DA terminal fields but not cell bodies of *Wld*^{S} mice are protected against MPTP injury [27] *in vivo* and MPP$^+$ toxicity *in vitro* (Fig. 2.1). To confirm and extend these observations in our modified microchamber system, primary mesencephalic cells obtained from both DA/GFP and *Wld*^{S}-DA/GFP mice were grown in compartmented chambers and treated with 2 μM MPP$^+$ on DIV14. Chambers were subsequently fixed at various time points and examined for axonal integrity using GFP fluorescence as a relevant indicator of DA axons. Like MPTP treated *Wld*^{S} mice [27] or MPP$^+$-treated dissociated DA neurons (Fig. 2.1), DA axons from DA/GFP/*Wld*^{S} mice were significantly protected from toxin treatment at all time points, most prominently at 12 h (Fig. 5.1A,B). Thus, *in vitro* as *in vivo* [23], *Wld*^{S} protects DA axons from MPTP/MPP$^+$ toxicity.

Studies in cultured cerebellar granule cells have shown that *Wld*^{S} cultures have higher baseline levels of acetylated tubulin compared to WT cultures [30]. To determine if *Wld*^{S} DA neurons exhibit higher levels of microtubule acetylation, we either stained DA axons with anti-acetylated tubulin or prepared lysates from

midbrain cultures for western blotting. Neither immunocytochemical techniques (Fig. 5.1C) nor western blots (Fig. 5.1D,E) detected differences in acetylated tubulin levels between WT and *Wld*^{S} cultures. Thus, differences, if any, are not apparent in *Wld*^{S} compared to wild type DA axons or cultures

5.3.2 *Wld*^{S} protein is present in DA mitochondria

Many studies have shown that the *Wld*^{S} fusion gene is primarily localized in the nucleus [31]. This is also true in DA neurons in the SN [27]. Despite the abundance of *Wld*^{S} in the nucleus, it can also be found in other locations including axons [32]. "Extranuclear" *Wld*^{S} is reportedly associated with small membranous structures including mitochondria [33]. To determine the subaxonal expression pattern of *Wld*^{S}, we labeled compartmentalized axonal mitochondria with MTR and then fixed and stained for *Wld*^{S} with the Wld18 antibody. *Wld*^{S} was axonally distributed in pleo-morphic globular organelles which significantly overlapped with MTR (56.14 $\pm$ 15 % overlap) (Fig. 5.2). Other studies have not identified any overt structural differences in mitochondria derived from WT or *Wld*^{S} mice [34-35]. In agreement with these findings, we did not see any differences in baseline mitochondrial density, number of moving mitochondria, mitochondrial velocity, mitochondrial length, or $\Delta\Psi_m$ between DA/GFP and *Wld*^{S}-DA/GFP DA axonal mitochondria (Table 1). These data indicate that extranuclear *Wld*^{S} is readily distributed to DA axons where it is associated with mitochondria but does not outwardly change any of their parameters.

5.3.3 *Wld*^{S} prevents MPP$^+$-induced changes in axonal mitochondrial transport

Recently, we demonstrated that MPP$^+$ rapidly decreases mitochondrial transport in DA axons [29]. Because *Wld*^{S} significantly co-localized with axonal mitochondria (Fig. 5.2), we tested whether mitochondrial transport was altered in *Wld*^{S}-DA/GFP axons. As we previously reported, MPP$^+$ decreased the numbers of moving mitochondria in DA/GFP axons by 50% within 30 min of treatment (Fig. 5.3A,B). We also confirmed in DA/GFP axons that MPP$^+$ treatment decreased the number and speed of moving mitochondria in the anterograde direction but increased speed in the retrograde direction (Fig. 4.3) [29]. In contrast, numbers of moving mitochondria in *Wld*^{S}-DA/GFP axons were not affected by MPP$^+$ treatment nor were there any differences in their anterograde or retrograde motility (Fig. 5.3A,B). Similarly, no change in mitochondrial velocity was measured following MPP+ treatment in either the anterograde or retrograde direction in *Wld*^{S}-DA/GFP cultures (Fig. 5.3A,C). Thus *Wld*^{S} prevents the rapid and directed effect of MPP$^+$ on DA axonal mitochondria.

To determine whether *Wld*^{S} had an effect on other types of organelles particularly synaptic vesicles, DA/GFP and *Wld*^{S}-DA/GFP cultures in microchamber devices were transduced using a lentivirus expressing synaptophysin fused in frame with cerulean (Syn-Cer). We did not observe any significant difference between DA/GFP and *Wld*^{S}-DA/GFP axons in terms of the number of moving Syn-Cer particles per 100 μm length of axon (2.88 $\pm$ 0.17 and 3.02 $\pm$ 0.44, respectively). Not surprisingly, no significant difference was apparent

in the velocity of the Syn-Cer particles in DA/GFP and *Wld*^{S}-DA/GFP cultures (0.47 $\pm$ 0.02 μm/sec and 0.41 $\pm$ 0.08 μm/sec, respectively) as well. Despite MPP$^+$-induced changes in mitochondrial axonal transport, (Fig. 5.3A,B) [29], MPP$^+$ did not affect synaptophysin motility and velocity in wild type or *Wld*^{S} cultures (Fig. 5.3D,E), indicating that the effect of *Wld*^{S} is specific for mitochondria.

5.3.4 *Wld*^{S} prevents MPP$^+$-induced decreases in axonal mitochondrial membrane potential

Because MPP$^+$ leads to a rapid loss of $\Delta\Psi_m$, in DA axons [18], we tested whether *Wld*^{S} affected that process. Compartmentalized DA/GFP and *Wld*^{S}-DA/GFP axons were labeled with the sensitive $\Delta\Psi_m$ indicator tetramethylrhodamine ethyl ester (TMRE) before acquiring baseline images. After 30 min of toxin treatment, $\Delta\Psi_m$ was significantly reduced in DA/GFP but not *Wld*^{S}-DA/GFP axonal mitochondria (Fig. 5.4A,B). Similarly there were no significant differences in the size of *Wld*^{S}-DA/GFP mitochondria following MPP+ treatment (not shown). Thus, MPP$^+$ rapidly depolarized DA/GFP mitochondria but not *Wld*^{S}-DA/GFP.

To test whether *Wld*^{S} also protects DA mitochondria from other types of depolarizing agents, we treated DA/GFP and *Wld*^{S}-DA/GFP axons with carbonyl cyanide *m*-chlorophenyl-hydrazone (CCCP), which depolarizes mitochondria by acting as an uncoupler [36]. DA/GFP and *Wld*^{S}-DA/GFP axons were labeled with TMRE and images were acquired at baseline as well as at 15 and 30 minutes

after the addition of CCCP. CCCP reduced $\Delta\Psi_m$ in both DA/GFP and *Wld*^{S}-DA/GFP axonal mitochondria at both time points examined (Fig. 5.4C,D), but there was a significant attenuation observed in *Wld*^{S} DA mitochondrial axons at 30 minutes. Taken together, these results show that *Wld*^{S} attenuates processes that alter mitochondrial membrane potential such as blocking complex I (MPP+) or uncoupling membrane potential (CCCP)

5.3.5 *Wld*^{S} protects DA neurons against MPP$^+$-induced autophagy

Decreases in $\Delta\Psi_m$ can induce mitophagy (autophagy of mitochondrial organelles) [32]. Given that we [18] and others [33] have shown that MPP$^+$ induces autophagy in DA neurons, we tested whether *Wld*^{S} could prevent autophagy in this model system. Using GFP-labeled LC3 (microtubule-associated protein 1, light chain 3; also known as ATG8), as a frequently used marker of autophagy, we confirmed our previous observation that LC3-GFP puncta were visible as early as 3 hours after MPP$^+$ treatment [29] (Fig. 5.5A). In contrast, *Wld*^{S} cultures transduced with LC3-GFP maintained the normal diffuse cytoplasmic distribution even after MPP+ treatment (Fig. 5.5). These data are consistent with the evidence that *Wld*^{S} prevents MPP$^+$-induced mitochondrial membrane depolarization and this in turn prevents the induction of mitophagy.

5.4 Discussion

Numerous studies suggest that axonal dysfunction precedes cell body death in many neurodegenerative disorders, especially PD. Halting or delaying

axonal degeneration would allow DA axons to stay “wired up” and hence, functional. Because *Wld*^{S} dramatically rescued DA terminal fields from MPTP *in vivo* [27] and since *Wld*^{S} also protects DA neurites *in vitro* (Fig. 2.1), we used optical, cellular and molecular techniques to demonstrate that *Wld*^{S} protects DA axons by maintaining $\Delta\Psi_m$, mitochondrial motility, and mitochondrial velocity such that autophagic processes are not activated.

What is the mechanism by which *Wld*^{S} protects DA terminals? Although many studies have emphasized that both Nmnat1 and cytoplasmically re-directed Nmnat can protect axons in many peripheral model systems, few studies have tested how *Wld*^{S} protects DA neurons from PD-linked genes and/or toxins. Studies on peripheral nervous system models attribute the protective phenotype of *Wld*^{S} to its Nmnat portion. *In vitro* studies have shown that overexpression of Nmnat1 by itself protects axons from many mechanical, genetic or toxin-induced injuries [24, 37]. However, transgenic animals expressing nuclear Nmnat1 are less neuroprotective than *Wld*^{S} [38-39]. In part, this might be due to where Nmnat1 is expressed [24] since cytoplasmically [40] or axonally targeted Nmnat1 [33] *in vivo* was equally if not more effective than *Wld*^{S} at protecting axons against injury. Interestingly, in either case Nmnat1 was expressed at higher levels in the mitochondrial fraction compared to nuclear Nmnat1 [33, 40]. Nmnat3, a mitochondrially expressed isoform of Nmnat, also showed comparable levels of protection to *Wld*^{S} when expressed *in vivo*, unlike native Nmnat1 [39]. Even the *Wld*^{S} fusion protein was more effective *in vivo* when it was targeted to the cytoplasm and it also showed higher levels of expression in the mitochondria

than native *Wld*^{S} [32]. Although we used the original *Wld*^{S} animals (albeit crossed with DA/GFP), our study shows that extranuclear *Wld*^{S} partially colocalizes with axonal DA mitochondria, attenuating MPP^+-induced changes in $\Delta\Psi_m$, mitochondrial motility and mitochondrial velocity. Thus, the present findings are consistent with the observations that *Wld*^{S} might regulate or affect an important mitochondrial process.

Data supporting this idea comes from a differential proteomics approach comparing WT and *Wld*^{S} striatal synaptosomes [34]. Sixteen proteins were found to be differentially expressed, eight of which were localized to the mitochondria. These included the VDAC2, a pore forming protein in the outer mitochondrial membrane which essentially serves as a metabolite exchanger [41]. The latter, although not part of the mPTP is thought to play a role in regulating it [42]. Of the three known VDACs each has a unique phenotype. For instance, VDAC2 inhibits apoptosis whereas VDAC1 is an activator of apoptotic processes [43]. Given the complexity of their protein structure and the numerous isoform-specific protein-protein interactions, there might be many target points for *Wld*^{S}/VDAC2 interactions. Nonetheless, since DA synapses would comprise a significant proportion of striatal synaptosomal preparations, the changes in mitochondrial proteins in *Wld*^{S} versus WT re-enforce the notion that *Wld*^{S} might be acting directly at the level of the mitochondria to prevent axonal dysfunction.

Mitochondria undergo complex fission and fusion processes in part to ensure a healthy pool of organelles [44]. Towards this end it is thought that depolarized mitochondria are quickly culled from the pack and marked for

destruction, possibly through the stabilization of PINK1 on the outer mitochondrial membrane followed by the recruitment of Parkin and other mitophagic components [45]. Earlier studies done in wild type or *Wld*^{S} superior cervical ganglion (SCG) cultures found that, as expected, *Wld*^{S} protected SCG neurites from vinblastine treatment. But for the first time, it also showed that *Wld*^{S} prevented a highly significant loss of $\Delta\Psi_m$ which occurred in wild type cultures [35]. In other studies using sciatic nerve preparations, axon degeneration was ascribed to activation of the mitochondrial permeability transition pore (mPTP) [46]. Opening of the mPTP is thought to trigger $\Delta\Psi_m$, ROS, loss of ATP, and release of pro-apoptotic factors, amongst other things [47]. In this same sciatic nerve study, *Wld*^{S} prevented the activation of mPTP after axons were cut but was unable to protect axons from pharmacological agents directly activating the pore [46]. These results prompted Barrientos *et al*. to propose a model in which *Wld*^{S} acts upstream of the mitochondria to prevent the opening of the mPTP [46].

Barrientos *et al*. also showed that both pharmacologic and genetic manipulation of cyclophilin D, a functional component of the mPTP, were able to prevent axon degeneration [46]. Recently Thomas *et al*. reported that cyclophilin D knockout mice were significantly resistant to MPTP toxicity, raising the possibility that this mechanism might hold true for this PD-linked toxin as well. However, several caveats for this idea exist. The authors found that knocking out cyclophilin D was ineffective against subacute or chronic MPTP models and only partially effective at rescuing SN neurons in the acute model. Although it

appeared that there was some preservation of DA terminal fields, that area most relevant to this study, densitometry was also not done in these animals [48].

Perhaps the most direct question is whether MPP^+ activates the mPTP in the dissociated culture system. Earlier experiments using bongkrekic acid and/or cyclosporine A to prevent mPTP opening following MPP^+ did not rescue DA neurons from cell death [Lotharius and O'Malley, unpublished observation]. It will be important to repeat these experiments using our current model system to see whether cyclosporine A prevents MPP^+-induced depolarization of DA axonal mitochondria.

This work and our previous work show that MPP^+ rapidly inhibits the motility of DA mitochondria [29]. Despite the MPP^+-induced decrease seen in $\Delta\Psi_m$, increasing ATP levels, blocking ROS production or JNK, PI3K or PKC pathways, or preventing rises in cytoplasmic calcium levels did not rescue mitochondrial motility. To date, the only pharmacologic agents that prevented MPP^+-induced mitochondrial immobility were *N*-acetylcysteine (NAC) and membrane permeable GSH [29]. Given the prevalence of redox-sensitive proteins in the mitochondria and the close connection between redox balance and membrane potential [49], redox regulation of depolarization might facilitate interactions between the bioenergetic membranes and homeostatic processes such as mitophagy. *Wld*^{S} could potentially work at the level of the mPTP by blocking pore activation or at the level of the mitochondrial thioredoxin/ or glutaredoxin/ reductase systems to maintain a reduced state [50]. Since

cyclophilin D itself is regulated by redox potential, mPTP could be indirectly strengthened via a *Wld*^{S} effect on redox potential.

Although maintenance of mitochondrial function may not be the sole trigger of axonal dysfunction, our data shows that it plays an early and pivotal role in the degeneration of axons. This study, together with the large amount of evidence suggesting that PD is associated with axonal "dying-back," underscores the necessity of developing therapeutics aimed at axons as well as cell bodies so as to preserve circuitry and function. Understanding how *Wld*^{S} protects axons is important in designing potential interventions that can delay or halt axonal dysfunction and ensuing disease progression.

5.5 Acknowledgements

This work was supported by National Institutes of Health Grants NS39084 (K.L.O.) and National Institutes of Health Neuroscience Blueprint Core Grant NS057105 to Washington University. This work was also supported by the Bakewell Family Foundation. We thank Steven K. Harmon for technical support and Drs. Michael Coleman, Jeffrey Milbrandt, Rachel Wong, Jeffrey Milbrandt, and Chris Weihl for plasmid constructs and Valeria Cavalli for materials and helpful discussions.

References:

1. Braak H, Ghebremedhin E, Rub U, Bratzke H, Del Tredici K: **Stages in the development of Parkinson's disease-related pathology.** *Cell Tissue Res* 2004, **318:**121-134.
2. Bernheimer H, Birkmayer W, Hornykiewicz O, Jellinger K, Seitelberger F: **Brain dopamine and the syndromes of Parkinson and Huntington. Clinical, morphological and neurochemical correlations.** *J Neurol Sci* 1973, **20:**415-455.
3. Scherman D, Desnos C, Darchen F, Pollak P, Javoy-Agid F, Agid Y: **Striatal dopamine deficiency in Parkinson's disease: role of aging.** *Ann Neurol* 1989, **26:**551-557.
4. Riederer P, Wuketich S: **Time course of nigrostriatal degeneration in parkinson's disease. A detailed study of influential factors in human brain amine analysis.** *J Neural Transm* 1976, **38:**277-301.
5. Cheng HC, Ulane CM, Burke RE: **Clinical progression in Parkinson disease and the neurobiology of axons.** *Ann Neurol* 2010, **67:**715-725.
6. Fearnley JM, Lees AJ: **Ageing and Parkinson's disease: substantia nigra regional selectivity.** *Brain* 1991, **114 (Pt 5):**2283-2301.
7. Li Y, Liu W, Oo TF, Wang L, Tang Y, Jackson-Lewis V, Zhou C, Geghman K, Bogdanov M, Przedborski S, et al: **Mutant LRRK2(R1441G) BAC transgenic mice recapitulate cardinal features of Parkinson's disease.** *Nat Neurosci* 2009, **12:**826-828.
8. Saha AR, Hill J, Utton MA, Asuni AA, Ackerley S, Grierson AJ, Miller CC, Davies AM, Buchman VL, Anderton BH, Hanger DP: **Parkinson's disease alpha-synuclein mutations exhibit defective axonal transport in cultured neurons.** *J Cell Sci* 2004, **117:**1017-1024.
9. Yang ML, Hasadsri L, Woods WS, George JM: **Dynamic transport and localization of alpha-synuclein in primary hippocampal neurons.** *Mol Neurodegener* 2010, **5:**9.
10. Weihofen A, Thomas KJ, Ostaszewski BL, Cookson MR, Selkoe DJ: **Pink1 forms a multiprotein complex with Miro and Milton, linking Pink1 function to mitochondrial trafficking.** *Biochemistry* 2009, **48:**2045-2052.
11. Reis K, Fransson A, Aspenstrom P: **The Miro GTPases: at the heart of the mitochondrial transport machinery.** *FEBS Lett* 2009, **583:**1391-1398.
12. Narendra DP, Jin SM, Tanaka A, Suen DF, Gautier CA, Shen J, Cookson MR, Youle RJ: **PINK1 is selectively stabilized on impaired mitochondria to activate Parkin.** *PLoS Biol* 2010, **8:**e1000298.
13. Van Laar VS, Arnold B, Cassady SJ, Chu CT, Burton EA, Berman SB: **Bioenergetics of neurons inhibit the translocation response of Parkin following rapid mitochondrial depolarization.** *Hum Mol Genet* 2011, **20:**927-940.

14. Narendra D, Tanaka A, Suen DF, Youle RJ: **Parkin is recruited selectively to impaired mitochondria and promotes their autophagy.** *J Cell Biol* 2008, **183:**795-803.
15. Schapira AH, Gegg M: **Mitochondrial contribution to Parkinson's disease pathogenesis.** *Parkinsons Dis* 2011, **2011:**159160.
16. Xilouri M, Stefanis L: **Autophagic pathways in Parkinson disease and related disorders.** *Expert Rev Mol Med* 2011, **13:**e8.
17. Herkenham M, Little MD, Bankiewicz K, Yang SC, Markey SP, Johannessen JN: **Selective retention of MPP+ within the monoaminergic systems of the primate brain following MPTP administration: an in vivo autoradiographic study.** *Neuroscience* 1991, **40:**133-158.
18. Meissner W, Prunier C, Guilloteau D, Chalon S, Gross CE, Bezard E: **Time-course of nigrostriatal degeneration in a progressive MPTP-lesioned macaque model of Parkinson's disease.** *Mol Neurobiol* 2003, **28:**209-218.
19. Serra PA, Sciola L, Delogu MR, Spano A, Monaco G, Miele E, Rocchitta G, Miele M, Migheli R, Desole MS: **The neurotoxin 1-methyl-4-phenyl-1,2,3,6-tetrahydropyridine induces apoptosis in mouse nigrostriatal glia. Relevance to nigral neuronal death and striatal neurochemical changes.** *J Biol Chem* 2002, **277:**34451-34461.
20. Li H, Guo M: **Protein degradation in Parkinson disease revisited: it's complex.** *J Clin Invest* 2009, **119:**442-445.
21. Mijatovic J, Piltonen M, Alberton P, Mannisto PT, Saarma M, Piepponen TP: **Constitutive Ret signaling is protective for dopaminergic cell bodies but not for axonal terminals.** *Neurobiol Aging* 2011, **32:**1486-1494.
22. Iseki E, Kato M, Marui W, Ueda K, Kosaka K: **A neuropathological study of the disturbance of the nigro-amygdaloid connections in brains from patients with dementia with Lewy bodies.** *J Neurol Sci* 2001, **185:**129-134.
23. Raff MC, Whitmore AV, Finn JT: **Axonal self-destruction and neurodegeneration.** *Science* 2002, **296:**868-871.
24. Coleman MP, Freeman MR: **Wallerian degeneration, wld(s), and nmnat.** *Annu Rev Neurosci* 2010, **33:**245-267.
25. Mi W, Beirowski B, Gillingwater TH, Adalbert R, Wagner D, Grumme D, Osaka H, Conforti L, Arnhold S, Addicks K, et al: **The slow Wallerian degeneration gene, WldS, inhibits axonal spheroid pathology in gracile axonal dystrophy mice.** *Brain* 2005, **128:**405-416.
26. Sajadi A, Schneider BL, Aebischer P: **Wlds-mediated protection of dopaminergic fibers in an animal model of Parkinson disease.** *Curr Biol* 2004, **14:**326-330.
27. Hasbani DM, O'Malley KL: **Wld(S) mice are protected against the Parkinsonian mimetic MPTP.** *Exp Neurol* 2006, **202:**93-99.
28. Mack TG, Reiner M, Beirowski B, Mi W, Emanuelli M, Wagner D, Thomson D, Gillingwater T, Court F, Conforti L, et al: **Wallerian**

degeneration of injured axons and synapses is delayed by a Ube4b/Nmnat chimeric gene. *Nat Neurosci* 2001, **4:**1199-1206.
29. Kim-Han JS, Antenor-Dorsey JA, O'Malley KL: **The Parkinsonian Mimetic, MPP+, Specifically Impairs Mitochondrial Transport in Dopamine Axons.** *J Neurosci* 2011, **31:**7212-7221.
30. Suzuki K, Koike T: **Mammalian Sir2-related protein (SIRT) 2-mediated modulation of resistance to axonal degeneration in slow Wallerian degeneration mice: a crucial role of tubulin deacetylation.** *Neuroscience* 2007, **147:**599-612.
31. Coleman M: **Axon degeneration mechanisms: commonality amid diversity.** *Nat Rev Neurosci* 2005, **6:**889-898.
32. Beirowski B, Babetto E, Gilley J, Mazzola F, Conforti L, Janeckova L, Magni G, Ribchester RR, Coleman MP: **Non-nuclear Wld(S) determines its neuroprotective efficacy for axons and synapses in vivo.** *J Neurosci* 2009, **29:**653-668.
33. Babetto E, Beirowski B, Janeckova L, Brown R, Gilley J, Thomson D, Ribchester RR, Coleman MP: **Targeting NMNAT1 to axons and synapses transforms its neuroprotective potency in vivo.** *J Neurosci* 2010, **30:**13291-13304.
34. Wishart TM, Paterson JM, Short DM, Meredith S, Robertson KA, Sutherland C, Cousin MA, Dutia MB, Gillingwater TH: **Differential proteomics analysis of synaptic proteins identifies potential cellular targets and protein mediators of synaptic neuroprotection conferred by the slow Wallerian degeneration (Wlds) gene.** *Mol Cell Proteomics* 2007, **6:**1318-1330.
35. Ikegami K, Koike T: **Non-apoptotic neurite degeneration in apoptotic neuronal death: pivotal role of mitochondrial function in neurites.** *Neuroscience* 2003, **122:**617-626.
36. Ganote CE, Armstrong SC: **Effects of CCCP-induced mitochondrial uncoupling and cyclosporin A on cell volume, cell injury and preconditioning protection of isolated rabbit cardiomyocytes.** *J Mol Cell Cardiol* 2003, **35:**749-759.
37. Yan T, Feng Y, Zheng J, Ge X, Zhang Y, Wu D, Zhao J, Zhai Q: **Nmnat2 delays axon degeneration in superior cervical ganglia dependent on its NAD synthesis activity.** *Neurochem Int* 2010, **56:**101-106.
38. Conforti L, Fang G, Beirowski B, Wang MS, Sorci L, Asress S, Adalbert R, Silva A, Bridge K, Huang XP, et al: **NAD(+) and axon degeneration revisited: Nmnat1 cannot substitute for Wld(S) to delay Wallerian degeneration.** *Cell Death Differ* 2007, **14:**116-127.
39. Yahata N, Yuasa S, Araki T: **Nicotinamide mononucleotide adenylyltransferase expression in mitochondrial matrix delays Wallerian degeneration.** *J Neurosci* 2009, **29:**6276-6284.
40. Sasaki Y, Vohra BP, Baloh RH, Milbrandt J: **Transgenic mice expressing the Nmnat1 protein manifest robust delay in axonal degeneration in vivo.** *J Neurosci* 2009, **29:**6526-6534.

41. Halestrap AP: **What is the mitochondrial permeability transition pore?** *J Mol Cell Cardiol* 2009, **46:**821-831.
42. Azarashvili T, Stricker R, Reiser G: **The mitochondria permeability transition pore complex in the brain with interacting proteins - promising targets for protection in neurodegenerative diseases.** *Biol Chem* 2010, **391:**619-629.
43. Shoshan-Barmatz V, Ben-Hail D: **VDAC, a multi-functional mitochondrial protein as a pharmacological target.** *Mitochondrion* 2011.
44. Westermann B: **Mitochondrial fusion and fission in cell life and death.** *Nat Rev Mol Cell Biol* 2010, **11:**872-884.
45. Narendra D, Tanaka A, Suen DF, Youle RJ: **Parkin-induced mitophagy in the pathogenesis of Parkinson disease.** *Autophagy* 2009, **5:**706-708.
46. Barrientos SA, Martinez NW, Yoo S, Jara JS, Zamorano S, Hetz C, Twiss JL, Alvarez J, Court FA: **Axonal degeneration is mediated by the mitochondrial permeability transition pore.** *J Neurosci* 2011, **31:**966-978.
47. Zorov DB, Juhaszova M, Yaniv Y, Nuss HB, Wang S, Sollott SJ: **Regulation and pharmacology of the mitochondrial permeability transition pore.** *Cardiovasc Res* 2009, **83:**213-225.
48. Thomas B, Banerjee R, Starkova NN, Zhang SF, Calingasan NY, Yang L, Wille E, Lorenzo BJ, Ho DJ, Beal MF, Starkov A: **Mitochondrial Permeability Transition Pore Component Cyclophilin D Distinguishes Nigrostriatal Dopaminergic Death Paradigms in the MPTP Mouse Model of Parkinson's Disease.** *Antioxid Redox Signal* 2011.
49. Halestrap AP, Woodfield KY, Connern CP: **Oxidative stress, thiol reagents, and membrane potential modulate the mitochondrial permeability transition by affecting nucleotide binding to the adenine nucleotide translocase.** *J Biol Chem* 1997, **272:**3346-3354.
50. Toman J, Fiskum G: **Influence of aging on membrane permeability transition in brain mitochondria.** *J Bioenerg Biomembr* 2011, **43:**3-10.

Table 5.1 - WT and *Wld*^{S} have similar mitochondrial characteristics

	DA		Non-DA	
	WT	***Wld*^{S}**	**WT**	***Wld*^{S}**
Density	**8.89 ± 0.86**	**8.43 ± 0.48**	**9.5 ± 0.82**	**10.08 ± 0.59**
Moving particles/ 100 mm	**1.93 ± 0.22**	**2.00 ± 0.19**	**2.49 ± 0.24***	**2.78 ± 0.19***
Speed (mm/s)	**0.28 ± 0.05**	**0.23 ± 0.20**	**0.79 ± 0.07****	**0.87 ± 0.06****
Length (mm)	**1.19 ± 0.04**	**1.17 ± 0.09**	**2.28 ± 0.12**	**2.7 ± 0.19**
$\Delta\Psi_m$(AU)	**50 ± 8.37**	**49.55 ± 10.3**	**55.14 ± 9.14**	**48.70 ± 6.32**

Mean ± SEM, total of 40 (control) and 82 (MPP^+-treated) axons derived from 8 independent experiments, *p<0.05, **p<0.01

Figure 5.1 - *Wld*^{S} prevents changes in axonal structure after MPP$^+$. (A) Integrity of DA/GFP and *Wld*^{S}-DA/GFP DA axons was assessed before and after MPP$^+$ treatment. Compartmented axons were fixed after 12, 24, and 48 hours of MPP$^+$ treatment. (B) Fragmentation of DA axons was quantified. Mean $\pm$ SEM made in three independent experiments, *$p<0.05$, **$p<0.001$. (C) Levels of acetylated tubulin (Ac-tub) were assessed by staining DA/GFP and *Wld*^{S}-DA/GFP DA axons with acetylated tubulin antibody. No significant difference in baseline acetylated tubulin levels was evident between WT and *Wld*^{S} axons. (D) Western blot shows similar expression levels of acetylated tubulin in lysates from WT and *Wld*^{S} primary mesencephalic cultures. (E) Quantification of the western blots done on cell lysates from three independent experiments, Mean $\pm$ SEM.

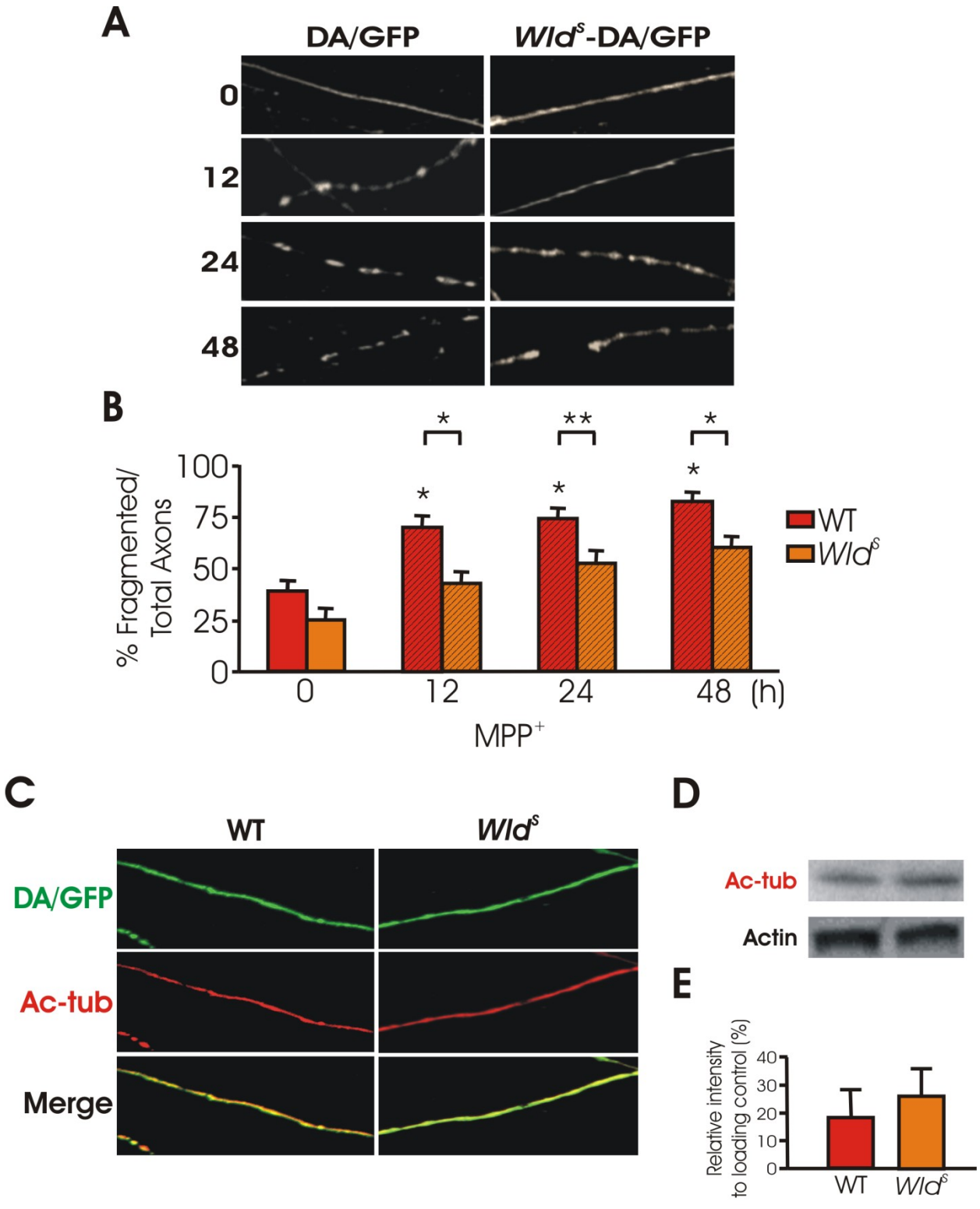
A
DA/GFP
Wld^S-DA/GFP
0
12
24
48
B
% Fragmented/ Total Axons
100
75
50
25
0
*
**
*
*
*
0
12
24
48 (h)
MPP+
WT
Wld^S
C
WT
Wld^S
DA/GFP
Ac-tub
Merge
D
Ac-tub
Actin
E
Relative intensity to loading control (%)
40
30
20
10
0
WT
Wld^S

Fig.5.1

Figure 5.2 - *Wld*^{S} partially colocalizes to axonal mitochondria. Sublocalization of WldS was assessed by labeling mitochondria with MTR and staining *Wld*^{S} DA axons with Wld18 antibody. Approximately 50% colocalization of Wld18 staining and MTR signal was observed (arrows).

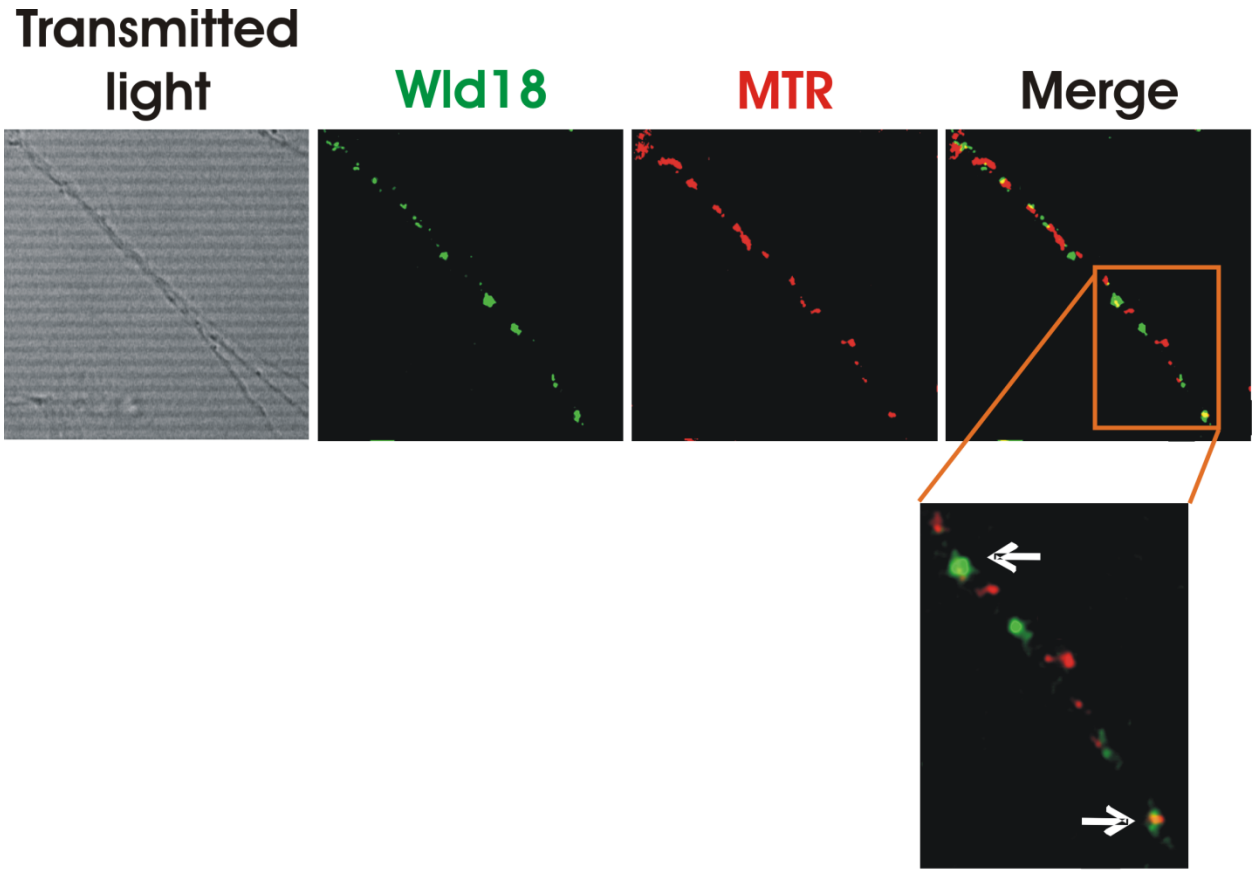

Fig.5.2

Figure 5.3 – *Wld*^{S} protects against MPP$^+$-induced changes in mitochondrial axonal transport. (A) *Wld*^{S}-DA/GFP DA mitochondria labeled with MTR were imaged for 5 min at 5 sec intervals after 30 min incubation with and without 2 μM MPP$^+$. For consistency, mitochondrial measurements were assessed near the axon terminal at least 2 mm away from the cell bodies. Resulting kymographs are shown below. (B) Number of moving mitochondria per 100 μm length of axon was calculated. Mean ± SEM, total of 40 (control) and 82 (MPP$^+$-treated) axons derived from 8 (control) and 16 (MPP$^+$-treated) dishes in 8 independent experiments. (C) Vesicular movement as measured using Syn-Cer was observed for 5 min before and after 30 min of incubation with and without 2 μM MPP$^+$. Quantification of moving particles was determined as described in Materials and Methods. Mean ± SEM. A total of 42 (control) and 80 (MPP$^+$-treated) axons from 8 (control) and 16 (MPP$^+$-treated) dishes in 8 independent experiments.

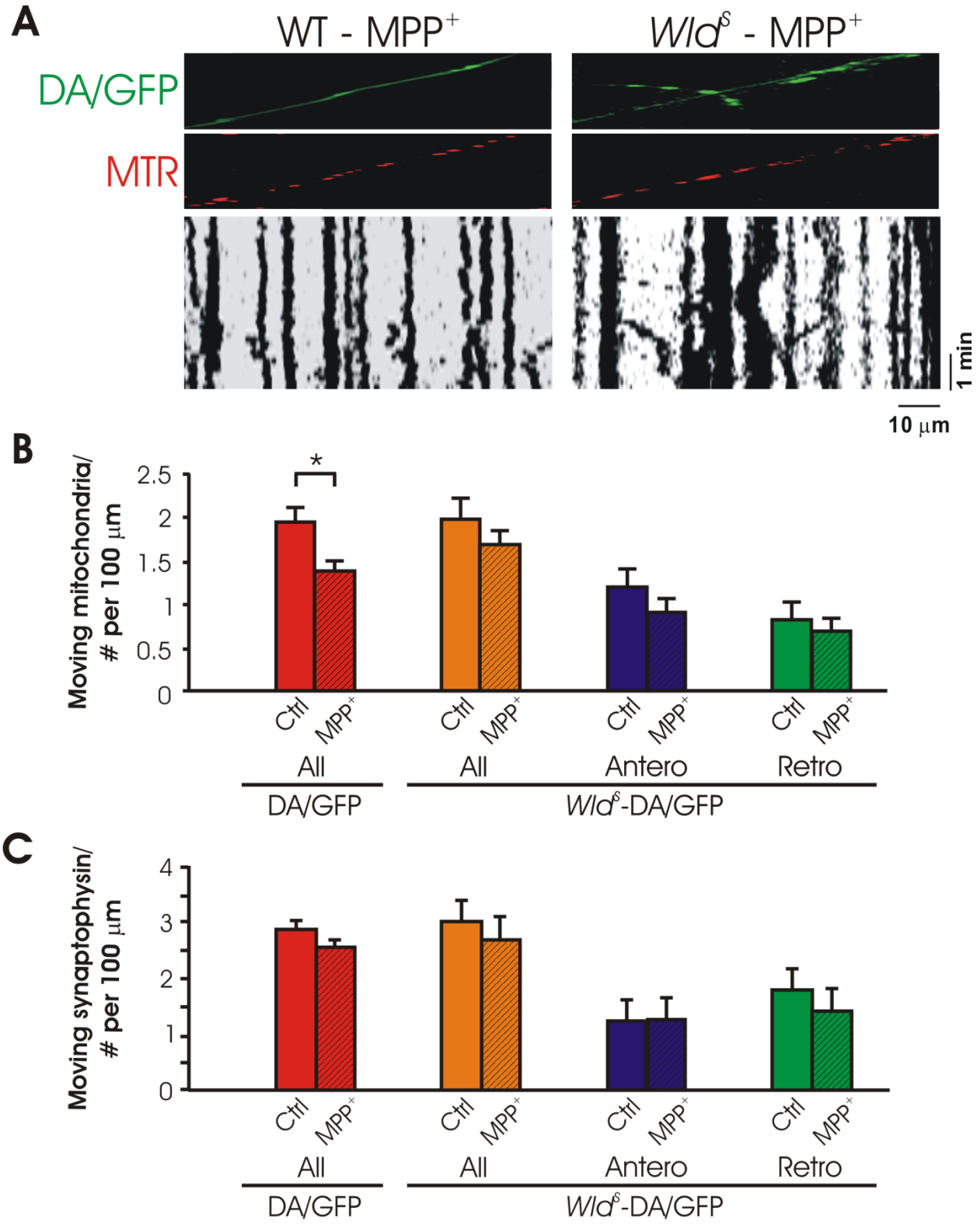
A
WT - MPP+
Wld^S - MPP+
DA/GFP
MTR
1 min
10 μm
B
Moving mitochondria/
per 100 μm
2.5
2
1.5
1
0.5
0
*
Ctrl
MPP+
All
DA/GFP
All
Antero
Retro
Wld^S-DA/GFP
C
Moving synaptophysin/
per 100 μm
4
3
2
1
0

Fig.5.3

Figure 5.4 - *Wld*^{S} prevents MPP$^+$-induced decreases in axonal mitochondrial membrane potential. (A) Mitochondria in axons from DA/GFP and *Wld*^{S}-DA/GFP cultures were labeled with 25 nM TMRE and then assessed before and 30 min after MPP$^+$ treatment. (B) MPP$^+$ led to significant differences in $\Delta\Psi_m$ in DA/GFP mitochondria but not in *Wld*^{S}-DA/GFP mitochondria. Mean ± SEM of representative determinations from six independent experiments, **p<0.001 (C) Mitochondria in axons from DA/GFP and *Wld*^{S}-DA/GFP cultures were again labeled with 25 nM TMRE and then assessed before and 30 min after 2 μm CCCP treatment. (D) CCCP led to decreases in $\Delta\Psi_m$ in DA/GFP and *Wld*^{S}-DA/GFP mitochondria at 15 and 30 minutes after addition of toxin, but *Wld*^{S}-DA/GFP attenuated the effects of CCCP 30 minutes after treatment. Mean ± SEM of representative determinations from six independent experiments, *p<0.05.

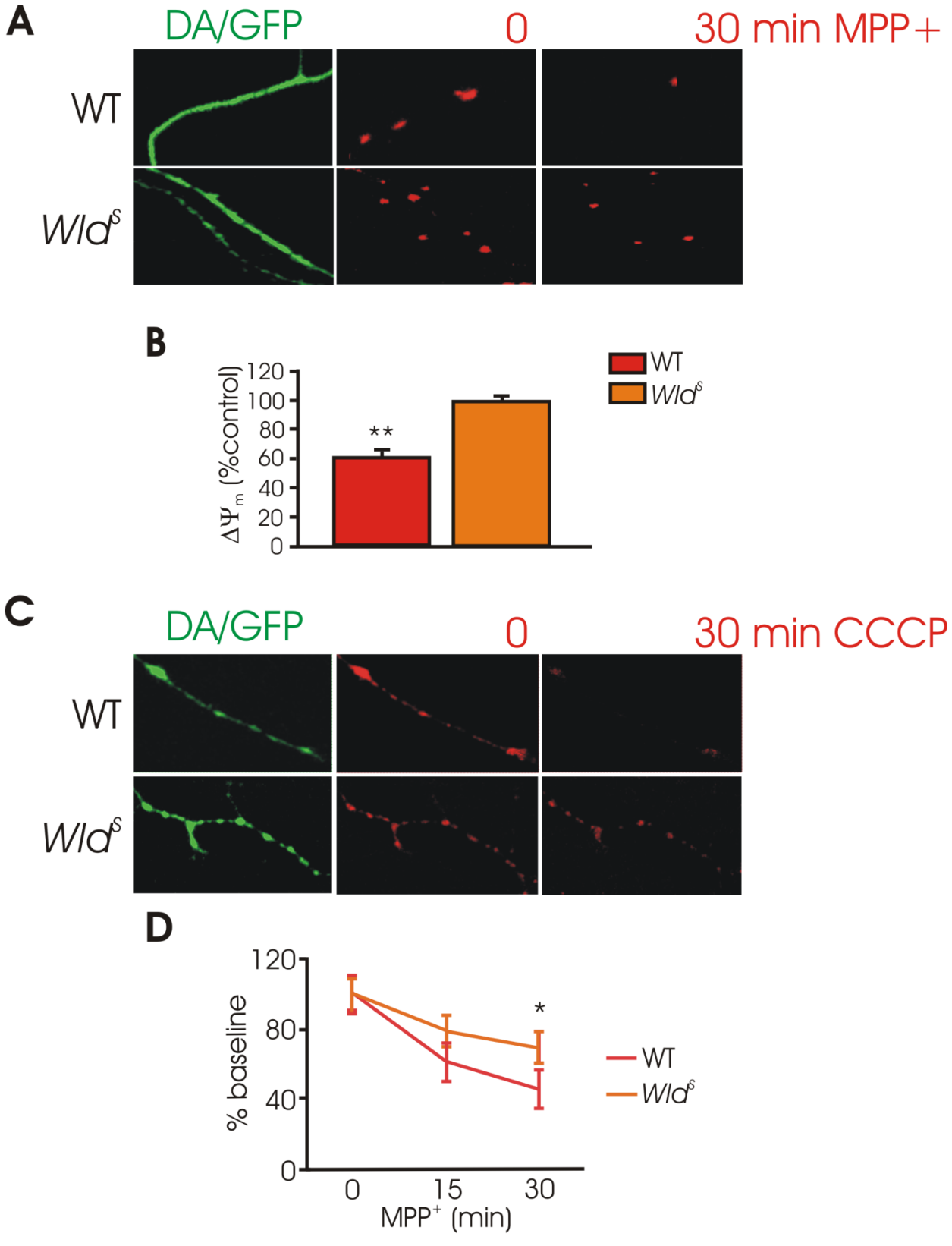
A
DA/GFP
0
30 min MPP+
WT
Wld^S
B
ΔΨm (%control)
120
100
80
60
40
20
0
**
WT
Wld^S
C
DA/GFP
0
30 min CCCP
WT
Wld^S
D
% baseline
120
80
40
0
*
0
15
30
MPP+ (min)
WT
Wld^S

Fig.5.4

Figure 5.5 - *Wld*^{S} prevents mitophagy after MPP^{+}. (A) Autophagy was assessed by introducing a GFP-tagged LC3 expression clone at DIV6 and treating DA neurons 1 day later with 2 μM MPP^{+}. The formation of LC3-positive granules (arrow) was measured as indicated by immunostaining. Right panels show LC3 fluorescence within TH-positive axons after toxin treatment. (B) The number of TH-positive neurons with at least three LC3-GFP granules was counted and expressed as percentage of all neurons that were both TH positive and LC3-GFP positive, regardless of whether the LC3-GFP signal in these neurons was diffuse or punctuate. Mean ± SEM in three independent experiments, *$p<0.05$.

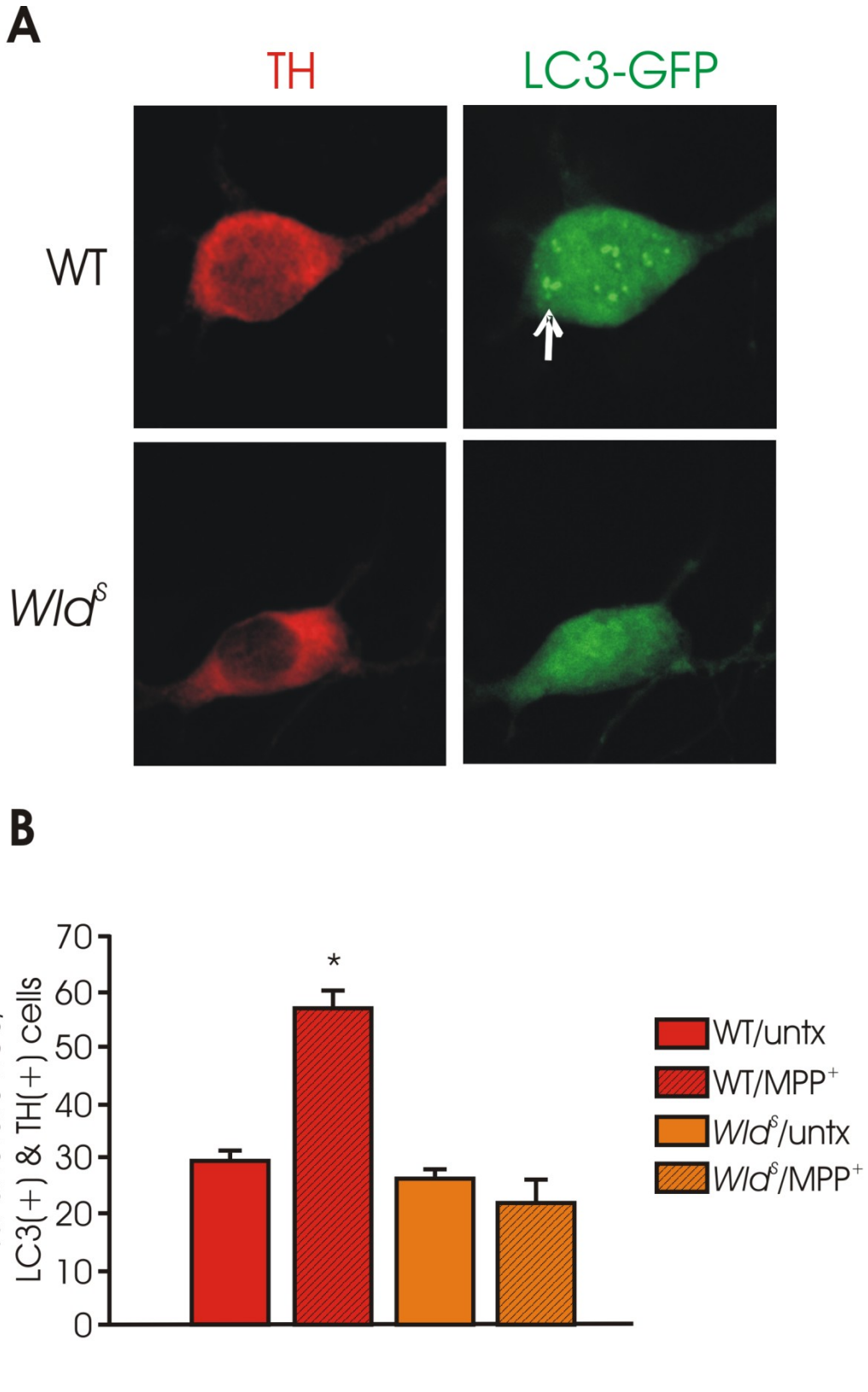
A
TH
LC3-GFP
WT
Wld^S
B
%Punctate LC3/
LC3(+) & TH(+) cells
70
60
50
40
30
20
10
0
*
WT/untx
WT/MPP+
Wld^S/untx
Wld^S/MPP+

Fig.5.5

Chapter 6

Conclusions and Future Directions

6.1 Conclusions

Axonal dysfunction and impaired axonal transport may play a key role in PD. This notion is dramatically supported by our earlier work showing that the WldS fusion protein completely rescued DA terminal fields from in vivo MPTP toxicity [1]. The current findings confirm and significantly extend these studies *in vitro* exploring mechanisms underlying *Wld*^{S} actions against additional PD-linked toxins. Our findings identify a novel role of *Wld*^{S} in DA axons that is independent of its NAD^+-synthesizing activity and further emphasizes a novel gain of function. Moreover, our new observations point to a significant role of *Wld*^{S} in maintaining or delaying changes in mitochondrial membrane bioenergetics .Finally, this dissertation reinforces the notion that DA neurons are more susceptible in the pathogenesis of PD due, in part, to unique characteristics of their mitochondria that are smaller and slower than their counterparts.

Given the many studies showing that Nmnat at least partially protects axons from a variety of insults both in the CNS but especially the PNS, our studies showing that Nmnat1, Nmnat3 and cytoplasmically-targeted Nmnat1 cannot protect DA axons from two different types of parkinsonian mimetics were surprising. Although it might be argued that the transduced levels of each variant were insufficient to protect DA neurites, the fact that the same if not greater numbers of DA neurons were transduced (Chapter 2), that expressed protein levels were the same (Fig. 2.3), and most importantly, that the same lentiviral preparations rescued DRG neurites from vincristine treatment, indicates that insufficient Nmnat is not the cause. Most studies also suggest that Nmnat's

NAD^+-synthesizing ability is essential in protecting axons [2-3], yet this did not seem to be the case in DA neurites either (Fig. 2.5). Moreover, while exogenous NAD^+ did protect cell bodies and neurites against MPP^+, its neuroprotective effect was additive with that of *Wld*^{S} suggesting that it was acting through a different mechanism (Fig. 2.8). Finally, even though *Wld*^{S} protected DA neurites from 6-OHDA, neither Nmnat1 nor exogenous NAD^+ did so, again suggesting that the entire *Wld*^{S} fusion protein is required for protection of DA neurites. Taken together, these findings argue that *Wld*^{S} plays a different role in DA neurons than it does in certain CNS or PNS neurons.

What is different about DA neurons? Besides producing a neurotransmitter that is prone to oxidation [4], DA neurons have long, thin-caliber, poorly myelinated axons. Typically, such axons use more energy to generate action potentials than more highly myelinated neurons [5]. Thus DA axons may require more energy making them more susceptible to energy loss than axons requiring less [5]. This idea is consistent with data demonstrating preferential effects on DA neurons of inhibitors of mitochondrial complex 1 such as MPP^+ and rotenone and even 6-OHDA, leading to ROS, loss of $\Delta\Psi_m$, and eventually loss of ATP [6]. DA neurons also exhibit a greater dependence on L-type Ca^{2+} channels than most neurons which can lead to deleterious amounts of intracellular calcium and increased stress on mitochondria [7]. Moreover, DA neurons have fewer mitochondria [8] and, as shown here [17], DA axonal mitochondria are smaller and move along the axon slower than mitochondria in non-DA neurons. These unique characteristics of DA neurons suggest that

protection of these neurons may employ a different type of mechanism(s), potentially one that protects DA mitochondria from bioenergetic challenges.

Wld^S is predominantly seen in the nucleus, but here, we present evidence that the *Wld*^{S} protein partially colocalizes with DA axonal mitochondria (Fig. 5.2), similar to what has been reported by others [9]. Thus, *Wld*^{S} can protect against axonal degeneration by preserving mitochondrial function. In support of this, we saw that *Wld*^{S} DA axonal mitochondria maintained their motility after MPP^+ treatment. *Wld*^{S} also protected axonal DA mitochondria against MPP^+-induced decrease in mitochondrial membrane potential ($\Delta\Psi_m$) and attenuated the effect of carbonyl cyanide *m*-chlorophenyl-hydrazone (CCCP) on $\Delta\Psi_m$. In addition, *Wld*^{S} neurites were protected against 6-OHDA, which our lab has previously reported to cause ROS generation and a rapid decrease in $\Delta\Psi_m$ of DA neurons [10]. These results are consistent with data showing that *Wld*^{S} cultures maintain their $\Delta\Psi_m$ and have intact neurites after vincristine treatment [11]. Taken together, our findings and other studies underscore the role of mitochondria in the neuroprotective phenotype of *Wld*^{S}.

So how does *Wld*^{S} protect DA axonal mitochondria? A recent study has shown that *Wld*^{S} was able to regulate the mitochondrial permeability transition pore (mPTP) and prevent calcium release, ATP loss, oxidative stress and release of proteins involved in axonal degeneration in sciatic nerve explants [12]. In addition, the mPTP inhibitor, promethazine, was reported to prevent MPTP-induced loss of SN DA neurons [13]. Because CCCP and oxidative stress can also induce mitochondrial permeability transition [14-15], one potential model is

that *Wld*^{S} protects axons by inhibiting mPTP activation, mitochondrial depolarization, and all the subsequent complications of mitochondrial dysfunction. *Wld*^{S} can potentially prevent opening of the mPTP in response to toxin injury in two ways. First, *Wld*^{S} can affect the mPTP through direct action on the pore since one of the proteins that was upregulated in *Wld*^{S} striatal synaptosomes is VDAC2 [16], which has been shown to regulate the mPTP [17]. The second way that *Wld*^{S} can affect pore opening is suggested by our findings that NAC and GSHEE protect against MPP^+-induced loss of mitochondrial motility. Since *Wld*^{S} has a similar phenotype, we hypothesize that *Wld*^{S} might affect redox balance such that the pore is less likely to open and hence can withstand various challenges in a more robust fashion. Future studies will continue to explore this role of *Wld*^{S} in protecting DA axons from degeneration.

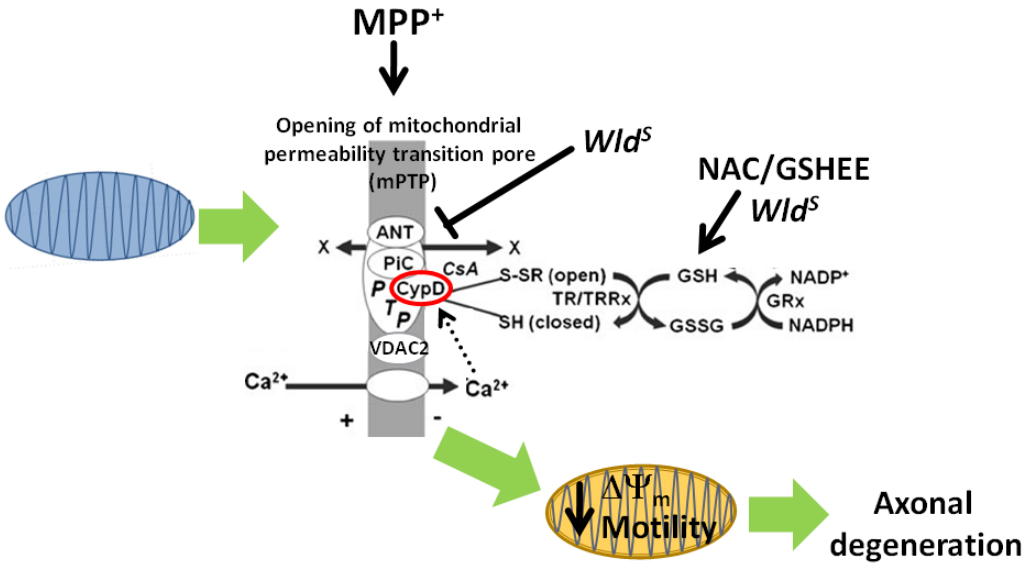

Figure 6.1 – Proposed model of how *Wld*^{S} protects DA axons from PD mimetics. Modified from Toman and Fiskum, 2011 [18].

6.2 Future Directions

6.2.1 Does disruption of the mitochondrial permeability transition pore in DA neurons inhibit the protective effect of *Wld*^{S}?

We hypothesize that *Wld*^{S} protects DA axons by inhibiting mitochondrial permeability transition (Fig. 6.1). To test this idea, we propose to examine if exogenous activation of mPTP causes degeneration of DA axons and if *Wld*^{S} cultures protect DA axons against this type of insult. Atractyloside (ATR) stimulates mPTP by inducing a conformational change in the adenine nucleotide translocator (ANT) [19]. Thus, we can utilize ATR for these experiments. We can also test if primary midbrain cultures from cyclophilin D knockout mice [20], which are available from Jackson Laboratories, are protected against 6-OHDA and MPP^+-induced toxicity and if this protection is similar to the *Wld*^{S} phenotype. Alternatively, we could use knockdown approaches to similarly manipulate the levels of cyclophilin D.

To determine whether delayed mPTP activation is intrinsic to *Wld*^{S} mitochondria, we can also examine the effect of ATR on the $\Delta\Psi_m$ of WT and *Wld*^{S} DA axonal mitochondria. If our model holds true, we predict that ATR will have less effect on axonal degeneration and $\Delta\Psi_m$ in *Wld*^{S} DA axons compared to WT.

6.2.2 Does *Wld*^{S} protect DA neurons through an effect on glutathione levels?

Similar to our findings in *Wld*^{S} cultures, pretreatment of DA axons with the redox-sensitive neuroprotectants NAC and GSHEE protected against MPP^+-induced changes in mitochondrial motility and DA neurite and cell body loss. Thus, it is worth investigating if *Wld*^{S} cultures protect in a similar manner as NAC and GSHEE by determining if WT and *Wld*^{S} exhibit similar levels of reduced GSH. Reduced GSH may be visualized using Ellman's reagent or bimane derivates such as monobromobimane [21]. Another way to measure glutathione is through the use of redox-sensitive green fluorescent protein (roGFP) [22]. These proteins have the advantage of enabling one to quantify the glutathione redox potential in live cells, but have the disadvantage of having poor sensitivity and slow response to redox potential changes. An alternative approach is to utilize the Grx1-roGFP2 fusion protein developed by Gutscher *et al.* [23]. Using this fusion protein, the authors were able to measure glutathione redox potential in different cellular compartments with high sensitivity and temporal resolution while still allowing one to conduct experiments in live cells. More importantly this construct, and one devised to look at thioredoxin function, can be targeted to the mitochondria allowing redox measurements of that organelle [23].

Aside from comparing baseline levels of GSH in WT and *Wld*^{S} mice, we can also examine how GSH affects the *Wld*^{S} phenotype by decreasing GSH levels in *Wld*^{S} mice. Treatment of animals with buthionine sulphoximine (BSO), an inhibitor of gamma-glutamylcysteine synthetase, has been shown to lower

tissue GSH concentration [24]. If treating *Wld*^{S} animals with BSO abrogates their protective effect against 6-OHDA or MPTP, this will suggest that maintenance of GSH levels plays a role in the neuroprotective phenotype of *Wld*^{S}.

6.2.3 How does *Wld*^{S} protect against 6-OHDA-mediated neurodegeneration?

We saw that *Wld*^{S} protects DA cell bodies and neurites against 6-OHDA-mediated toxicity through an Nmnat-independent mechanism. However, the exact mechanism by which *Wld*^{S} protects against 6-OHDA has not been fully explored. Data from this lab has shown that ROS production from 6-OHDA upregulates the unfolded protein response (UPR) and causes p53-dependent cell death through two parallel pathways [25]. 6-OHDA also causes a rapid decrease in $\Delta\Psi_m$ of DA neurons [10]. Accordingly, the following questions need to be addressed: (1) Does *Wld*^{S} protect DA neurons against oxidative stress? (2) Does *Wld*^{S} protect DA neurons against upregulation of UPR? (3) Does *Wld*^{S} protect DA neurons against p53 activation? (4) Does *Wld*^{S} protect against 6-OHDA-mediated decrease in $\Delta\Psi_m$?

6.2.3.1 Does *Wld*^{S} protect DA neurons against oxidative stress?

Mouse embryonic fibroblasts from *Wld*^{S} mice were protected against paraquat, a PD-linked toxin known to generate ROS [26]. 6-OHDA has also been

shown to rapidly and robustly generate ROS in DA cell bodies [10], This emphasizes the need to examine if *Wld*^{S} protects against 6-OHDA-mediated increases in oxidative stress. Measuring ROS in axons can be difficult but recently other studies have shown that MitoSox, a dye derived from DHE, has the sensitivity to see changes *in situ* using optical imaging techniques. Thus, using MitoSox, we can quantify the generation of ROS in the mitochondria of WT and *Wld*^{S} DA axons in response to 6-OHDA treatment.

6.2.3.2 Does *Wld*^{S} protect DA neurons against upregulation of UPR?

6-OHDA causes upregulation of proteins associated with the unfolded protein response (UPR) [27]. Since Nmnat has been suggested to have chaperone activity [28-29], it is possible that *Wld*^{S} prevents 6-OHDA injury by inhibiting the initiation of the UPR. To determine if WT and *Wld*^{S} cultures have differential regulation of UPR after 6-OHDA, we can probe WT and *Wld*^{S} primary midbrain cultures with antibodies for UPR markers at baseline and at the appropriate time points after addition of 6-OHDA. Two UPR markers that would be interesting to utilize for this purpose are ATF3, which is an early UPR maker, and CHOP, which is a late UPR marker. If *Wld*^{S} has a chaperone-like activity similar to Nmnat1, we would predict that *Wld*^{S} will prevent the upregulation of the both ATF3 and CHOP.

6.2.3.3 Does *Wld*^{S} protect DA neurons against activation of p53?

Our lab has recently shown that 6-OHDA-generated ROS induces DNA damage and causes cell death through a p53-dependent mechanism. Intriguingly, primary midbrain cultures from p53 knockout mice were almost completely protected from 6-OHDA toxicity both at the level of the cell body and neurites [25]. To investigate if *Wld*^{S}' neuroprotective effect is potentially mediated by p53, WT and *Wld*^{S} primary midbrain cultures can be stained with phospho-p53 antibody before and after 6-OHDA treatment to determine if these two types of cultures have a similar induction of p53 activity after addition of toxin. Because our previous work showed that DA cell bodies, but not neurites, of Puma (p53-upregulated mediator of apoptosis)-null mice were protected against 6-OHDA [25], we would predict that if *Wld*^{S} prevents the activation of p53, it will also prevent the upregulation of its downstream effector, Puma.

6.2.3.4 Does *Wld*^{S} protect against decreased mitochondrial membrane potential due to 6-OHDA toxicity?

Since 6-OHDA causes a rapid decrease in $\Delta\Psi_m$ in DA cell bodies [10], we can test if *Wld*^{S} can prevent against changes in $\Delta\Psi_m$ from 6-OHDA injury. This can be done in a similar manner as described in Chapter 4 and 5 in MPP^+-treated cultures through the use of tetramethylrhodamine ethyl ester (TMRE) as a $\Delta\Psi_m$ indicator dye. Since we hypothesize that *Wld*^{S} protects axons through its action on the mitochondria, we predict that *Wld*^{S} will also prevent changes in $\Delta\Psi_m$

axonal DA mitochondria after 6-OHDA treatment. Data from these proposed experiments will help elucidate how *Wld*^{S} protects against predicted 6-OHDA-induced axonal injury.

6.2.4 Does 6-OHDA affect axonal mitochondrial dynamics?

MPP^+ and 6-OHDA cause DA cell death through distinct cell death mechanisms [10], thus what we've shown for MPP^+ may not necessarily be the same processes triggered by 6-OHDA toxicity. One similarity however is that, like MPP+, 6-OHDA causes a rapid decrease in $\Delta\Psi_m$ in DA cell bodies [10]. This implies that 6-OHDA may also cause mitochondrial dysfunction and/or mitochondrial permeability transition. Hence, one can investigate if 6-OHDA also causes (1) a decrease in mitochondrial motility, (2) slower anterograde mitochondrial velocity, and (3) faster retrograde mitochondrial velocity, before disruptions in microtubule stability are observed using the microchamber device utilized in the experiments described in Chapter 4. We predict that 6-OHDA effects on axon transport will overlap to a significant extent with those of MPP^+. As previously described, Burke and colleagues found that, similar to MPTP, 6-OHDA also lead to depletion of striatal nerve terminals followed by retrograde degeneration of neurons in the SN and that *Wld*^{S} protected against this loss of DA terminals [30]. Thus, we predict that *Wld*^{S} will also protect DA mitochondria against 6-OHDA-induced perturbations in mitochondrial dynamics.

Taken together this will further support our hypothesis that mitochondrial transport dysfunction leads to axonal degeneration in DA neurons. Therefore, these data suggest that while MPP^+ and 6-OHDA cause DA cell death through distinct mechanisms, they may share a common mechanism of axonal degeneration.

6.2.5 Does MPTP affect mitochondrial motility and velocity *in vivo*?

The current work shows that MPP^+ decreases mitochondrial motility, changes mitochondrial velocity, and decreases $\Delta\Psi_m$ in DA axons *in vitro.* Extending results from cellular systems to *in vivo* systems is essential in further establishing if MPP^+-specific effects in mitochondrial health and dynamics are integral to the role of axonal degeneration in PD pathogenesis. *In* vivo imaging of the basal ganglia at the resolution needed to see individual mitochondrion is impossible at the moment given its location deep in the animal's brain. However, an *ex vivo* approach would get us one step closer. To do this, parasagittal brain slices can be prepared from DA/GFP mice such that DA projections from the SN to the striatum are preserved. Protocols exist for maintaining brain slices in a special chamber that allows for live imaging. MTR can be used to label mitochondria and time lapse confocal imaging to monitor mitochondrial dynamics to determine if our *in vitro* observations are recapitulated *ex vivo*. Problems with this approach might be the excessive mitochondrial labeling seen with MTR and the difficulty in assigning mitochondria to DA/GFP axons. Alternatively, we can

image mitochondria by crossing DA/GFP mice with transgenic mice that express CFP in the mitochondria (*Thy1-mitoCFP*-H) [31]. One caveat of this approach is the potential difficulty of identifying the cyan fluorescence signal labeling the mitochondria in the background of a green fluorescence signal signifying DA axons. Another way to assess mitochondrial transport is by using static time points in an intact animal. MTR can be stereotactically injected into either the SN or the striatum before treating mice with an acute regimen of MPTP. Mice can then be sacrificed at a range of time points after MPTP administration. Changes in mitochondrial transport can be visualized by assessing differences in the distribution of MTR distally and proximally from the site in injection, whether it is the striatum or SN, in fixed parasagittal brain slices. Regardless of the experimental approach utilized, we predict that mitochondrial motility and velocity are affected by MPTP in brain slices, similar to the effect of MPP^+ in primary mesencephalic cultures.

6.2.6 Does *Wld^S* protect against MPTP-induced changes in mitochondrial motility and velocity *in vivo*?

As our findings on the effect of MPP^+ on mitochondrial motility are seen *in vitro*, we need to confirm that the protection seen in *Wld^S* axonal DA mitochondria is replicated *in vivo*. We can test if *Wld^S* protects against MPTP-induced changes in mitochondrial motility and velocity *in vivo* by using the method(s) described in the previous section using *Wld^S*-DA/GFP brain slices.

Given that *Wld*^{S} protected axons against MPTP *in vivo* [1], we predict that *Wld*^{S} will also protect midbrain projections to the striatum against MPTP-induced changes in mitochondrial health and dynamics.

Our work has shed light on the role of mitochondria in MPP^+-mediated DA axonal degeneration and how *Wld*^{S} protects against this injury *in vitro*. The results of these proposed experiments will further establish how *Wld*^{S} protects DA axons against both MPTP and 6-OHDA and extend our *in vitro* results *in vivo*.

References:

1. Hasbani, D.M. and K.L. O'Malley, *Wld(S) mice are protected against the Parkinsonian mimetic MPTP.* Exp Neurol, 2006. **202**(1): p. 93-9.
2. Sasaki, Y., T. Araki, and J. Milbrandt, *Stimulation of nicotinamide adenine dinucleotide biosynthetic pathways delays axonal degeneration after axotomy.* J Neurosci, 2006. **26**(33): p. 8484-91.
3. Conforti, L., et al., *Wld S protein requires Nmnat activity and a short N-terminal sequence to protect axons in mice.* J Cell Biol, 2009. **184**(4): p. 491-500.
4. Hastings, T.G., *The role of dopamine oxidation in mitochondrial dysfunction: implications for Parkinson's disease.* J Bioenerg Biomembr, 2009. **41**(6): p. 469-72.
5. Braak, H., et al., *Stages in the development of Parkinson's disease-related pathology.* Cell Tissue Res, 2004. **318**(1): p. 121-34.
6. Ali, S.F., et al., *MPTP-induced oxidative stress and neurotoxicity are age-dependent: evidence from measures of reactive oxygen species and striatal dopamine levels.* Synapse, 1994. **18**(1): p. 27-34.
7. Surmeier, D.J., et al., *What causes the death of dopaminergic neurons in Parkinson's disease?* Prog Brain Res, 2010. **183**: p. 59-77.
8. Liang, C.L., et al., *Mitochondria mass is low in mouse substantia nigra dopamine neurons: implications for Parkinson's disease.* Exp Neurol, 2007. **203**(2): p. 370-80.
9. Beirowski, B., et al., *Non-nuclear Wld(S) determines its neuroprotective efficacy for axons and synapses in vivo.* J Neurosci, 2009. **29**(3): p. 653-68.
10. Lotharius, J., L.L. Dugan, and K.L. O'Malley, *Distinct mechanisms underlie neurotoxin-mediated cell death in cultured dopaminergic neurons.* J Neurosci, 1999. **19**(4): p. 1284-93.
11. Ikegami, K. and T. Koike, *Non-apoptotic neurite degeneration in apoptotic neuronal death: pivotal role of mitochondrial function in neurites.* Neuroscience, 2003. **122**(3): p. 617-26.
12. Barrientos, S.A., et al., *Axonal degeneration is mediated by the mitochondrial permeability transition pore.* J Neurosci, 2011. **31**(3): p. 966-78.
13. Cleren, C., et al., *Promethazine protects against 1-methyl-4-phenyl-1,2,3,6-tetrahydropyridine neurotoxicity.* Neurobiol Dis, 2005. **20**(3): p. 701-8.
14. Lim, M.L., T. Minamikawa, and P. Nagley, *The protonophore CCCP induces mitochondrial permeability transition without cytochrome c release in human osteosarcoma cells.* FEBS Lett, 2001. **503**(1): p. 69-74.
15. Juhaszova, M., et al., *The identity and regulation of the mitochondrial permeability transition pore: where the known meets the unknown.* Ann N Y Acad Sci, 2008. **1123**: p. 197-212.
16. Wishart, T.M., et al., *Differential proteomics analysis of synaptic proteins identifies potential cellular targets and protein mediators of synaptic*

neuroprotection conferred by the slow Wallerian degeneration (Wlds) gene. Mol Cell Proteomics, 2007. **6**(8): p. 1318-30.
17. Halestrap, A.P., *What is the mitochondrial permeability transition pore?* J Mol Cell Cardiol, 2009. **46**(6): p. 821-31.
18. Toman, J. and G. Fiskum, *Influence of aging on membrane permeability transition in brain mitochondria.* J Bioenerg Biomembr, 2011. **43**(1): p. 3-10.
19. Halestrap, A.P., K.Y. Woodfield, and C.P. Connern, *Oxidative stress, thiol reagents, and membrane potential modulate the mitochondrial permeability transition by affecting nucleotide binding to the adenine nucleotide translocase.* J Biol Chem, 1997. **272**(6): p. 3346-54.
20. Thomas, B., et al., *Mitochondrial Permeability Transition Pore Component Cyclophilin D Distinguishes Nigrostriatal Dopaminergic Death Paradigms in the MPTP Mouse Model of Parkinson's Disease.* Antioxid Redox Signal, 2011.
21. Meyer, A.J., M.J. May, and M. Fricker, *Quantitative in vivo measurement of glutathione in Arabidopsis cells.* Plant J, 2001. **27**(1): p. 67-78.
22. Meyer, A.J., et al., *Redox-sensitive GFP in Arabidopsis thaliana is a quantitative biosensor for the redox potential of the cellular glutathione redox buffer.* Plant J, 2007. **52**(5): p. 973-86.
23. Gutscher, M., et al., *Real-time imaging of the intracellular glutathione redox potential.* Nat Methods, 2008. **5**(6): p. 553-9.
24. Drew, R. and J.O. Miners, *The effects of buthionine sulphoximine (BSO) on glutathione depletion and xenobiotic biotransformation.* Biochem Pharmacol, 1984. **33**(19): p. 2989-94.
25. Bernstein, A.I., et al., *6-OHDA generated ROS induces DNA damage and p53- and PUMA-dependent cell death.* Mol Neurodegener, 2011. **6**(1): p. 2.
26. Yu, Q., et al., *Wld Reduces Paraquat-Induced Cytotoxicity via SIRT1 in Non-Neuronal Cells by Attenuating the Depletion of NAD.* PLoS One, 2011. **6**(7): p. e21770.
27. Holtz, W.A. and K.L. O'Malley, *Parkinsonian mimetics induce aspects of unfolded protein response in death of dopaminergic neurons.* J Biol Chem, 2003. **278**(21): p. 19367-77.
28. Zhai, R.G., et al., *Drosophila NMNAT maintains neural integrity independent of its NAD synthesis activity.* PLoS Biol, 2006. **4**(12): p. e416.
29. Zhai, R.G., M. Rizzi, and S. Garavaglia, *Nicotinamide/nicotinic acid mononucleotide adenylyltransferase, new insights into an ancient enzyme.* Cell Mol Life Sci, 2009. **66**(17): p. 2805-18.
30. Cheng, H.C. and R.E. Burke, *The Wld(S) mutation delays anterograde, but not retrograde, axonal degeneration of the dopaminergic nigro-striatal pathway in vivo.* J Neurochem, 2010. **113**(3): p. 683-91.
31. Misgeld, T., et al., *Imaging axonal transport of mitochondria in vivo.* Nat Methods, 2007. **4**(7): p. 559-61.